MATHEMATICAL MODELLING OF SOLID OXIDE FUEL CELL SYSTEM BY USING BIOGAS

GUNNIGA PORNSOPIN

A THESIS SUBMITTED IN PARTIAL FULFILLMENT

OF THE REQUIREMENT FOR THE DEGREE OF

MASTER OF ENGINEERING IN AUTOMOTIVE ENGINEERING

(INTERNATIONAL PROGRAM)

INTERNATIONAL COLLEGE

KING MONGKUT'S INSTITUTE OF TECHNOLOGY LADKRABANG

2011

KMITL-2011-IC-M-004-004

Thesis Title	Mathematical Modelling of Solid Oxide Fuel Cell System by Using Biogas
Student	Ms.Gunniga Pornsopin
Student ID	51061905
Degree	Master of Engineering
Program	Automotive Engineering (International Program)
Year	2011
Thesis Advisor	Assoc.Prof.Dr.Jarruwat Charoensuk Dr. Sumittra Charojrochkul Prof.Dr.Katsunori Hanamura

ABSTRACT

A solid oxide fuel cell (SOFC) is an electrochemical device which converts chemical energy to electricity. It consumes hydrogen which can be converted from any sources of hydrocarbon fuel. A renewable fuel source such as biogas is an interesting alternative for SOFC. The feasibility in using biogas as a cheap energy resource is unexplored. This study uses biogas as fuel supply in the SOFC system. Biogas is a mixture of methane and carbon dioxide. The system has a fuel processing unit for removing CO_2, the hydrogen production unit for converting methane to hydrogen and the SOFC unit for producing 1 kW electrical output. The SOFC system is investigated for the energy input and output by using computer program to make the empirical model of the sub-unit. The SOFC system consumed very high energy for 42% of the chemical reaction and 48% of the SOFC bundle heater. Mechanical energy input such as pump power consumed only 10%. Moreover, there is 98% waste energy due to the heat loss. When compared the energy consumption with the electrical output of the SOFC, it is only 2% of the overall system. The energy output is regarded as only a small amount of energy.

ACKNOWLEDGEMENT

This thesis could not be completed without the assistance of many persons to whom I would like to express my sincere appreciation.

First, author would like to sincerely thank my advisors, Assoc.Prof.Dr.Jaruwat Charoensuk, who has given me many helpful suggestions and the main idea of this thesis. Also I would like to sincerely thank Dr.Sumittra Charojrochkul for willingly filled the role of revising this thesis and Prof.Dr.Katsunori Hanamura for kind advising, suggestion and helping.

I really appreciate to National Science and Technology Development Agency (NSTDA) which provided the full scholarship for studying in the master program and National Metal and Materials Technology Center (MTEC), especially for providing the laboratory equipment and instruments. Moreover, I would like to thank to electrochemical materials and system (EMS) lab members for their assistances in knowledge, equipment and running the experiments.

Finally, I am very grateful to my family for all love, caring, understanding and motivation throughout my life.

Gunniga Pornsopin

CONTENTS

CONTENTS (CONT.)

CONTENTS (CONT.)

LIST OF TABLES

LIST OF FIGURES

LIST OF FIGURES (CONT.)

LIST OF FIGURES (CONT.)

LIST OF FIGURES (CONT.)

Figure Page

NOMENCLATURE

$C_{p\ exhaust}$	Specific heat capacity of exhaust gas	kJ/kg K
ΔH	Heat of reaction	kJ/mol
ΔH_{SMR}	Heat of steam methane reforming reaction	kJ/mol
ΔH_{WGS}	Heat of water gas shift reaction	kJ/mol
h_{NT}	Enthalpy at normal temperature	kJ/kg
h_{reform}	Enthalpy of reformer at operation temperature	kJ/kg
$h_{sensible,\ reformate\ gas}$	Enthalpy of sensible reformate gas	kJ/kg
I	Current	A
LHV_{H_2}	Lower Heating Value of hydrogen	MJ/kg
LHV_{LPG}	Lower Heating Value of LPG	MJ/kg
$\dot{m}_{biogas}$	Mass flow rate of biogas	kg/s
$\dot{m}_{CH_4}$	Mass flow rate of methane	kg/s
$\dot{m}_{CO}$	Mass flow rate of carbon monoxide	kg/s
$\dot{m}_{CO_2}$	Mass flow rate of carbon dioxide	kg/s
$\dot{m}_{exhaust}$	Mass flow rate of exhaust gas	kg/s
$\dot{m}_{H_2}$	Mass flow rate of hydrogen	kg/s
$\dot{m}_{LPG}$	Mass flow rate of LPG	kg/s
$\dot{m}_{reformate\ gas}$	Mass flow rate of reformate gas	kg/s
m_{NaOH}	Mass of NaOH	kg
M_{CH_4}	Molecular weight of methane	kg/kmol
M_{H_2O}	Molecular weight of water	kg/kmol
$\mathrm{NaOH}_{consump}$	NaOH consumption	kg/day
n_{CH_4}	Mole flow rate of methane	mol/s
$\dot{n}_{CO_2}$	Mole flow rate of carbon dioxide	mol/s
$\eta_{combustion}$	Efficiency of LPG combustion	%
$\eta_{furnace}$	Efficiency of furnace	%
η_{SOFC}	Efficiency of SOFC	
Q_{latent}	Latent heat of water	J/g
$Q_{sensible\ steam}$	Sensible heat of steam	J/s

NOMENCLATURE (CONT.)

$Q_{sensible\ water}$	Sensible heat of water	J/g
$\dot{Q}_{boiler}$	Heat of boiler	W
$\dot{Q}_{chem}$	Chemical energy	kW
$\dot{Q}_{loss,reformate\ gas}$	Heat energy loss from reformate gas	kW
$\dot{Q}_{LPG}$	Heat of LPG combustion	kW
$\dot{Q}_{exhaust}$	Heat of exhaust gas	kW
$\dot{Q}_{reformer}$	Heat of reformer	kW
$\dot{Q}_{reforming}$	Heat of steam methane reforming reaction	kW
$\dot{Q}_{SOFC}$	Heat of reformate gas in SOFC	kW
$\dot{Q}_{wall}$	Heat loss to wall	kW
$Power_{SOFC}$	Electrical power output of SOFC	kW
$P_{pump\ air}$	Power pump of air	kW
t_{CO_2}	CO_2 absorption time	min
T_{BP}	Temperature at boiling point	°C
T_{in}	Temperature at the inlet of furnace	°C
T_{NT}	Temperature at normal temperature	°C
T_{out}	Temperature at the outlet of furnace	°C
T_{reform}	Temperature at reformer operation	°C
$\dot{W}_{pump}$	Power of NaOH pump	W
V	Voltage	V
X_{CH_4}	Conversion of methane	
X_{CO_2}	Conversion of carbon dioxide	
Y_{CH_4}	H_2 yield	

Acronym	
AFC	Alkaline Fuel Cell
CHP	Combine Heat and Power
DMFC	Direct Methanol Fuel Cell
GC	Gas Chromatography

NOMENCLATURE (CONT.)

LHV	Lower Heating Value
LPG	Liquefied Petroleum Gas
MCFC	Molten Carbonate Fuel Cell
PAFC	Phosphoric Acid Fuel Cell
PEMFC	Polymer Electrolyte Fuel Cell
SOFC	Solid Oxide Fuel Cell
HC	Hydrocarbon
SG	Synthesis Gas
NT	Normal Temperature
BP	Boiling point
S/C	Steam to Carbon ratio

CHAPTER 1

INTRODUCTION

1.1 Significance and Background

Renewable energy sources are of widely interest nowadays such as biogas. Biogas is produced from farm waste or domestic animals disposal. It is cheap and readily available since Thailand is the country of agriculture. Biogas composes of methane, carbon dioxide, hydrogen sulphide and etc. Solid Oxide Fuel Cell, or in short SOFC, is a device that consumes hydrogen which can be derived from any forms of hydrocarbon. Thus biogas is an alternative fuel which can be the fuel supply for SOFC. Before feeding biogas into an SOFC, biogas needs to be treated or upgraded by fuel processing which are CO_2 removal and H_2S removal. These processes are necessary for removing unwanted and toxic gases. SOFC is supplied by hydrogen, thus hydrogen production process is needed to convert methane to hydrogen. Therefore, the major processes for the SOFC system are; fuel processing, hydrogen production and SOFC.

SOFC is an energy conversion device which converts a gaseous fuel to electricity and heat in the presence of an oxidant. Since SOFCs have high energy efficiency and are environmentally friendly, they are potentially attractive in producing electricity. To study the energy for the production of 1 kW electrical output of SOFC at the National Metal and Materials Technology Center (MTEC), the SOFC system is developed. The main unit in the SOFC system are CO_2 removal, reformer and the SOFC stack. First, Biogas is fed into the CO_2 removal in which CO_2 will be removed by the chemical absorption process. Now, there was only methane to be converted to hydrogen via a reforming process. Hydrogen product is supplied into the SOFC with certain amount of heat being removed from the reformed gas to meet the temperature level as required by the SOFC stack. Finally, the SOFC stack operates at 850-920°C and produce electrical energy as the output. Overview of the process is shown in Figure 1.1. The study of energy conservation is necessary. Mass and energy balance is investigated to determine the energy input and output on sub-units and overall system.

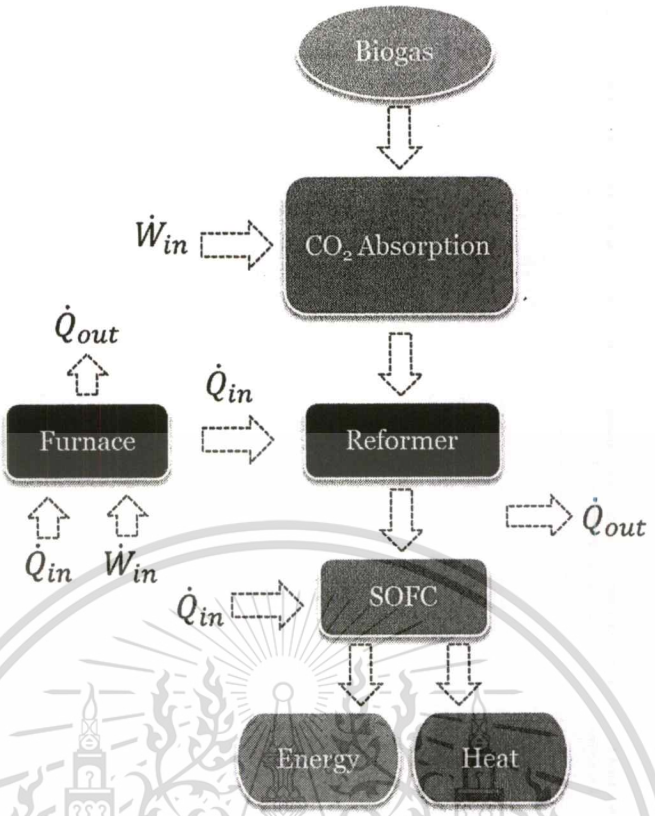

Figure 1.1 Flowchart of SOFC system

1.2 Objectives

To study and develop an empirical modelling of the sub-unit of the SOFC system; i) Fuel processing system, ii) Hydrogen production system, and iii) SOFC system and to assess the energy budget for the production of 1 kW electrical output of the SOFC.

1.3 Scopes

1.3.1 Use a computer program for the development of an empirical modelling of the sub-unit of the SOFC system as follows;

1) CO_2 absorption model

2) Reformer model

3) SOFC model

1.3.2 Study the empirical modelling of the SOFC system to investigate the energy conservation.

1.4 Expected Benefits

1.4.1 Understanding the process of the fuel processing, hydrogen production and the SOFC unit operated in the SOFC system.

1.4.2 Capability in developing and improving the empirical model of the SOFC system on MATLAB SIMULINK.

1.4.3 Capability in developing a mathematical model using a computer program

CHAPTER 2

LITERATURE REVIEW

In several decades, fossil fuel has significantly increased demand for electrical power generation, although this fuel is a non-renewable energy resource. The consumption demand makes this kind of energy almost running out. This is the reason why people look for alternative fuel such as biofuel, biomass, biogas, hydrogen etc.

2.1 Biogas

Biogas is a renewable resource which is normally produced from waste in farm or domestic animal. A potential of biogas production from biomass in Thailand is approximately 2,100 million m^3 of biogas. (eqv. 1,040 ktoe), however only 18% of these are practical in the production and in use. Currently, there are almost 2,300 biogas plants installed. These systems annually produce 380 million m^3 of biogas (eqv. 188 ktoe) from cassava starch wastewater (53%), pig manure (39%) and others (8%). More than 70% of these biogas plants employ small digesters called fixed dome technology, which is used mainly in small pig and dairy farms. Whereas, industrial scale technologies, such as up flow anaerobic sludge blanket, anaerobic fixed film, anaerobic covered lagoon, completely stirred tank reactor and anaerobic baffle reactor are implemented in large animal farms and agro-industries i.e. cassava starch, distilleries, beer, canned seafood, slaughterhouse, palm oil mill, etc. (P. Kullavanijaya et al. 2007).

2.1.1 Biogas Composition

Biogas is mainly comprised of methane and carbon dioxide as shown in Table 2.1. Methane is the main composition of combustion fuel such as natural gas. Thus, biogas can be used as a combustion fuel in gas engines to generate electricity. Furthermore, biogas is applied to use with an SOFC for the utilization in SOFC, CO_2 and H_2S have to be removed from the biogas because CO_2 causes dilution of reaction and H_2S has eroded SOFC. Therefore, biogas needs to be cleaned to fulfil the requirements of SOFC.

Table 2.1 Composition of biogas

Component	% by volume
Methane	60 - 65
Carbon Dioxide	30 - 38
Nitrogen	2 - 5
Sulphide, Disulphide, Merceptane	2 - 5
Ammonia	0 - 1.0
Hydrogen	0.1 - 1.0
Carbon Monoxide	0 - 0.2
Other trace gases	0 - 0.2

Pollution Control Department. 2544

2.2 CO_2 Removal Technologies

When using biogas for SOFC, all contaminants as well as CO_2 need to be removed to increase the concentration of hydrogen in the reforming process. There are several methods for removing CO_2

2.2.1 Water Absorption

Water is the most common solvent in which case the process is called water scrubbing. The absorption process is purely physical. Biogas is pressurised and fed to the bottom of a packed column while water is fed on the top as shown in Figure 2.1. The absorption process is designed for a counter flow pattern. The column is filled with packing to create a large surface between gas and liquid. CO_2 as well as H_2S are more soluble in water than methane. The biogas which is brought out from the top of the column is enriched in methane and saturated with water. To reduce the water vapour the biogas needs to be dried. The water which exits the column with absorbed CO_2 can be regenerated and re-circulated back to the absorption column.

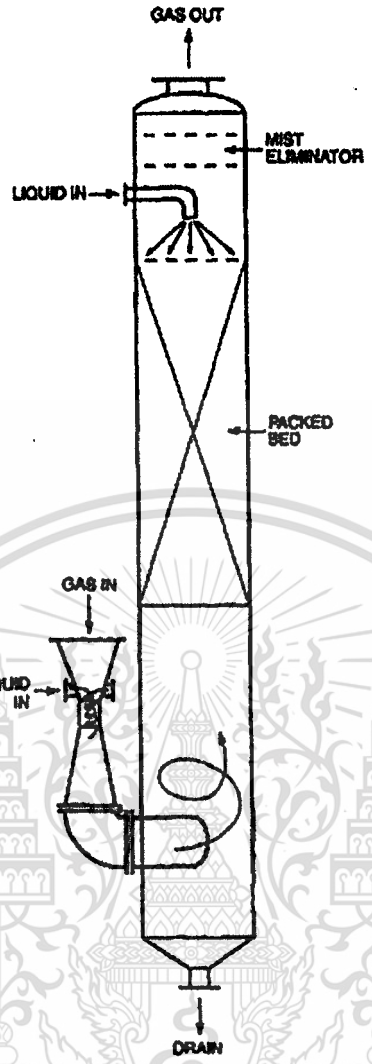

Figure 2.1 Diagram of venture scrubber-packed absorber combination system *Croll-Reynolds CO., Inc* (Gas Purification, 5th ed.)

There are two types of water scrubbing (Wahyudin, W. 2007):

i) Single pass scrubbing

In a single pass scrubbing, the washing water is used only once. The advantage of this type of scrubbing is that no contamination in the water occurs like traces of H_2S and CO_2. This gives the total amount of CO_2 and H_2S at its maximum. The disadvantage of this technique is that it requires a large amount of water. This technique is only feasible when working near a sewer water cleaning plant from which water can be used.

ii) Regenerative absorption

In a regenerative absorption, the washing water is regenerated after washing the biogas as shown in Figure 2.2. The main advantage of this technique is that the total amount of water required is much lower compared to a single pass scrubbing.

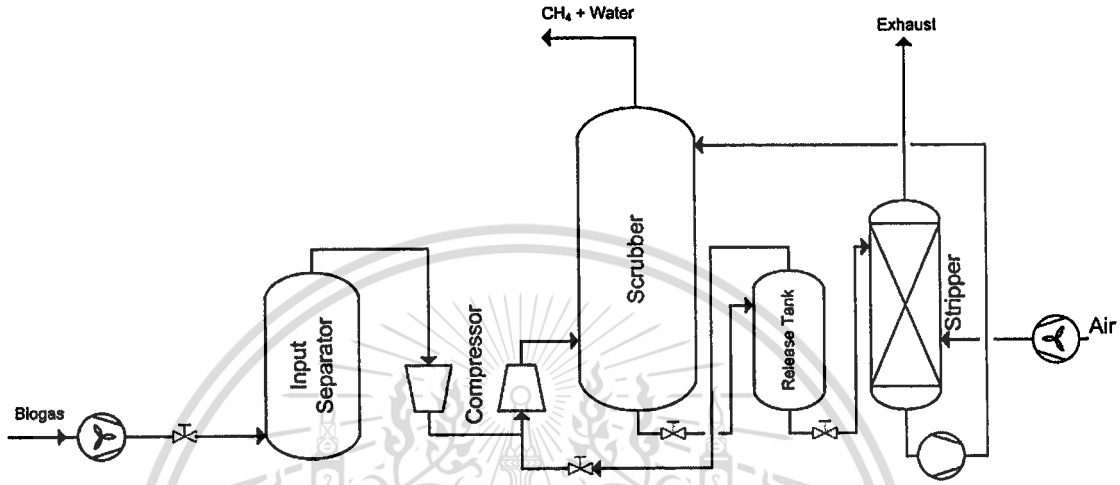

Figure 2.2 Diagram of high pressure water scrubbing (J. de Hullu, et al. 2008)

The use of water as an absorbent offers the advantages as the following (Gas Purification, 5th ed.).

1) Simple plant design
2) No heat load
3) Inexpensive solvent
4) Solvent not reactive with O_2 and other possible trace constituents

The principal disadvantages of the water-wash process are (Gas Purification, 5th ed.)

1) Requires a large volume of water that must be purified and recycled
2) Substantial loss of hydrogen or other valuable constituents of the gas stream
3) Very high pumping load
4) Poor CO_2 removal efficiency

In view of these disadvantages, the water-wash process is rarely used today for carbon dioxide removal.

2.2.2 Cryogenic Separation

Methane has a boiling point of -160°C at atmospheric pressure whereas carbon dioxide has a boiling point of -78°C. This means that carbon dioxide can be separated from biogas as a liquid by cooling the gas mixture at elevated pressure. Methane can be taken out in gas or liquid phase, depending on how the system is constructed. When methane is condensed, nitrogen which has an even lower boiling point is separated and this is an advantage when dealing with landfilled gas. The separated carbon dioxide is clean and can be sold. To avoid freezing and other problems in the cryogenic process, water and hydrogen sulphide need to be pre-separated. The principle of cryogenic separation is that biogas is compressed and then cooled by heat exchangers followed by an expansion step for instance in an expansion turbine. The cooling and the expansion cause the carbon dioxide to condense. Compression as well as chilling can be done in several steps. After carbon dioxide has been removed as a liquid, the gas can be cooled further to condense the methane.

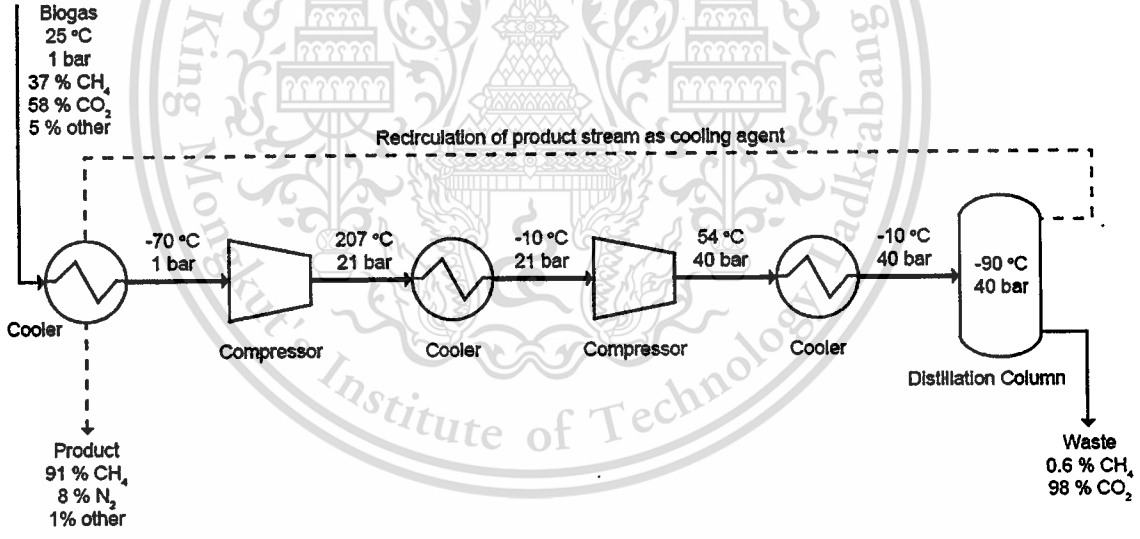

Figure 2.3 Cryogenic separation of biogas (J. de Hullu, et al. 2008)

Among the existing techniques for biogas upgrading, cryogenic separation of impurities from biogas is still in the early stage of research and development. J. de Hullu, et al. (2008) investigated the feasibility of this technique. In the first designing steps, the focus has been on the separation under low temperature and high pressure. When the desired purity of the upgraded gas is achieved, the design of the cooling and compressing unit in this technique can be continued.

Finally, these two models for compressing and separating of biogas, is put together to achieve the final separation model which is shown in Figure 2.3.

2.2.3 Membrane Separation

Biogas can be separated between methane and carbon dioxide using a membrane separation technology. CH_4 and CO_2 are different in particle size. The principle is that some components of the raw gas could be transported through a thin membrane (<1 mm) while others are retained. The transportation of each component is driven by the difference in partial pressure over the membrane and is highly dependent on the permeability of the component in the membrane material.

Wellinger and Lingberg (1999) described two basic systems of gas scrubbing with membranes: a high pressure gas separation with gas phases on both sides of the membrane and a low pressure gas liquid absorption on separation where a liquid absorbs the molecule diffusing through the membrane. The high pressure gas separation membranes can last up to 3 years which is comparable to the life time of membranes used for natural gas purification.

J. de Hullu, et al. (2008) had investigated the membrane separator. A major disadvantage of this technique is the low methane yield. The waste gas still contains CH_4 which is highly polluting. A use of a multistage setup also increases the yield. Positive results have been found using an internally staged permeator as shown in Figure 2.4.

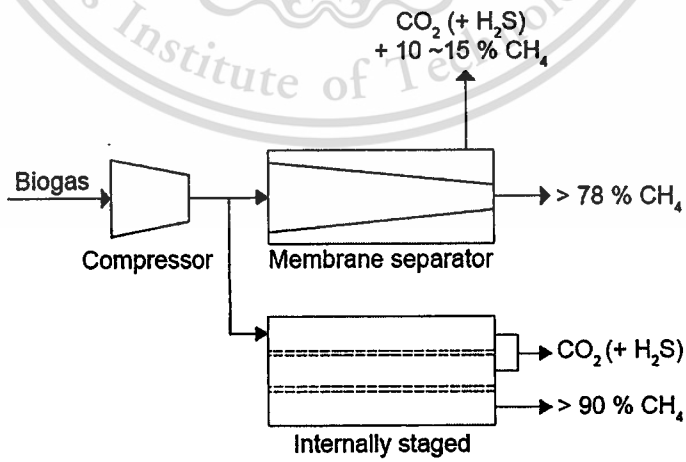

Figure 2.4 Diagram of an internally staged membrane separator (J. de Hullu, et al. 2008)

2.2.4 Carbon Molecular Sieves

The carbon molecular sieve method uses differential adsorption characteristics to separate CH_4 and CO_2. This adsorption is carried out at high pressure and is also known as "*pressure swing adsorption (PSA)*". For this process to be successful, H_2S should be removed before the adsorption process.

The process requires dry gas. Water vapour is usually condensed in a cooler. H_2S needs to be pre-separated before the gas is fed into the bottom of the adsorption vessel. This is done by using an additional tank of activated carbon. Usually when its surface is saturated with hydrogen sulphide, the material is exchanged. An addition of air to the biogas stream can extend the lifetime of the sulphide removal unit. However, it bares the risk if there are traces of oxygen in the upgraded biogas. In the pressurized vessels, carbon dioxide is adsorbed. The gas leaving from the top of the vessel is enriched with methane. When the material in the vessel is saturated, biogas is led to a new vessel. There are several (most often four) vessels linked together to create a continuous operation and to reduce the energy needed for gas compression as shown in Figure 2.5. Regeneration of the saturated vessel is achieved through stepwise depressurization. First, the pressure is reduced through linking the vessel with an already regenerated vessel. Then the pressure is reduced to almost atmospheric pressure. The gas released in this step contains significant amounts of methane and is therefore recycled to the gas inlet (Wellinger and Lingberg. 1999).

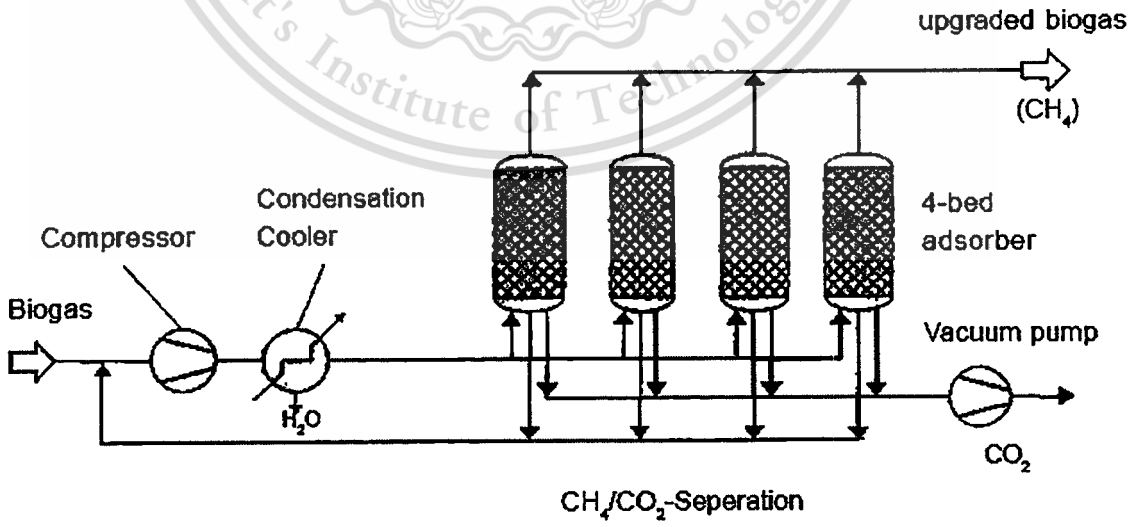

Figure 2.5 Diagram of flow sheet for upgrading of biogas to vehicle fuel standards with carbon molecular sieves (Wellinger and Lingberg. 1999)

Finally, the vessel is completely evacuated using a vacuum pump. The gas that leaves the vessel in this step mainly consists of carbon dioxide which is in one system released to the atmosphere. In another system, it is burned in a burner designed for low calorie gases. In the first system, more upgraded biogas is produced whereas the second system needs less absorber surface and has no methane slip to the atmosphere.

2.2.5 Chemical Process

Chemical absorption involves a formation of reversible chemical bonds between the solute and the solvent. A regeneration of the solvent therefore, involves breaking of these bonds and correspondingly, a relatively high energy input. Chemical solvents generally employ either aqueous solution of amines, i.e. mono-, di- or tri-ethanolamine or aqueous solution of alkaline salts, i.e. sodium, potassium and calcium hydroxides.

2.2.5.1 Chemical Absorption with Alkanolamine

The basic flow arrangement for all alkanolamine acid-gas absorption-process systems is shown in Figure 2.6. Gas to be purified is passed upward through the absorber, countercurrent to a stream of the solution. The rich solution from the bottom of the absorber is heated by heat exchange with lean solution from the bottom of the stripping column and is then fed to the stripping column at some point near the top.

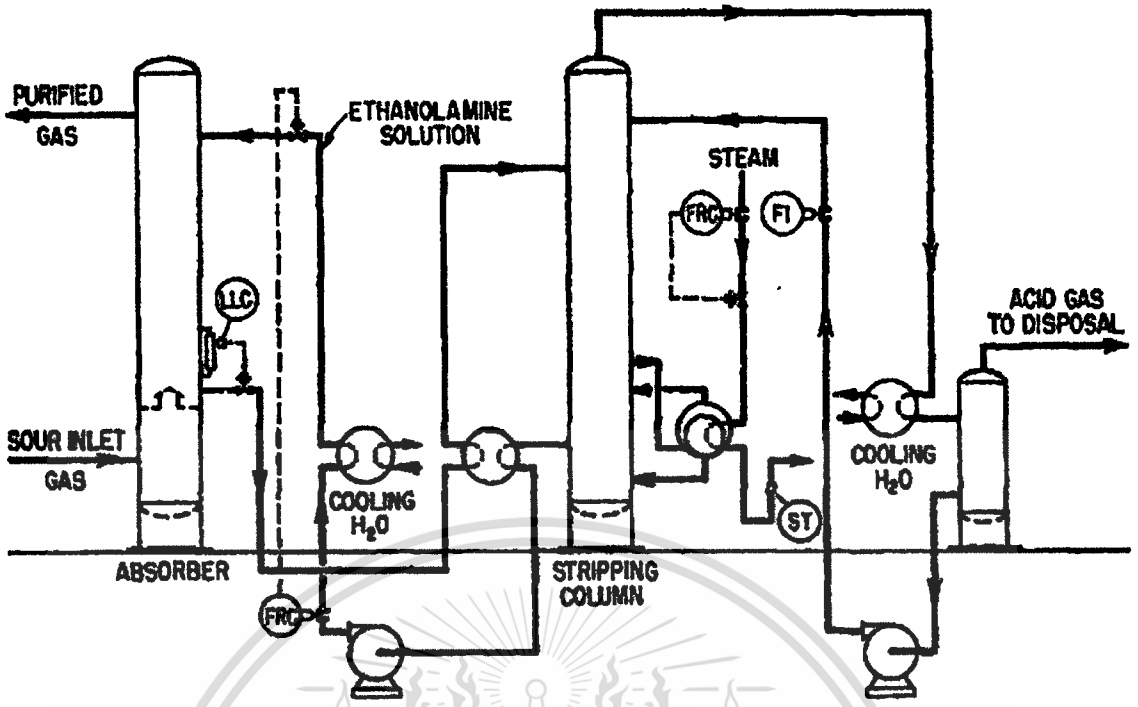

Figure 2.6 Basic flow scheme for alkanolamine acid gas removal processes (Gas Purification, 5th ed.)

In units treating sour hydrocarbon gases at high pressure, it is customary to flash the rich solution in a flash drum maintained at an intermediate pressure to remove dissolved and entrained hydrocarbons before acid gas stripping. When heavy hydrocarbons condense from the gas stream in the absorber, the flash drum may be used to skim off liquid hydrocarbons as well as to remove dissolved gases. The flashed gas is often used locally as a fuel.

Lean solution from the stripper, after partial cooling in the lean-to-rich solution heat exchanger, is further cooled by heat exchange with water or air, and fed into the top of the absorber to complete the cycle. Acid gas that is removed from the solution in the stripping column is cooled to condense a major portion of the water vapor. This condensate is continually fed back to the system to prevent the amine solution from becoming progressively more concentrated. Generally, all of this water, or a major portion of it, is fed back to the top of the stripping column at a point above the rich-solution feed and serves to absorb and return amine vapors carried by the acid gas stream.

A. Lawal et al. (2009) described one of the popular technologies proposed for post combustion capture as shown in Figure 2.7. The facility consists of two main units the absorber and stripper columns which are both packed columns. Flue gas from the power plant is

contacted counter-currently with lean MEA solution in the absorber. MEA chemically absorbs CO_2 in the flue gas. This leaves a treated gas stream of lower CO_2 content. The solvent solution (now rich MEA) is regenerated in the stripper column using steam derived from the power generation process. CO_2 from the top of the column is compressed and transported away while the lean (regenerated) MEA solution is returned to the absorber column to complete the cycle.

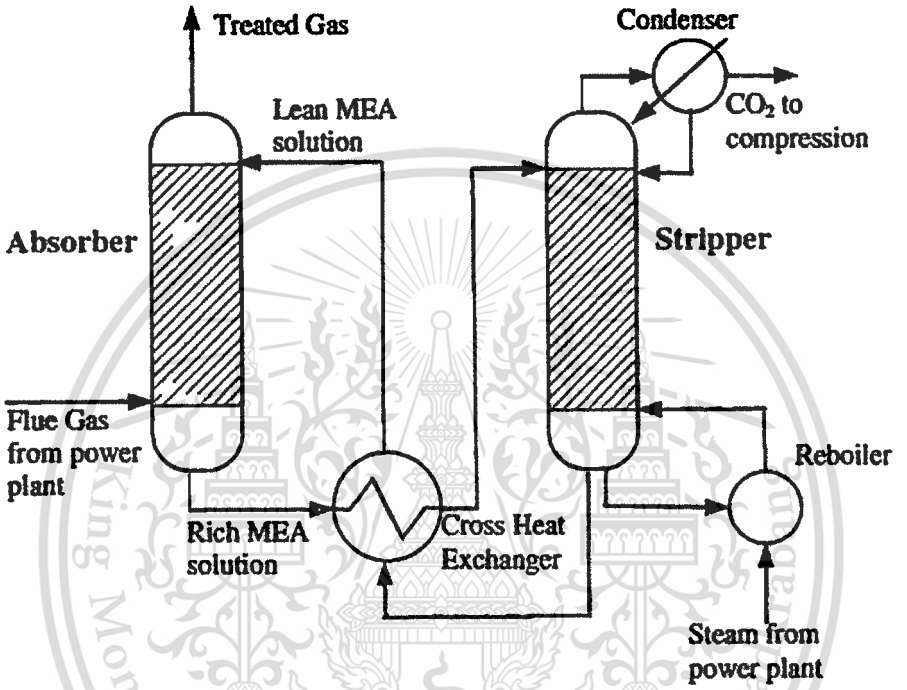

Figure 2.7 Simplified process flow diagram of chemical absorption process for post combustion capture (A. Lawal et al. 2009)

2.2.5.2 Chemical Absorption with Alkaline Salt Solutions

The processes employ an aqueous solution of salt containing sodium or potassium as the cation with an anion. There are many processes which have been developed on salts to absorb CO_2. The mechanisms of these processes require knowledge of the reaction path and rate as well as liquid phase physical properties.

The chemical reaction of absorbed carbon dioxide with alkaline carbonate solutions takes place through two parallel mechanisms: (1) direct formation of HCO_3^- by reaction of CO_2 with the hydroxyl ion and (2) reaction of CO_2 with water followed by dissociation of carbonic acid. According to Astarita et al. (1981), the predominant mechanism at pH > 10 involves the direct reaction of dissolved CO_2 with OH^-:

$$CO_2 + OH\text{-} = HCO_3^- \quad \text{(fast)} \tag{2.1}$$

$$HCO_3^- + OH^- = CO_3^{=} + H_2O \quad \text{(instantaneous)} \tag{2.2}$$

At pH < 8 the principal mechanism is based on the hydration of dissolved CO_2 to form carbonic acid followed by reaction of the carbonic acid with OH^-:

$$CO_2 + H_2O = H_2CO_3 \quad \text{(slow)} \tag{2.3}$$

$$H_2CO_3 + OH^- = HCO_3^- + H_2O \quad \text{(instantaneous)} \tag{2.4}$$

In the pH range of interest for commercial operations, pH > 8, the mechanism involving the direct reaction of carbon dioxide to form bicarbonate ions predominates (Astarita et al. 1981).

C. Fleischer et al. (1996) detailed the chemical absorption of carbon dioxide into an aqueous solution of sodium hydroxide in bubble column. At high sodium hydroxide concentration, the reaction is so fast that CO_2 bubbles are dissolved completely during their rise and a significant change of gas hold-up occurs over the reactor height.

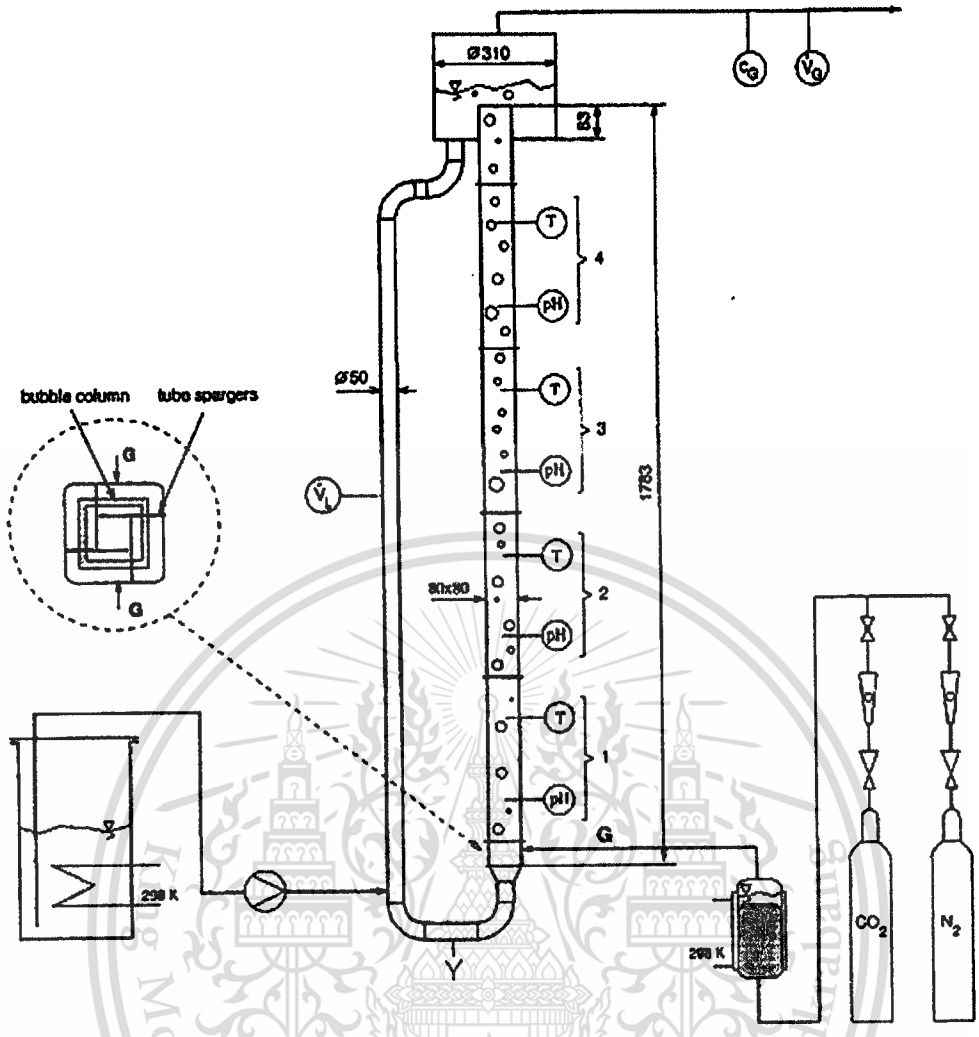

Figure 2.8 Experimental setup of the chemical absorption of CO_2 into NaOH. The bubble column can be operated with or without the external circulation loop (C. Fleischer et al. 1996)

In Figure 2.8, the reactor is operated in batch mode with respect to the liquid phase. The progress is measured by recording the temperature, the pH-value and the conductivity at different reactor heights. The hydrodynamic investigations of the bubble flow are limited to visual observation and measurement of the integral gas hold-up. The reaction gas has a purity of 99.99 %. The feed gas is saturated with water and kept at constant 25°C. The gas flow is controlled with a calibrated rotameter. In some experiments, nitrogen is added to the feed gas as an inert gas component. The effluent gas flow and its carbon dioxide concentration are measured continuously using a flow-meter and an IR gas analyzer.

The chemical absorption with salt solution has a simple plant design. The operation mechanism is similar to a water absorption. Salt solution is also cheap and has high

ability to absorb CO_2. In addition, research and development of this kind of technology is applied in the industrial field extensively.

2.3 Hydrogen production

Hydrogen is very rare in the Earth's atmosphere (1 ppm by volume) because of its light weight, which enables it to escape from Earth's gravity. However, hydrogen is still the third most abundant element on the Earth's crust (Argonne National Laboratory. 2003). Most of the Earth's hydrogen is in the form of chemical compounds such as hydrocarbons and water. Thus all hydrogen production processes are based on the separation of hydrogen from hydrogen-containing feedstock. The feed stock dictates the selection of the separation methods. In this chapter, two main methods are proposed to separate hydrogen from the feedstock, those of which are thermo-chemical and biological methods. The comparison of various hydrogen production technologies based on three main methods is summarized in Table 2.2.

Table 2.2 Current technology of hydrogen production

Process	Status of current technology	Efficiency (%)	Cost relative to SMR
Thermo-chemical process			
- Grid electrolysis of water	R&D	27	3-10
- High-temp. electrolysis of steam (100-800 °C)	R&D	41-61	-
- Methanol electrolysis	R&D	-	-
- Steam methane reforming (SMR)	Mature	70-80	1
- Partial oxidation of methane	Mature	70	1.8
Biological process			
- Photo-biological	Early R&D	<1	-

T-Raissi and Block. (2004)

From Table 2.2, the most interesting process is Steam Methane Reforming (SMR) because this technology is already mature in terms of research and development. Furthermore, it provides

the highest efficiency and the cheapest process when compared with others. However, the details and advantages of each process are described in the following section.

2.3.1 Thermo-chemical Method

2.3.1.1 Electrolysis process

Water electrolysis

This process produces high-purity hydrogen as high as 99.7% (Austin. 1984). The process can be performed by passing direct electric current through an aqueous solution of alkaline and decomposing the water to hydrogen and oxygen as shown in Figure 2.9. The involved reactions are indicated in Reactions (2.5) to (2.6).

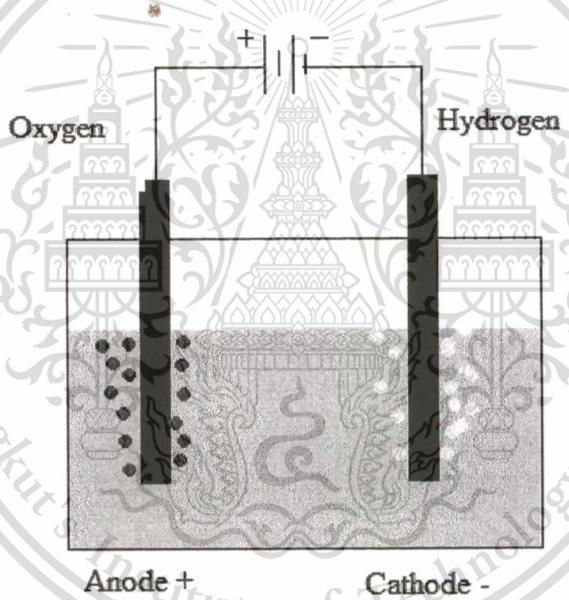

Figure 2.9 Basic configurations of water electrolysis

Cathode (reduction) $4H^{+}_{(aq)} + 4e^{-} \rightarrow 2H_{2(g)}$ (2.5)

Anode (oxidation) $2H_2O_{(l)} \rightarrow O_{2(g)} + 4H^{+}_{(aq)} + 4e^{-}$ (2.6)

Overall reaction $2H_2O_{(l)} \rightarrow 2H_{2(g)} + O_{2(g)}$ (2.7)

From Figure 2.9, the black dots are hydrogen bubble generated at the anode of the cell because molecules of water receive electron and decompose to hydrogen and hydroxide ion as indicated in Reaction (2.5). Generated oxygen is the white dot produced at the

cathode as indicated in Reaction (2.6). Water decomposes to proton, oxygen and gives off four electrons.

The water electrolysis process is divided into two types, low temperature and high temperature processes operating at 333-343 K and 373-1123 K, respectively. The efficiency of these processes are about 32% for low temperature (Austin. 1984), and 41-61 % for high temperature.

The advantage of water electrolysis is CO_2-free process because the reactant involves water only and it contains no carbon in its molecule. Unfortunately, the main disadvantage of this method is its low energy efficiency.

Methanol electrolysis

The major cost to produce hydrogen by water electrolysis method is electrical energy and oxygen produced from the process is not so valuable. An alternative way to reduce energy consumption in electrolytic process is to use methanol solution. The main reason is that an operating voltage of methanol electrolysis process is lower than water electrolysis process for about three times. It is about 0.3 volt for methanol and higher than 1.4 volt for water (Jeffries-Nakamura et al. 2002). The electrical energy used in methanol electrolysis is less than a half of water electrolysis in producing a given amount of hydrogen so the efficiency of methanol process is three times higher than the water electrolysis process (NASA Tech Briefs. 1999). A schematic diagram of an apparatus for methanol electrolysis process is shown in Figure 2.10 and corresponding reactions are indicated as follows:

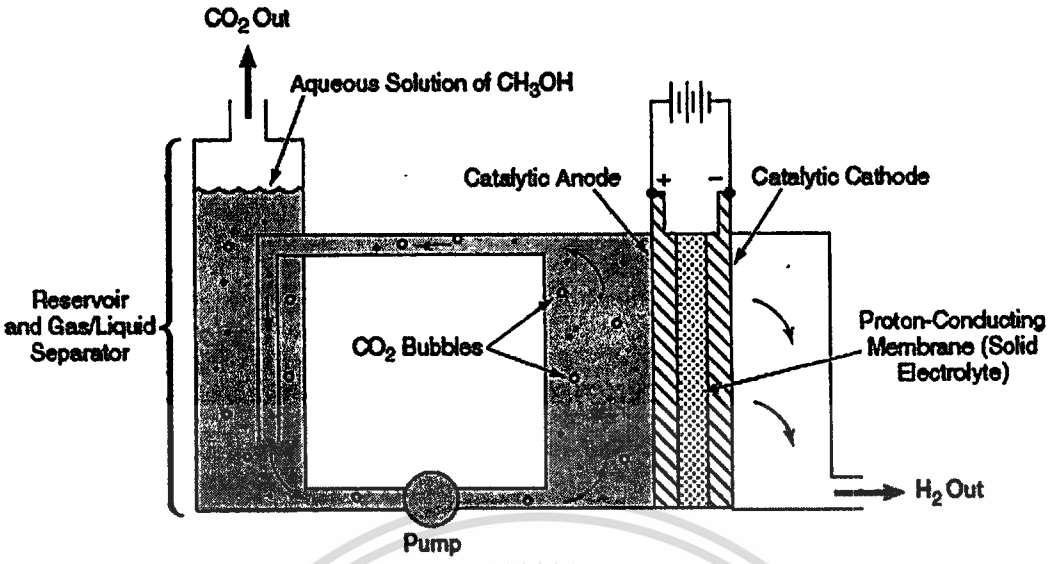

Figure 2.10 Schematic diagrams of methanol electrolysis apparatus (NASA Tech Briefs. 1999)

Anode $$CH_3OH + H_2O \rightarrow CO_2 + 6H^+ + 6e^- \quad (2.8)$$

Cathode $$6H^+ + 6e^- \rightarrow 3H_2 \quad (2.9)$$

Overall $$CH_3OH + H_2O \rightarrow CO_2 + 3H_2 \quad (2.10)$$

These reactions can be done at the temperature between 278 - 393 K. At the anode, methanol reacts with water to give off hydrogen ions and carbon dioxide, which can be further separated and purified to be a valuable product. The proton was conducted through the membrane to the cathode and combine with electron to give hydrogen.

In current technology, some of methanol and water are allowed to crossover the membrane from the side of solution to the side of hydrogen production (Jeffries - Nakamura et al. 2002). With this technology, methanol and water have to be removed to purify the produced hydrogen.

2.3.1.2 Steam Methane Reforming (SMR) process

Steam methane reforming converts methane to synthesis gas consisting mainly of CO and H_2. The conventional feed stocks for this process are natural gas or biogas. This is one of the most common methods for producing commercial bulk hydrogen as well as the hydrogen used in industrial synthesis of ammonia. It is the least expensive method (W. Crabtree et al. 2004). Steam reacts with methane to yield carbon monoxide and hydrogen as indicated in Reaction (2.11) (Hoang et al. 2005) at high temperature of 973–1373 K and in the presence of a nickel-based catalyst. Then, the water-gas shift reaction further takes place to convert CO into H_2 as indicated in Reaction (2.12). The Enthalpy changes as indicated in Reactions (2.11) to (2.13) were calculated at standard temperature of 298 K (Xu and Froment. 1989).

SMR	$CH_4 + H_2O \rightarrow CO + 3H_2$	$\Delta H = +206.1\ kJ/mol\ CH_4$	(2.11)
Water-gas shift	$CO + H_2O \rightarrow CO_2 + H_2$	$\Delta H = -41.15\ kJ/mol\ CO$	(2.12)
Overall	$CH_4 + 2H_2O \rightarrow CO_2 + 4H_2$	$\Delta H = +165.0\ kJ/mol\ CH_4$	(2.13)

From the heat of overall reaction as indicated in Reaction (2.13), the SMR reaction is an endothermic reaction. Then, this process requires extensive amount of heat from an external source to sustain the operating temperature of the reaction. To reduce the external heat requirement, a limited amount of oxygen is added to the steam methane reformer. Oxygen reacts with methane to yield CO, H_2O and heat. This reaction is called partial oxidation of methane. The process involves steam methane reforming and partial oxidation of methane are described in the next part.

2.3.1.3 Partial oxidation process or autothermal reforming

From an energy intensity process, SMR, the partial oxidation process is conducted to overcome external heat supplied by introducing limited amount of oxygen to methane and steam. A combustion of oxygen and some of methane in the reactor generates heat to supply SMR and water-gas shift reaction. Because of limited amount of oxygen, it reacts with methane yielding synthesis gas while carbon monoxide is converted to carbon dioxide and hydrogen by a water-gas shift reaction.

Total combustion $CH_4 + 2O_2 \rightarrow CO_2 + 2H_2O \quad \Delta H = -802\ kJ/mol\ CH_4$ (2.14)

Partial oxidation $CH_4 + \frac{1}{2}O_2 \rightarrow CO + 2H_2 \quad \Delta H = -36\ kJ/mol\ CH_4$ (2.15)

A large amount of heat produced by exothermic reactions (Equations (2.14) and (2.15)) is high enough to sustain the amount of heat consumed by endothermic reactions of SMR process (Equation (2.13)). The overall heat of reaction for SMR and partial oxidation reaction is still exothermic reaction then the excess heat can be recovered by preheating the feed stock. The drawback of this partial oxidation process is the lower yield of hydrogen as oxygen comes from air so hydrogen that comes out from this reactor is diluted with nitrogen.

The difference between partial oxidation process and auto-thermal process is that the partial oxidation (PO) uses oxygen to react with methane to achieve H_2 and CO. Catalytic partial oxidation (CPO) is used to permit partial combustion reaction which occur at lower temperature to produce synthesis gas. This process operates at low steam/carbon ratio (S/C from 0 to 1) and gives H_2/CO ratio in a range of 1.6 to 1 in the production of synthesis gas (Halabi et al. 2008). In contrast, auto-thermal reforming (ATR) uses a burner followed by a catalyst bed with methane, steam and oxygen to produce synthesis gas with higher H_2 to CO ratios of 2 to 1 and it operates at relatively higher steam load (S/C > 1).

2.3.2 Biological Hydrogen production process

The thermo-chemical process requires extensive amount of energy from fossil fuel to produce hydrogen. However, to make hydrogen fully renewable energy, it requires a method which does not require energy intensively to produce hydrogen. A biological method is the method that produces hydrogen by some types of anaerobic metabolism and is produced by several microorganisms, usually via reactions catalyzed by iron- or nickel-containing enzymes in the microorganisms. Most of this process can operate at room temperature and atmospheric pressure, therefore; it needs less energy than the thermo-chemical process. Furthermore, hydrogen production by biological method uses waste materials as a feedstock such as agricultural waste or waste water. From this method, it is a new option to produce hydrogen as a fully renewable energy.

The biological hydrogen production process can be classified into three mechanisms, first is the lighting process which occur by light and enzyme called hydrogenase, such as,

biophotolysis process of water by algae and cyanobacteria, or nitrogenase in photo-fermentation of organic substrate and water by photosynthesis bacteria. The second is the dark fermentation process. Hydrogen is produced without lighting. The third is a combined system between photosynthetic and fermentation of bacteria by separating the system into two stages. The first stage is fermentation by which organic waste is fermented to organic acid. The second stage is photolysis process to convert organic acid to hydrogen. An advantage of the combined system is a reduction of light energy demand in photolysis process but increasing in hydrogen production.

However, the disadvantage of the biological hydrogen production process is low efficiency, theoretically maximum hydrogen yield is up to 40%. However, in practice the efficiency is less than 10% (Esper et al. 2006).

From many kinds of hydrogen production technologies discussed above, the steam-methane reforming process is the cost effective process. It provides the highest efficiency and less complicated system than partial oxidation process. Therefore, the steam methane reforming process is an incentive technology to produce hydrogen where methane-containing gas is supplied such as natural gas and biogas.

In Thailand, biogas is more suitable fuel to power fuel cell than natural gas. The reason is that biogas is a renewable energy resource and it can be produced by anaerobic fermentation of agricultural waste such as cassava root and bagasse which are available in Thailand. The biogas mainly contains methane (~60%), carbon dioxide (~40%) and a trace amount of H_2S (~2000 ppm).

2.4 Fuel Cells

A fuel cell is an energy conversion device which converts a gaseous fuel to electricity and heat in the presence of an oxidant. Because fuel cells have high energy efficiency and are environmentally friendly, they are potentially attractive in producing electricity. Moreover, they can be operated in a flexible and modular design since they do not suffer appreciably from problems of lubrication, wear, leakage and heat loss, which affect the reliability of traditional heat engines (Hirschenhofer et al. 1998).

The fuel cell was invented in 1839 by Sir William Grove (Grove. 1839); however, the first real application was in the NASA space program on-board Apollo spacecraft in the 1960s when it was used to produce electricity and a by product as drinking water (UTC).

A fuel cell consists of an electrolyte sandwiched between two electrodes, called cathode and anode where the electrochemical reactions take place. The electro catalytic oxidation of hydrogen at the anode and the reduction of oxygen at the cathode create a potential difference between these electrodes. This can be exploited if a gas-tight electrolyte between the electrodes allows for ionic mass and charge transport. In an actual application, fuel cells are connected in series to obtain a greater output potential. An interconnect plate is always installed to provide the electronic contact between the anode of one cell to the cathode of the adjacent cell (Hirschenhofer et al. 1998).

Although the operational principles of a fuel cell are similar to those of a typical primary battery, they differ in several aspects. A battery is an energy storage device and the amount of energy available is determined by the amount of chemical reactant stored within the battery itself. The electrical energy produced decreases as the chemical reactant is consumed. A fuel cell, in contrast, can produce electrical energy continuously at a constant rate as long as the fuel and oxidant are supplied.

2.4.1 Types of Fuel Cells

Fuel cells are classified by the types of electrolyte. The characteristics of chemical reactions which occur in the fuel cell, the kind of catalysts required, the operating temperature range, the fuel and the oxidizing agent required, affect the applications for which these cells are most suitable. Some of the popular fuel cells and their characteristics are listed in Table 2.3.

Table 2.3 Types of fuel cells (Fuel cell handbook 4th ed.)

Fuel cell type	Electrolyte	Charge carrier	Operating temp.	Fuel	Electric efficiency	Application
AFC	KOH	OH^-	60 -120°C	Pure H_2	35-55%	<5kW military, space
PEMFC	Solid polymer	H^+	50 - 100°C	Pure H_2, tolerates CO_2	35-45%	5-250kW automotive, portable CHP
DMFC	Solid polymer	H^+	50 - 250°C	CH_3OH, C_2H_5OH,	35-45%	mobile application
PAFC	Phosphoric acid	H^+	~ 220°C	Pure H_2, tolerates CO_2	40%	200kW CHP
MCFC	Lithium and potassium carbonate	CO_3^{2-}	~ 650°C	H_2, CO, CH_4, tolerates CO_2	>50%	200kW-MW CHP and stand alone
SOFC	Yttria, stabilized Zirconia	O^{2-}	~ 1000°C	H_2, CO, CH_4, tolerates CO_2	>50%	2kW-MW CHP and stand alone

2.4.1.1 Alkaline Fuel Cells (AFCs)

An Alkaline fuel cell (AFC) is the first type used on spacecraft to produce electrical energy and water. The electrolyte is a solution of potassium hydroxide in water. A variety of non-precious metals can be used as a catalyst at both the anode and cathode. High-temperature AFC operates at temperatures between 100°C and 250°C. However, recent designs of AFC operate at lower temperatures of roughly 23°C to 70°C.

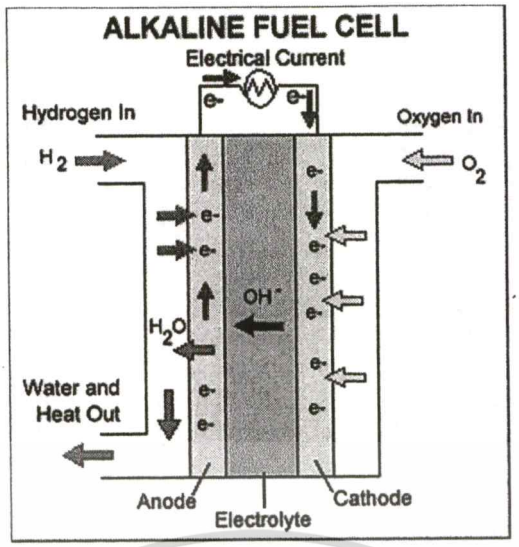

Figure 2.11 Alkaline fuel cell diagram (U.S. Department of Energy. 2008)

The chemical reactions which occur in the cell are responsible for high performance of AFC. They have also demonstrated efficiencies close to 60% in the space applications.

The disadvantage of this fuel cell type is that it is easily poisoned by carbon dioxide. In fact, even a small amount of CO_2 in air affect this cell operation, making it necessary to purify both hydrogen and oxygen used in the cell. This purification process is costly. Susceptibility to poisoning also affects the cell's lifetime, further adding to the cost.

Cost is less of a factor for remote locations, such as space or under the sea. However, to effectively compete in most mainstream commercial markets, these fuel cells will have to become more cost-effective. AFC stacks have been shown to maintain sufficiently stable operation for more than 8,000 operating hours. To be economically viable in large-scale utility applications, these fuel cells need to reach operating times exceeding 40,000 hours, something that has not yet been achieved due to material durability issues. This obstacle is possibly the most significant in commercializing this fuel cell technology.

2.4.1.2 Polymer Electrolyte Fuel Cell (PEFC)

Polymer electrolyte fuel cell or proton exchange membrane fuel cell (PEMFC) delivers a high-power density and offers advantages of low weight and volume, compared with other fuel cells. PEM fuel cells use a solid polymer as an electrolyte and porous carbon electrodes containing platinum catalyst. They need only hydrogen, oxygen from air, and

water to operate and do not require corrosive fluids like other fuel cells. They are typically fueled with pure hydrogen supplied from storage tanks or on-board reformers. For a system efficiency, a small 30 kW AC power plants will likely be 35% fuel to electricity efficient, 200 kW units 40% and large units 45% (Ben Wiens. 2008).

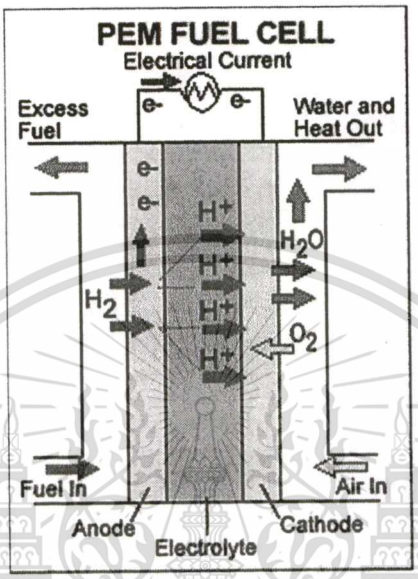

Figure 2.12 Polymer electrolyte membrane fuel cell (U.S. Department of Energy. 2008)

Polymer electrolyte fuel cells operate at relatively low temperatures, around 80°C. Low-temperature operation allows them to start quickly (less warm-up time) and results in less wear on system components, resulting in better durability. However, due to its operation at low temperature, it requires a noble-metal catalyst (typically platinum). The platinum catalyst is also extremely sensitive to carbon monoxide (CO) poisoning, making it necessary to employ an additional reactor to reduce CO in the fuel gas if hydrogen is derived from alcohol or hydrocarbon fuel. This also adds to cost. Developers are currently exploring platinum/ruthenium catalysts which are more resistant to CO.

PEMFCs are used primarily for transportation applications and some stationary applications. Due to their fast start-up time, low sensitivity to orientation, and favourable power-to-weight ratio, PEMFCs are particularly suitable for use in passenger vehicles, such as cars and buses.

A significant barrier in using these fuel cells in vehicles is hydrogen storage. Most fuel cell vehicles (FCVs) powered by pure hydrogen must store hydrogen on-board as a compressed gas in pressurized tanks. Due to the low-energy density of hydrogen, it is difficult to

store enough hydrogen on-board to allow vehicles to travel the same distance as gasoline-powered vehicles before refuelling, typically 300–400 miles. Higher-density liquid fuels, such as methanol, ethanol, natural gas, liquefied petroleum gas, and gasoline, can be used as a fuel, but the vehicles must have an on-board fuel processor to reform them to hydrogen. This requirement increases costs and maintenance. The reformer also releases carbon dioxide, though less than that emitted from current gasoline-powered engines.

2.4.1.3 Direct Methanol Fuel Cell (DMFC)

Most fuel cells are powered by hydrogen, which can be fed to the fuel cell system directly or can be generated within the fuel cell system by reforming hydrogen-rich fuels such as methanol, ethanol, and hydrocarbon fuels. However, direct methanol fuel cells are powered by pure methanol, which is mixed with steam and fed directly to the fuel cell anode.

Direct methanol fuel cells do not have many of the fuel storage problems typical of some fuel cells because methanol has a higher energy density than hydrogen though less than gasoline or diesel fuel. Methanol is also easier to be transported and supplied to public using our current infrastructure because it is liquid, like gasoline.

Direct methanol fuel cell technology is relatively new compared with other types of fuel cells powered by pure hydrogen.

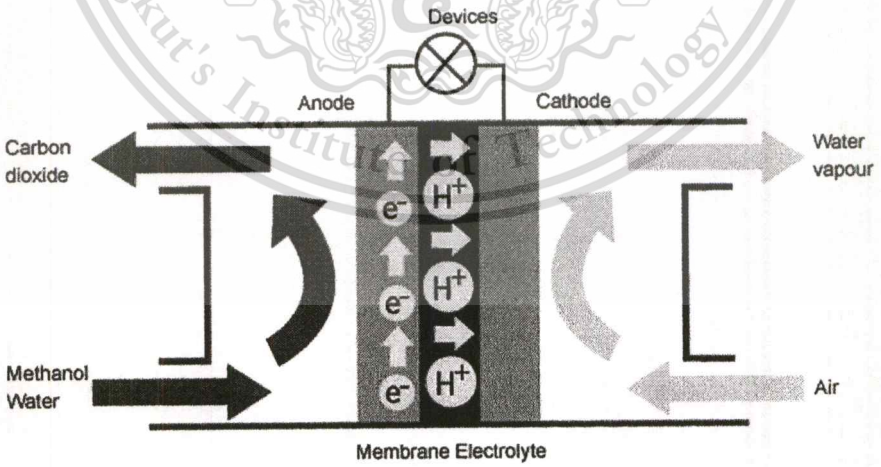

Figure 2.13 Direct methanol fuel cell (www.sfc.com 2009)

2.4.1.4 Phosphoric Acid Fuel Cell (PAFC)

Phosphoric acid fuel cells use phosphoric acid as an electrolyte, in which the acid is contained in a Teflon-bonded silicon carbide matrix, and porous carbon electrodes containing a platinum catalyst.

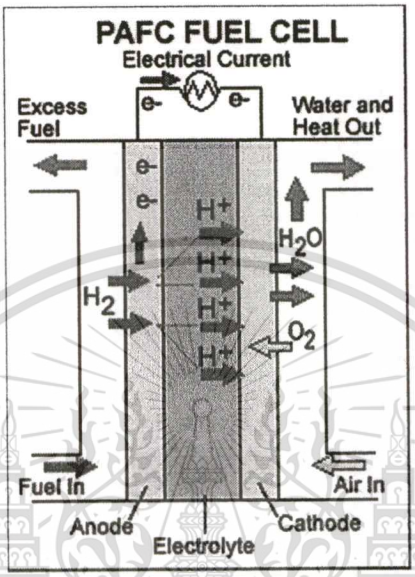

Figure 2.14 Phosphoric acid fuel cell (U.S. Department of Energy. 2008)

The phosphoric acid fuel cell (PAFC) is considered the "first generation" of modern fuel cells. This type of fuel cell is typically used for stationary power generation, but some PAFCs have been used to power large vehicles such as city buses.

PAFCs are more tolerant to impurities in fossil fuels that have been reformed to hydrogen than PEMFCs, which are easily "poisoned" by carbon monoxide because carbon monoxide binds to the platinum catalyst at the anode, hence decreasing the fuel cell's efficiency. They are 85% efficient when used for the co-generation of electricity and heat but less efficient when generating electricity alone (37%–42%). This is only slightly more efficient than combustion-based power plants, which is typically operated at 33%–35% efficiency. PAFCs are also less powerful than other fuel cells, given the same weight and volume. As a result, these fuel cells are typically large and heavy. PAFCs are also expensive. Like PEM fuel cells, PAFCs require an expensive platinum catalyst, which raises the cost of the fuel cell.

2.4.1.5 Molten Carbonate Fuel Cell (MCFC)

Molten carbonate fuel cells are currently being developed for natural gas and coal-based power plants for electric utility, industrial, and military applications. MCFCs are high-temperature fuel cells which use an electrolyte composed of a molten carbonate salt mixture suspended in a porous, chemically inert ceramic lithium aluminium oxide ($LiAlO_2$) matrix. Because they operate at extremely high temperatures of 650°C and above, non-precious metals can be used as catalysts at the anode and cathode, thus reducing the costs.

Improved efficiency is another reason why MCFCs offer significant cost reductions over phosphoric acid fuel cells. Molten carbonate fuel cells can reach efficiencies approaching 60%, considerably higher than the 37%–42% efficiencies of a phosphoric acid fuel cell plant. When the waste heat is captured and used, the overall fuel efficiencies can be as high as 85%.

Unlike alkaline, phosphoric acid, and polymer electrolyte fuel cells, MCFCs do not require an external reformer to convert more energy-dense fuels to hydrogen. Due to the high temperatures at which MCFCs operate, these fuels are converted to hydrogen within the fuel cell itself by a process called internal reforming, which also reduces cost.

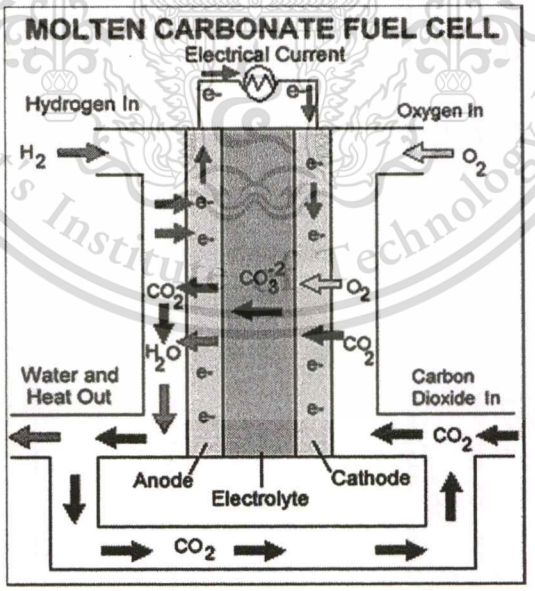

Figure 2.15 Molten carbonate fuel cell (U.S. Department of Energy. 2008)

Molten carbonate fuel cells are not prone to carbon monoxide or carbon dioxide poisoning, they can even use carbon monoxides as a fuel, making them more attractive

for fuelling with gases made from coal. Because they are more resistant to impurities than other fuel cell types, scientists believe that they could even be capable of internal reforming of coal, assuming they can be made resistant to impurities such as sulphur and particulates that result from converting coal, a dirtier fossil fuel source than many others, into hydrogen.

The primary disadvantage of current MCFC technology is durability. The high temperatures at which these cells operate and the corrosive electrolyte used accelerate component breakdown and corrosion, decreasing the cell life. Scientists are currently exploring corrosion-resistant materials for components as well as fuel cell designs which increase the cell life without decreasing the performance.

2.4.1.6 Solid Oxide Fuel Cell (SOFC)

Solid oxide fuel cells use a non-porous ceramic compound as the electrolyte. Because the electrolyte is solid, the cells do not have to be constructed in the plate-like configuration typical of other fuel cell types. SOFCs are expected to be around 50% - 60% efficient in converting fuel to electricity. In applications designed to capture and utilize the system's waste heat (co-generation), the overall fuel efficiencies could top 80%–85%.

SOFCs are also the most sulphur-resistant fuel cell type. They can tolerate several orders of magnitude of sulphur than other cell types. In addition, they are not poisoned by CO, which can even be used as a fuel (K. Sasaki. 2002 ; R. Suwanwarangkul. 2006) by using an internal reforming process. This property allows SOFCs to use gases from various hydrocarbon fuels such as natural gas, biogas, methanol and ethanol. However, these fuels must be reformed or gasified to produce synthesis gas mainly composing of H_2 and CO prior to entering an SOFC to increase the cell's efficiency.

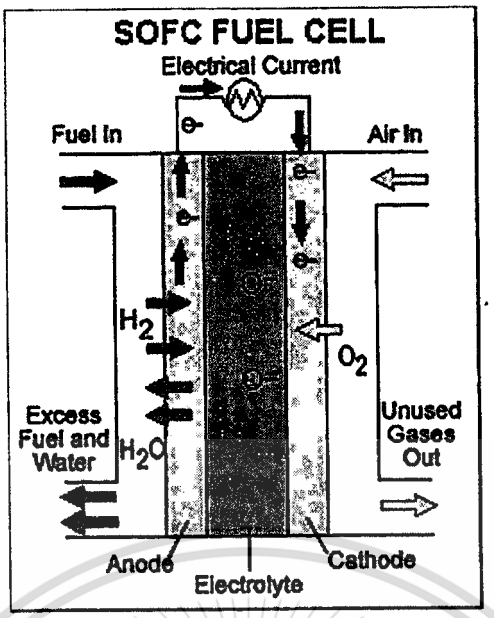

Figure 2.16 Solid oxide fuel cell (U.S. Department of Energy. 2008)

Solid oxide fuel cells operate at very high temperature around 1000°C. High-temperature operation removes the need for precious-metal catalyst, thereby reducing cost. It also allows SOFCs to reform fuels internally, which enables the use of a variety of fuels and reduces the cost associated with adding a reformer to the system. Another advantage of high operating temperature is some of high temperature waste gases can be fed back to the system.

High-temperature operation has disadvantages. It results in a slow start up and requires significant thermal shielding to maintain heat and protect personnel, which may be acceptable for utility applications but not for transportation and small portable applications. The high operating temperatures also place stringent durability requirements on materials. The development of low-cost materials with high durability at the cell operating temperatures is the key technical challenge facing this technology.

Researchers are currently exploring the potential for developing lower-temperature SOFC operating below 800°C which are more durable and less costly. However, a lower-temperature SOFC produces less electrical power.

2.5 SOFC System Model

S.H. Chan et al. (2002) studied on SOFC power system fed by hydrogen and methane. The simulation program developed consisted of two mathematical models which are H_2-fed and CH_4-fed SOFC system. They were written in Visual Basic. The H_2-fed SOFC system is comprised of two pre-heaters, a SOFC stack and an afterburner as shown in Figure 2.17. The CH_4-fed SOFC system incorporated a mixer, a vaporizer, two pre-heaters, an external reformer, a SOFC stack and an afterburner as shown in Figure 2.18.

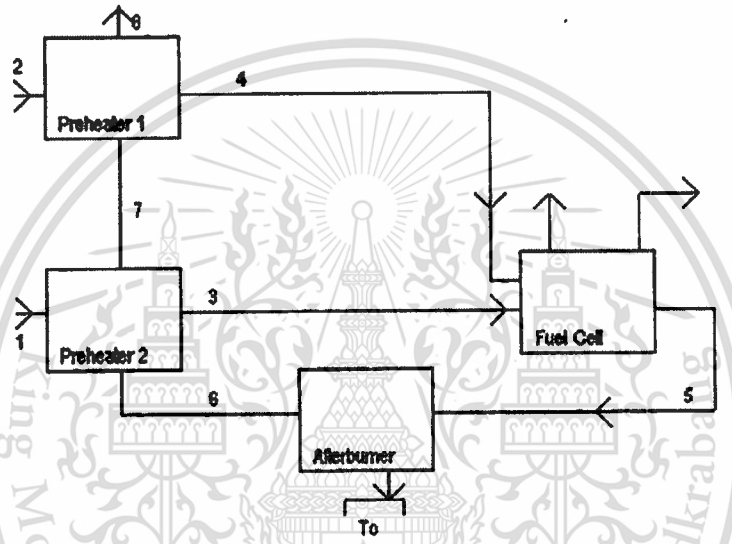

Figure 2.17 H_2-fed fuel cell system (S.H. Chan et al. 2002)

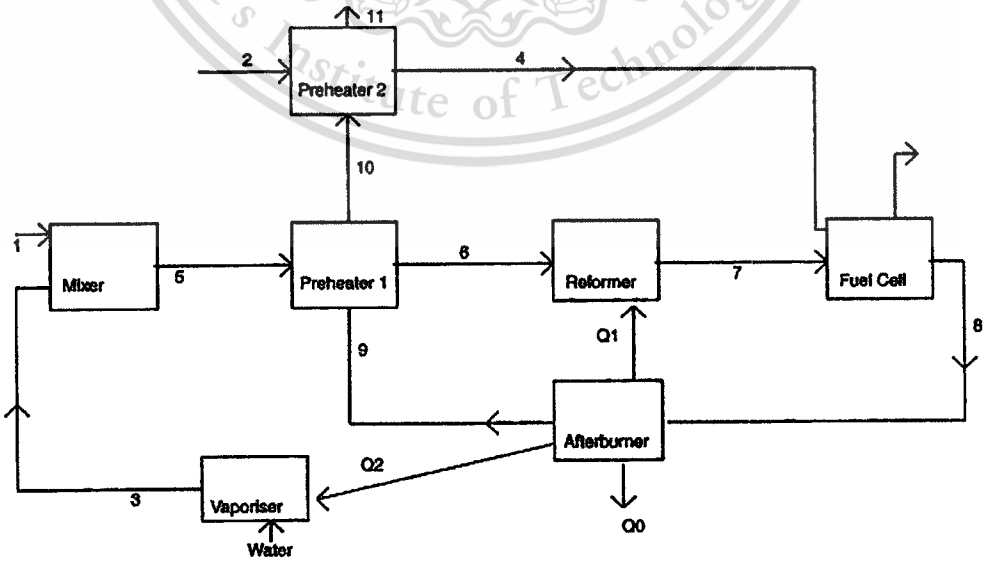

Figure 2.18 CH_4-fed fuel cell system (S.H. Chan et al. 2002)

This system based on thermodynamic modelling of the SOFC by analysis of the energy and exergy of the SOFC power system as shown in Equation (2.16). This study focused on physical and chemical exergies Equation (2.17) where subscript n refers to the state points of a system, " ° " refers to environment condition, H is the enthalpy, and S the entropy.

$$Exergy = E_{kinetic} + E_{potential} + E_{physical} + E_{chemical} \quad (2.16)$$

$$E_{physical} = E_{chemical} = (H_n - H^o) - T_o(S_n - S^o) \quad (2.17)$$

The electrochemical model considers the effect on the SOFC performance associated with heat loss and electrical energy output of the SOFC stack. The heat exchanger model was used to model the preheaters in fuel cell systems.

The simulation results showed the efficiency of H_2-fed system is 50.97 and 52.28% of the first and second law, respectively. For the CH_4-fed system are 62.19 and 59.96%. The waste heat was recovered for pre-heating the fuel and air in both system.

J. Van herle et al. (2003) studied on a small cogeneration system based on a SOFC fed on biogas. The model of this system based on the energy balance analysis. A diagram in Figure 2.19 shows the process flow model, Q represented exchanged heating power and W represent mechanical or electrical power. The composition of biogas is 60%CH_4 and 40%CO_2 by volume mixed with air in a 1:1 ratio for the partial oxidation reforming (POX).

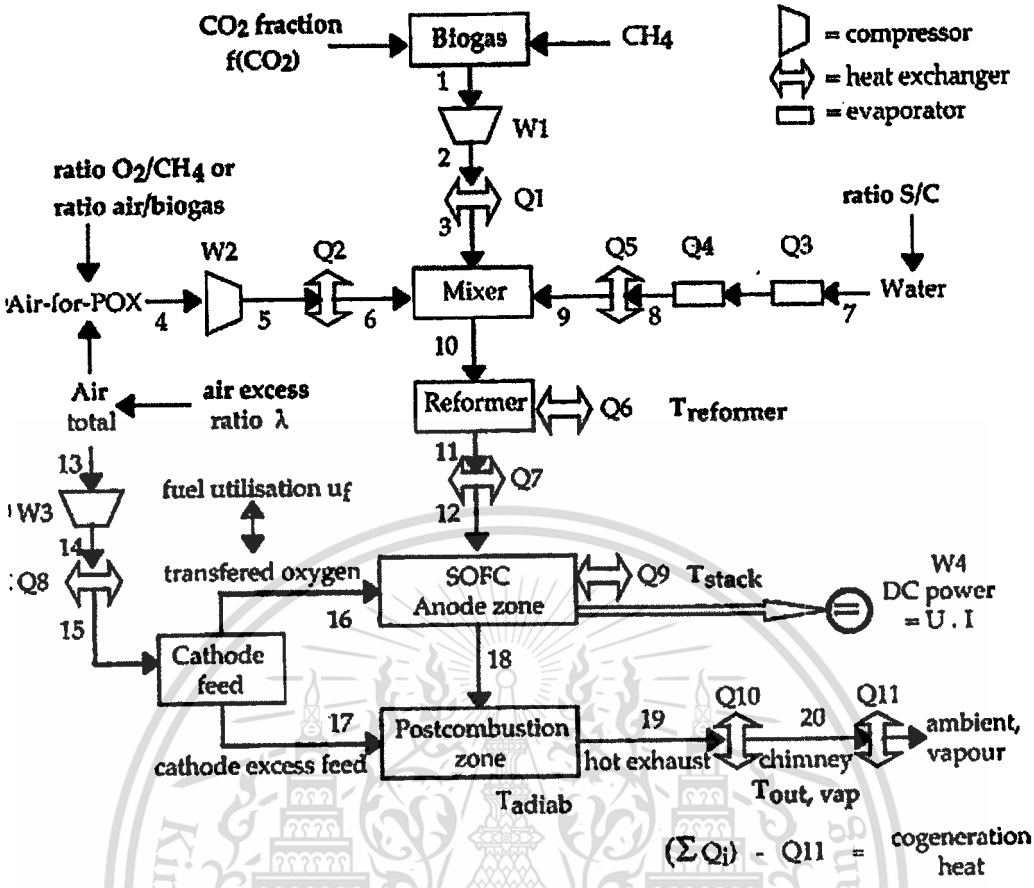

Figure 2.19 Process flow diagram of the considered SOFC system fed on biogas mixtures (J. Van herle et al. 2003)

A model stack was calculated to deliver 3.1 kW electrical and 5.16 kW thermal from an input of 8.95 kW LHV of biogas. The efficiency of this system is 33.8% and 57.6% electrical and cogeneration thermal efficiency, respectively.

J. Van herle et al. (2004) modelled a 100 kW SOFC system running on sewage biogas. Real data of sewage biogas adopted into the model. Biogas composition is 63%CH_4, 35%CO_2, 0.5%air and 1.5%H_2O. This system is comprised of reformer, SOFC stack and afterburner as shown in Figure 2.20. It is similar to J. Van herle et al.'s previous work.

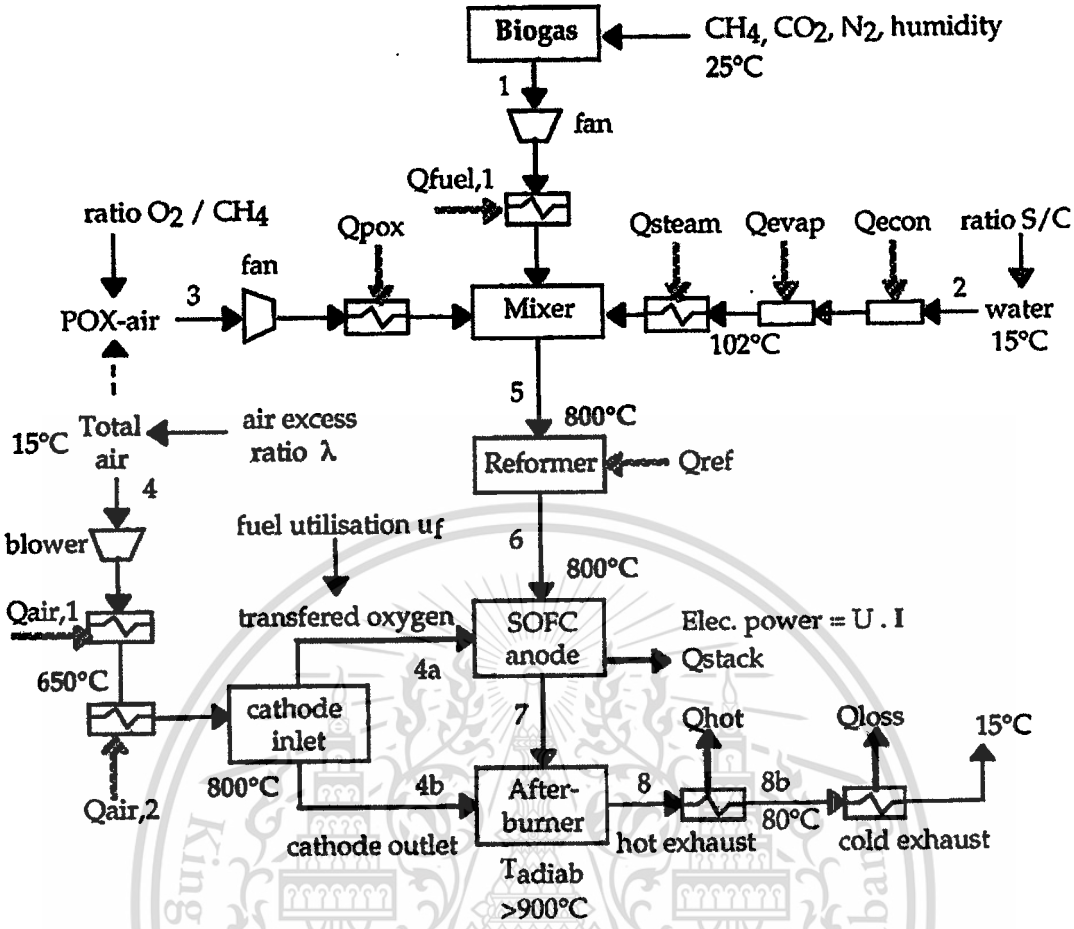

Figure 2.20 Process flow diagram of a solid oxide fuel cell system fed with sewage biogas (J. Van herle et al. 2004)

This study concerns with the investigation on input parameters selection of reforming condition (S/C ratio) and air excess ratio. The minimum steam quantity required and can be determined form thermodynamic equilibrium concentration calculation as shown in Figure 2.21.

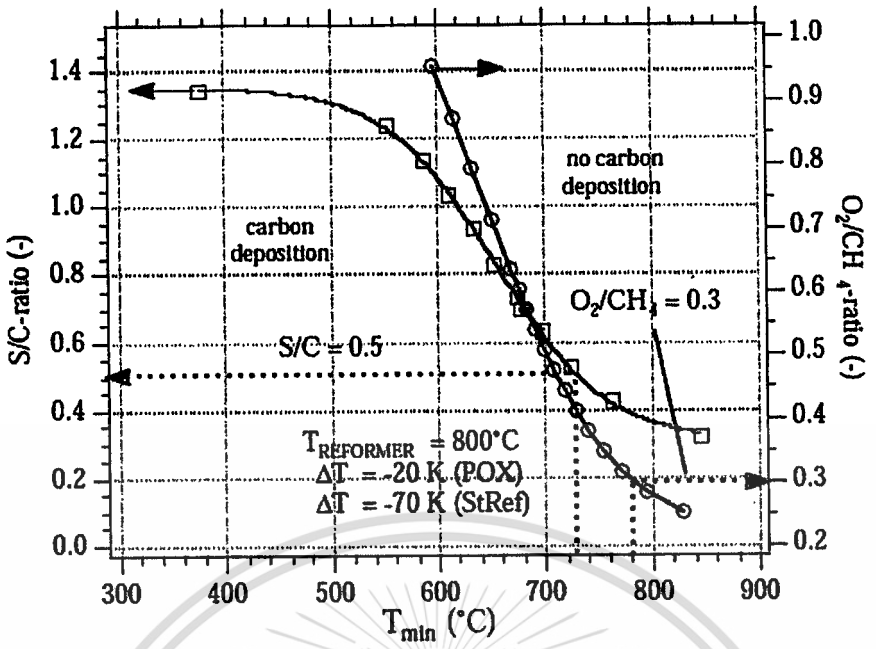

Figure 2.21 Minimal temperature and corresponding required ratios of steam-to-carbon (S/C) and oxygen-to-methane (O_2/CH_4) above which no carbon deposition takes place thermodynamically (J. Van herle et al. 2004)

At 800°C, the minimal S/C ratio is 0.37. Thus, the safety factor of S/C ratio is chosen at 0.5. From the input of biogas (63%CH_4) is equivalent to 269 kW (HHV). The electrical output of the SOFC was calculated to 131 kW (48%) using S/C ratio = 0.5.

P. Piroonlerkgul et al. (2008) studied on the fuel processor appropriation for biogas-fuelled SOFC system which is air-fed, steam-fed and co-fed SOFC as shown in Figures 2.22-2.24. Biogas was fed at different biogas compositions. Main reaction on reforming reaction is dry reforming. Steam was added for steam reforming on stem-fed SOFC system. Air was fed along with biogas for partial oxidation. The power density and electrical efficiency was investigated. The open circuit voltage (E) can be calculated from the Nernst equation as following in Equation (2.18).

$$E = E^0 + \frac{RT}{2F}\ln\left(\frac{P_{H_2}P_{O_2}^{1/2}}{P_{H_2O}}\right) \tag{2.18}$$

The actual cell potential (V) is calculated from Equation (2.19). The loss of cell can be consisted of ohmic loss (η_{act}), activation loss (η_{ohmic}) and concentration loss (η_{conc}).

$$V = E - \eta_{act} - \eta_{ohmic} - \eta_{conc} \tag{2.19}$$

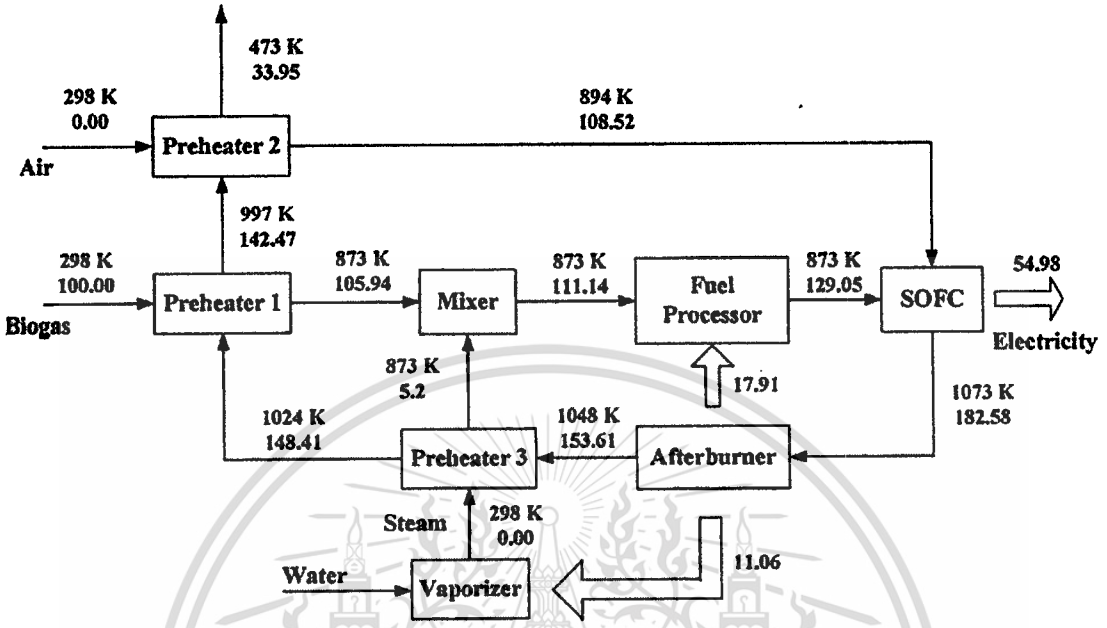

Figure 2.22 The plant configuration and energy balance for the steam-fed SOFC system (P. Piroonlerkgul et al. 2008)

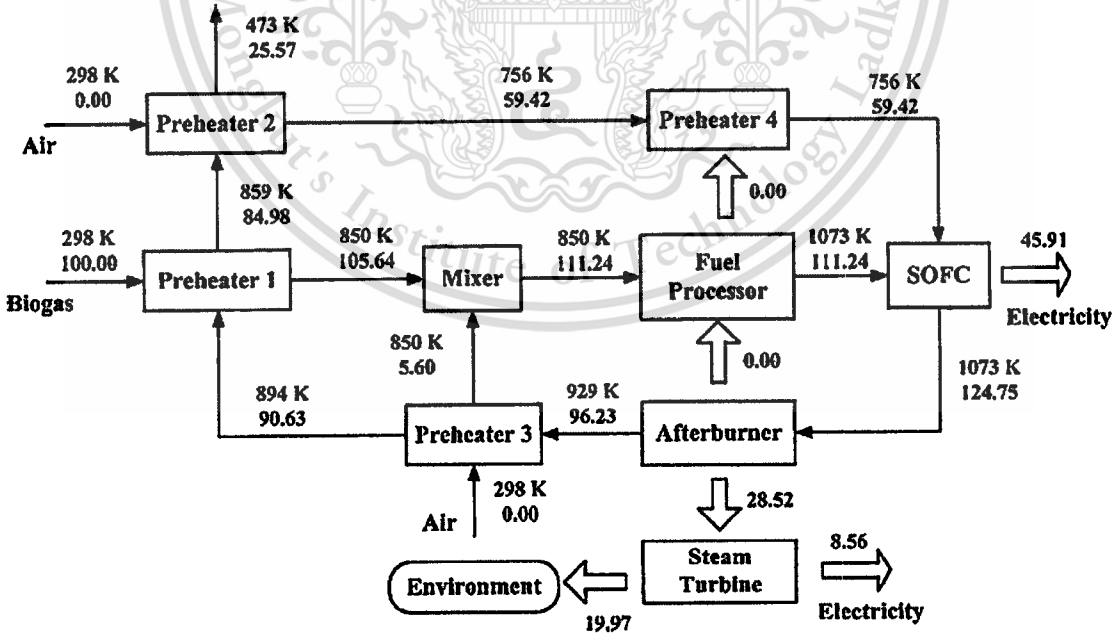

Figure 2.23 The plant configuration and energy balance for the air-fed SOFC system (P. Piroonlerkgul et al. 2008)

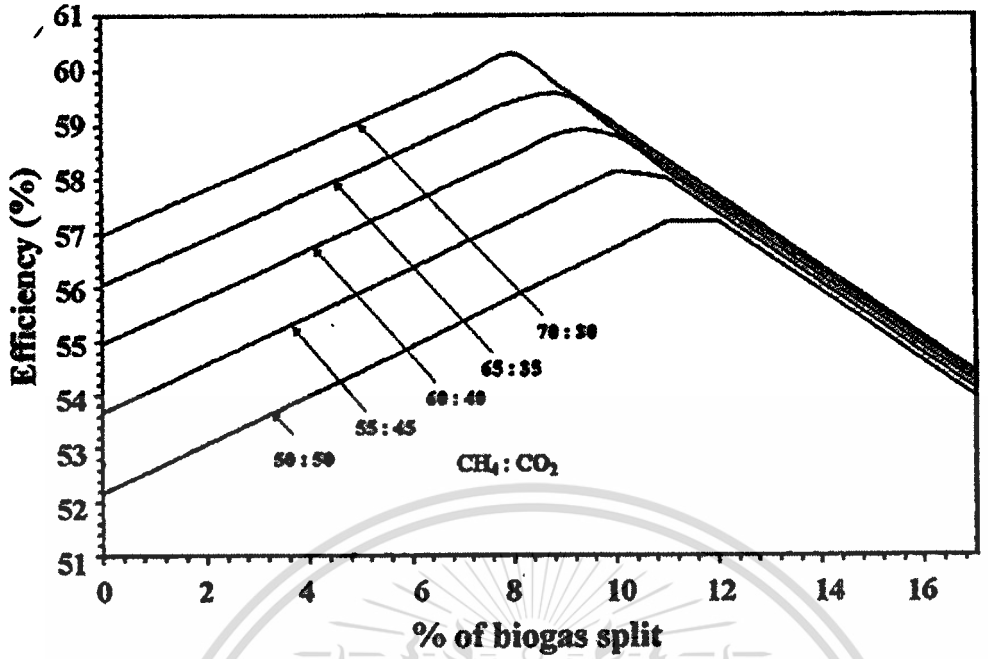

Figure 2.25 The effect of %biogas split on overall electrical efficiency (P. Piroonlerkgul et al. 2008)

Those works use SOFC type to run biogas because of ability to tolerate fuel contaminants. The studies on the SOFC system are based on thermodynamic. The SOFC performance associated with heat loss and electrical energy output of the SOFC. Previously, J. Van herle et al. worked on the partial oxidation for fuel processor and then changed to steam methane reforming which apply to use in the experimental. Results of P. Piroonlerkgul et al. (2008) prefer steam methane reforming because it offers high power density.

From literatures, the SOFC system normally has afterburner attached with the heat exchanger and preheater. They cloud achieve higher performance and reduced heat losses which occur in the SOFC system. Our study on the mathematical modelling of the solid oxide fuel cell by using biogas does not have an afterburner. Thus, the overall SOFC system may loss most performance to heat loss.

CHAPTER 3

EXPERIMENTAL PROCEDURES AND RESULTS

The SOFC system mainly comprise of CO_2 absorption unit, reformer for hydrogen production and SOFC stack as shown in Figure 3.1. This study has investigated the mass and energy conservation of SOFC system by using a computer program for developing an empirical modelling of the sub-units of the SOFC system.

A primary fuel for the SOFC system is biogas. In the first unit, CO_2 removal is carried out using NaOH solution for a chemical absorption process to remove CO_2 form biogas. Thus, it still remains methane only. CO_2 absorption experimental has been investigated at various $\%CO_2/CH_4$ by vol. at the inlet of CO_2 removal. Then, the experimental data and results were supplied into the computer program to model the mass and energy input and output of this unit.

The next unit is a reformer unit. It is used for hydrogen production to convert methane to hydrogen to supply as fuel to the SOFC. Methane and steam react on the steam methane reforming process. The empirical model of the reformer is investigated on hydrogen production which depends on the operation temperature at 650°C – 850°C. Heat is supplied by furnace using LPG as the combustion fuel. At the outlet of reformer unit, the product gases need to cool down to room temperature before feeding into the SOFC.

The last major unit, the SOFC operates at 920°C. On the experimental, it is supplied with hydrogen as a fuel at various flow rates to investigate the power output at different current-voltage drop of 1 kW electrical output of SOFC.

The energy conservation for all sub-unit are determined whether they worthwhile or not for the SOFC system using biogas.

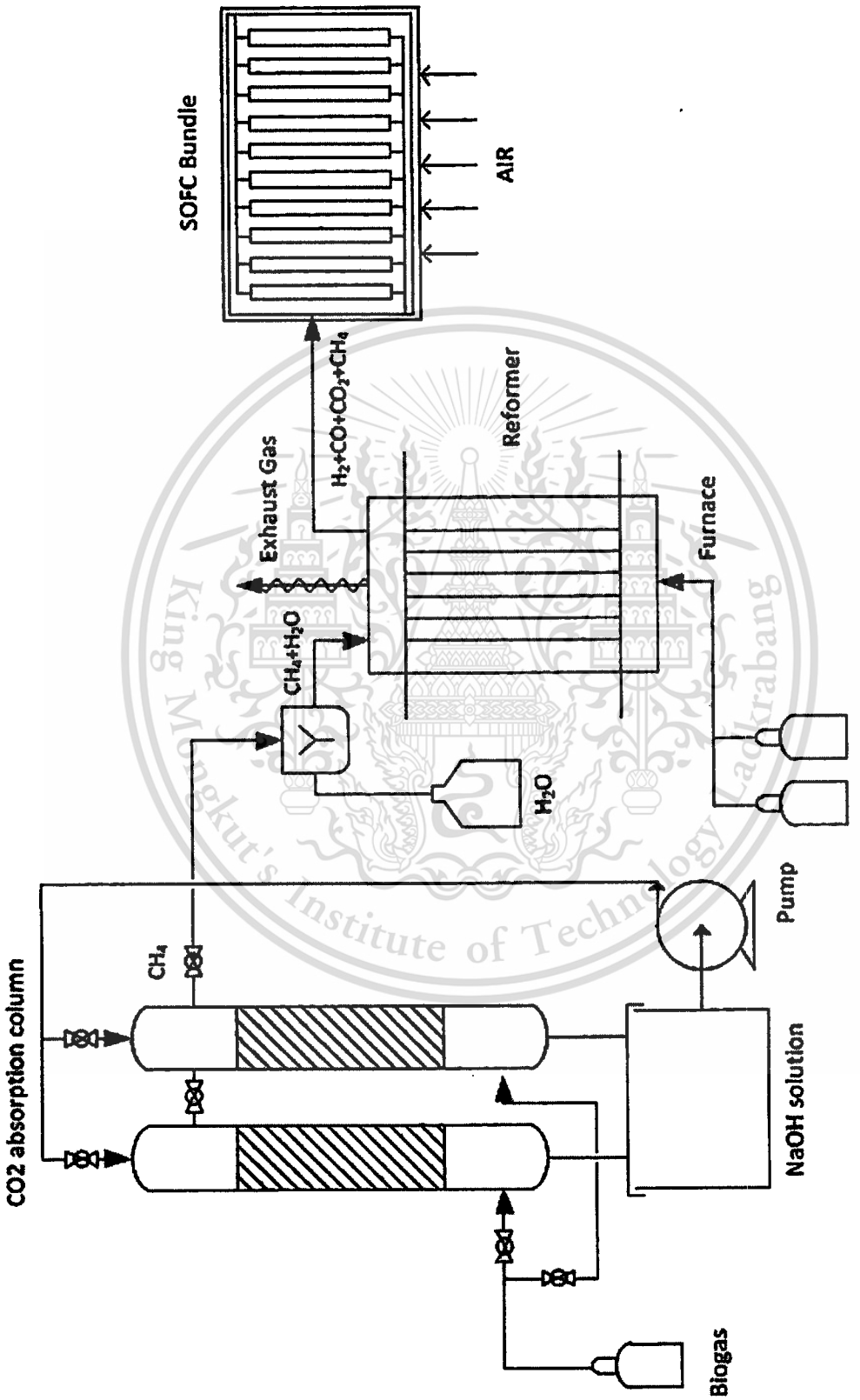

Figure 3.1 The SOFC system diagram

3.1 CO_2 Removal

The first unit of the SOFC system is CO_2 removal. It is a fuel processing to treat biogas by removing CO_2. In this study, it is focused on the chemical absorption by using sodium hydroxide (NaOH) solution. This solution is a kind of aqueous solution. It is convenient and cheap to use in a pilot scale. Basic chemical reaction of CO_2 and aqueous salt solution is represented by the following reaction.

$$CO_{2(g)} + OH^-_{(aq)} \rightarrow HCO^-_{(aq)} \quad (3.1)$$

$$HCO^-_{(aq)} + OH^-_{(aq)} \rightarrow CO^{2-}_{3(aq)} + H_2O_{(l)} \quad (3.2)$$

$$2Na^+_{(aq)} + CO^{2-}_{3(aq)} \rightarrow Na_2CO_{3(aq)} \quad (3.3)$$

Overall $CO_{2(g)} + 2NaOH_{(aq)} \rightarrow Na_2CO_{3(aq)} + H_2O_{(l)} \quad \Delta H = -107.52\ kJ/mol\ CO_2$ (3.4)

Products of the absorption reaction are disodium carbonate (Na_2CO_3) and water (H_2O). This is exothermic reaction which releases thermal energy. Heat absorption usually takes place at about 55 °C.

3.1.1 CO_2 Absorption Unit

The CO_2 absorption unit diagram is shown in Figure 3.2. The absorption column is 4 inch in diameter packed with raschig ring packing of 1.5 m high to increase the surface area of gas-liquid contact. The absorption column is designed for a counter flow pattern. At the top of the column locates a spray nozzle to spray solution into the column. NaOH solution tank supplies and receives absorbed solution in the experiment. Gas and liquid flow rates are calibrated using air and liquid rotameters. The CO_2 analysis is carried out using a gas chromatography (GC) which measures the CO_2 concentration from collected gas.

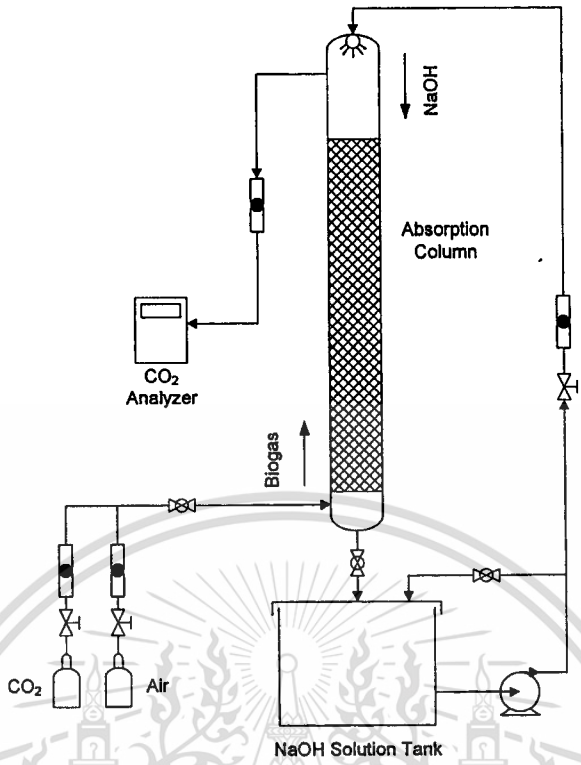

Figure 3.2 CO_2 Absorption unit

3.1.2 Experimental Procedure

The experiment setup is shown in Table 3.1. This experiment used synthesis gas between CO_2 and air as a simulated biogas. Various concentrations of the mixed gas can be quantified using a GC. Then, each gas flow was adjusted at 10 l/min to mix in the line to be 20 l/min and to flow into the column as shown in Figure 3.2. The mixed gas was left blending for 15 minutes. For aqueous solution, 6000 gram of NaOH is prepared with 50 litres of water to obtain 3 molar concentrations. The solution is pumped up to the top of the column at 10 l/min and sprayed into the column. Mixed gas and NaOH solution are flown in the opposite directions. A chemical reaction between CO_2 and aqueous salt solution occurs in the packed bed column. After the solution is used in the reaction, it flows back to the NaOH solution tank and is circulated until the concentration of NaOH solution decrease to the level that cannot absorb CO_2 anymore.

The experimental product gases obtained from the reaction are collected every 15 minutes and analysed using a GC to identify the concentration of gas compositions until CO_2 can be detected. The pH of the aqueous solution was checked using a pH paper. Before starting the experiment, the pH is 14. If CO_2 occurs in the product gas, the pH of the solution is changed.

Table 3.1 Experimental condition of CO_2 removal

Case	Gas			Aqueous (NaOH)		
	CO_2 Inlet (% by volume)	Flow rate (l/min)	Inlet pressure (Bar)	Concentration (M)	Volume (l)	Flow rate (l/min)
1	**45**	20	1.0	3	50	10
2	**55**	20	1.0	3	50	10
3	**60**	20	1.0	3	50	10
4	**70**	20	1.0	3	50	10

The results from the experimental are shown in Figures 3.3-3.6. They showed the details of the absorption duration in various concentrations of CO_2 at the inlet and the pH value. The absorption duration is counted from the beginning until the last point of 0%by vol. of CO_2 concentration at the outlet.

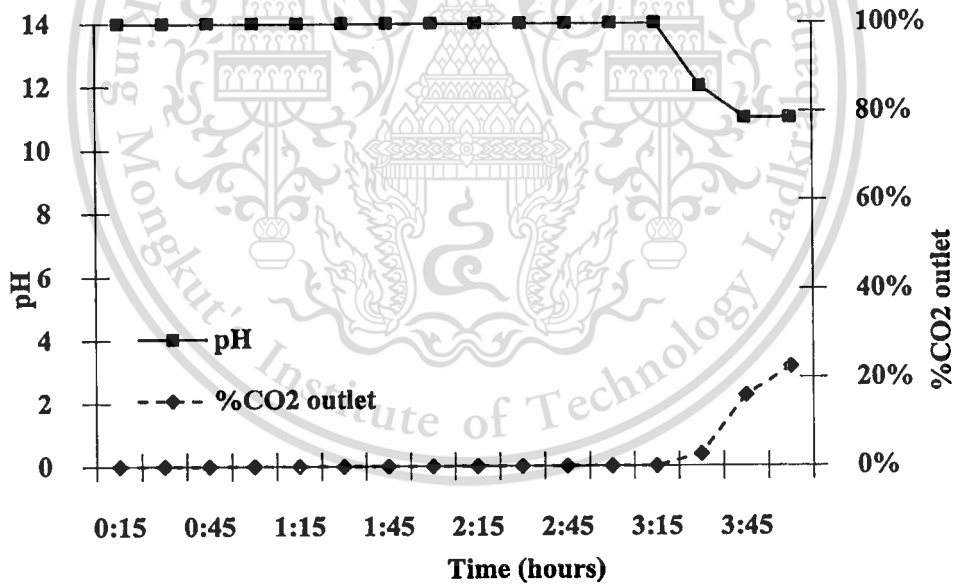

Figure 3.3 Relationship between CO_2 at the outlet and pH with time at 45%CO_2 by vol.

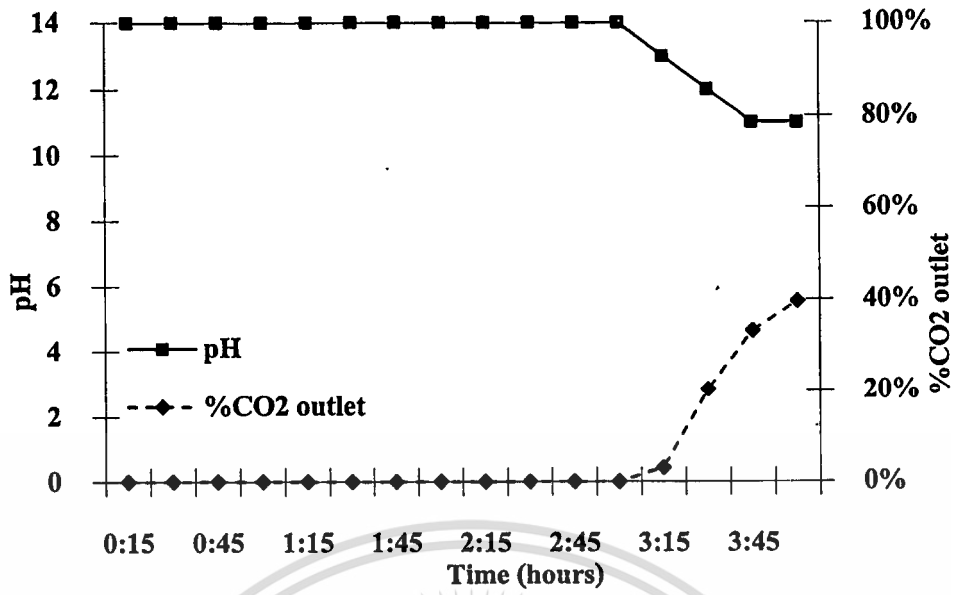

Figure 3.4 Relationship between CO_2 at the outlet and pH with time at 55%CO_2 by vol.

As shown in Figures 3.3-3.6, the %CO_2 by vol. at the outlet and pH value is changed in the same characteristic. While GC detected CO_2 at the outlet, pH indicator which checks on the NaOH solution was changed too.

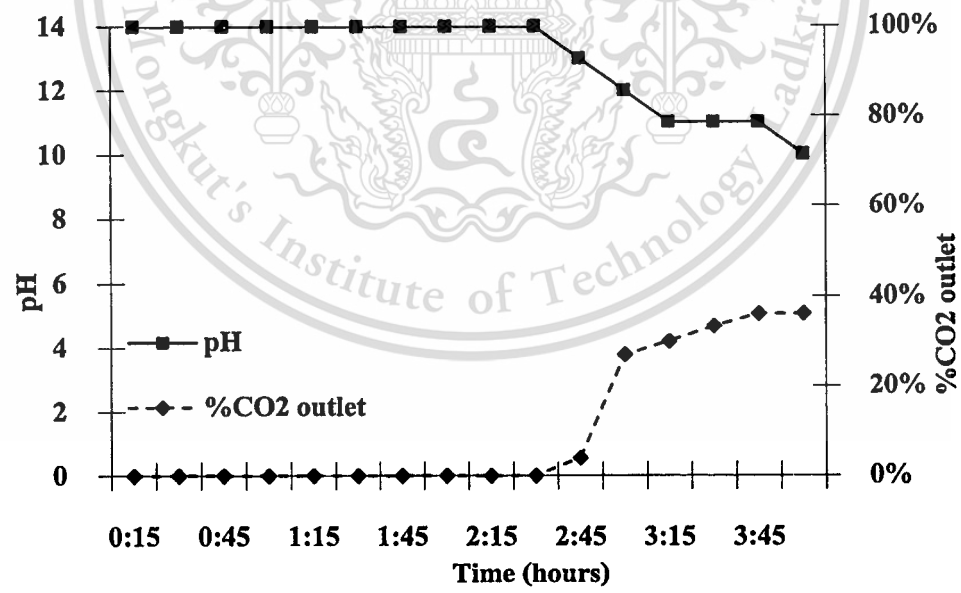

Figure 3.5 Relationship between CO_2 at the outlet and pH with time at 60%CO_2 by vol.

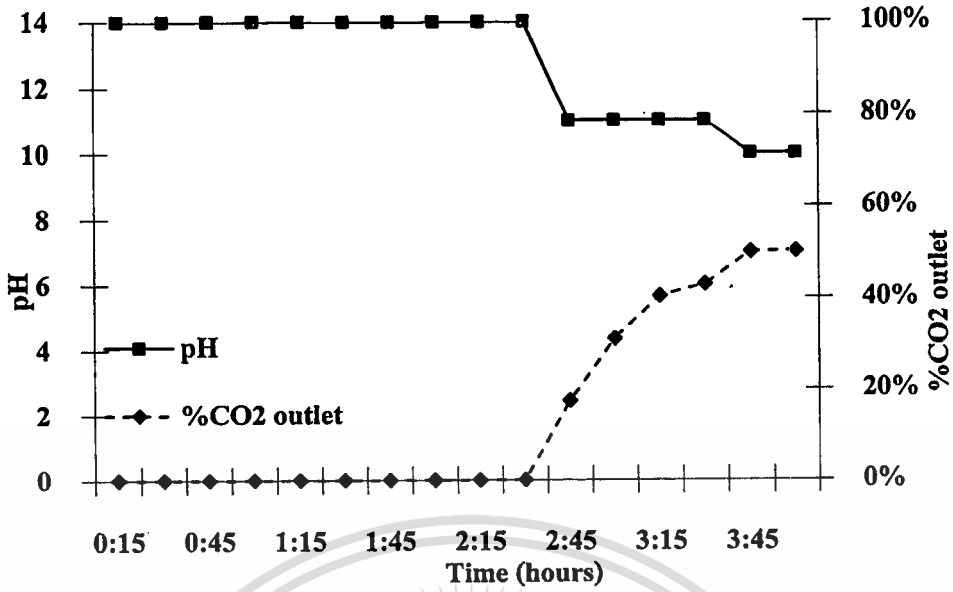

Figure 3.6 Relationship between CO_2 at the outlet and pH with time at 70%CO_2 by vol.

From the experimental, the study of CO_2 absorption is applied to develop the mathematical model in the next topic.

3.1.3 Mathematical Model of CO_2 Removal

Computer program, MATLAB Simulink is used to model mathematical of CO_2 removal model. In this model energy and mass balance are focused. There are 2 parts in CO_2 removal model which are CO_2 removal itself and NaOH solution pump. On the CO_2 removal, beside the mass balance of the chemical absorption reaction, it looks for the consumption of NaOH solution which reacts with CO_2. On the solution pump model, it is the power input model in which the pump consumes energy to pump up the solution into the absorption column.

To model CO_2 removal, the data which bring to use is in various %CO_2 by vol. of biogas test results as shown in Figures 3.3-3.6. The conditions of the operation are 45 – 70% CO_2 by vol. at the inlet and 3 Molar of NaOH. This result is modelled for the consumption of NaOH relating with %CO_2 by vol. of biogas, %CO_2 by vol. at the outlet and time. The assumptions of this empirical model are;

- only methane output from the CO_2 removal
- ideal gas condition
- negligible pressure drop

From the assumption, we can determine the mass flow rate of CH_4 from mass balance of biogas as given in Equation (3.5).

$$\dot{m}_{biogas} = \dot{m}_{CH_4} + \dot{m}_{CO_2} \tag{3.5}$$

The NaOH consumption (kg/day) at 3 Molar of solution can be calculated by following equation.

$$\mathrm{NaOH}_{consump} = \frac{m_{NaOH}}{t_{CO_2}} \times 1440\left(\mathrm{min}/_{day}\right) \tag{3.6}$$

The heat of reaction in a chemical reaction given in Reaction (3.4) can calculated the power input of CO_2 absorption as given in Equation (3.7).

$$\dot{Q}_{chem} = -107.52\ \mathrm{kJ/mol}CO_2 \times \dot{n}_{CO_2} \tag{3.7}$$

The CO_2 removal unit has a power input to NaOH solution pump. The work of the pump depends on NaOH solution volume flow rate as shown in Figure 3.7 which measures the current-voltage drop from the experimental.

$$\dot{W}_{pump} = IV \tag{3.8}$$

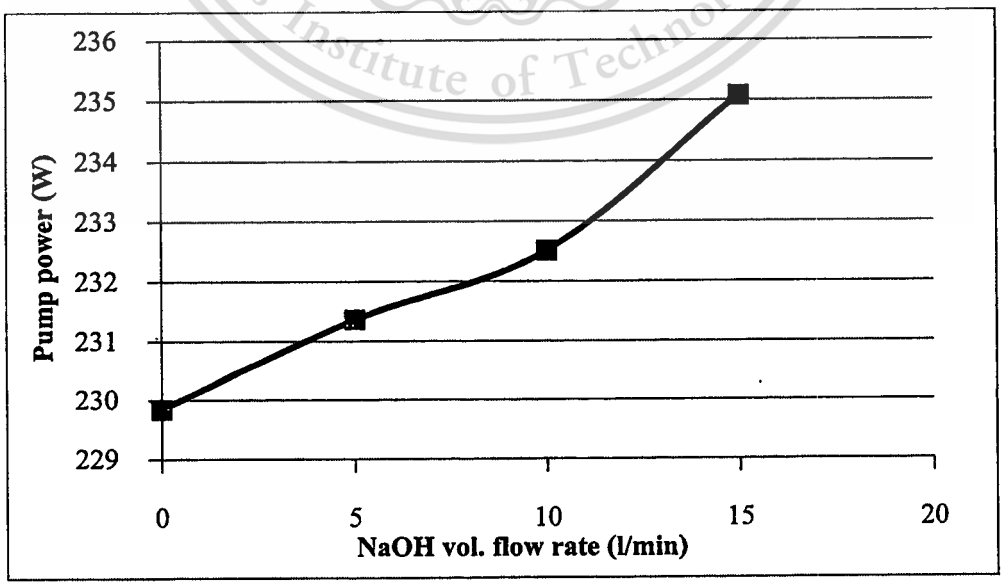

Figure 3.7 Relationship between NaOH volume flow rate and pump power

3.2 Reformer Unit

A reformer is a unit which produce hydrogen from the steam methane reforming (SMR) process. In this study, the model of the reformer supplied heat energy for the operation using a furnace by heat transfer principle. Thus, the reformer unit can be separated into two parts which are furnace and reforming reaction.

3.2.1 Furnace

The furnace is based on the fuel combustion which uses LPG as a fuel. This furnace is a kind of porous burner which is packed with 25 mm spherical alumina (Al_2O_3). The furnace is 220 mm in diameter and 600 mm high. The air input has 3 stages which are 1st air stage feeding air at the bottom of furnace, 2nd air stage feeding air at 50 mm from the bottom and 3rd air stage feeding air at 300 mm from the bottom as shown in Figure 3.8.

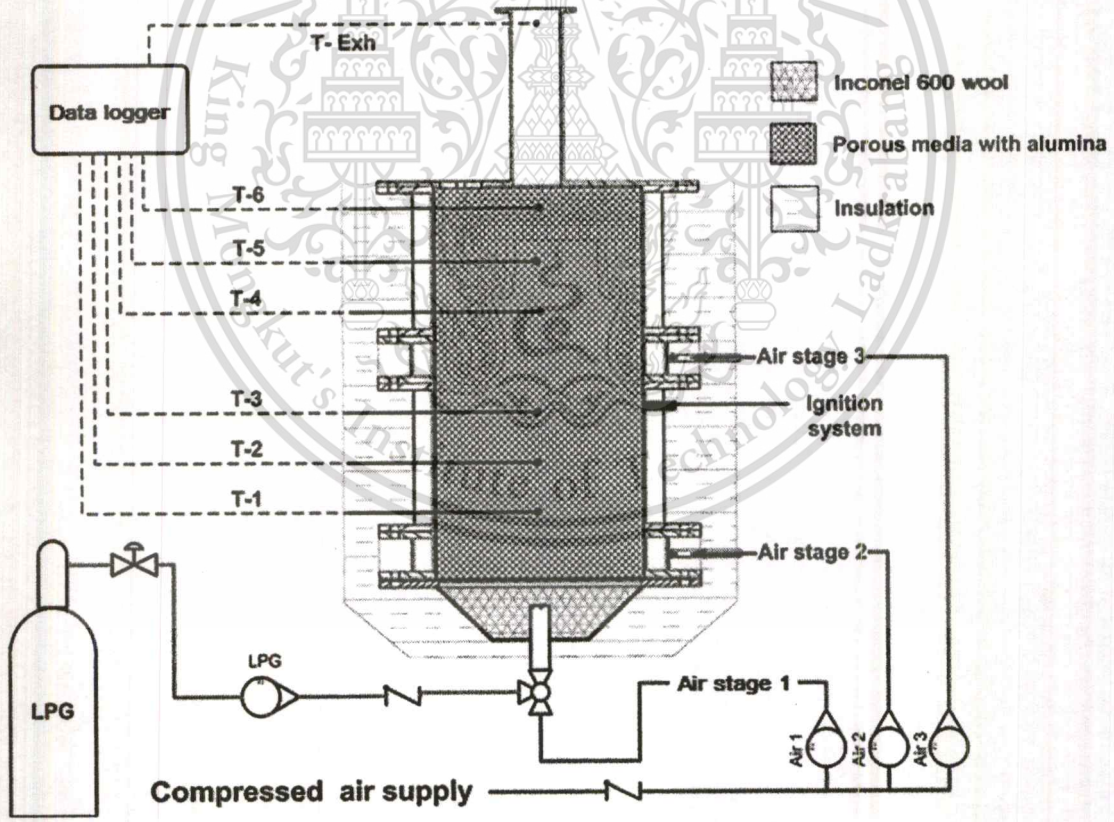

Figure 3.8 Porous burner diagram (Wittaya W.)

3.2.1.1 Experimental Procedure

Air is supplied at 4 bar for LPG combustion which is investigated on the amount of excess air at 85% as shown in Table 3.2. In the experimental, rotameter was need to control the volume flow rate of LPG and air. Grand Data Logger 2010 series is used to collect the temperature from the experimental. There are 6 positions of thermocouple type K which are 80, 150, 230, 380, 440 and 510 mm high from the bottom of furnace, respectively. When the temperature is at steady state, the exhaust gas is measured using a gas analyser (TECHNOTEST Type STARGAS 898) at the outlet of the furnace.

Table 3.2 Experimental condition

Energy input (kW)	Excess air (%)	Flow rate of air (l/min)			Flow rate of fuel (l/min)
		Stage 1 st	Stage 2 nd	Stage 3 rd	
10	85	50	100	200	7
A/F ratio	15.6				

3.2.1.2 Experimental Results

In Table 3.3, the exhaust gas emission was detected at 85% of excess air. The exhaust gas composition is shown in Table 3.3 which is CO, CO_2, O_2, and HC, respectively.

Table 3.3 Emissions result

%Excess air	Emissions (%Vol.)			
	CO	CO_2	O_2	HC (ppm)
85	0.027	4.65	13.61	3

Heat energy of the exhaust gas is calculated from exhaust gas composition. Hydrocarbon (HC) is neglect because it is very less value.

At 85% of the excess air, the experimental result shows the temperature at each positions of the furnace and includes exhaust gas at the outlet as shown in Figure 3.9. The temperature result decreases slightly from 1st position of temperature sensor (T1) to temperature

sensor at the outlet of the exhaust gas (Texhaust). T1-T3 are at high temperature greater than 1000 °C as a result of near stoichiometric combustion. Between T3-Texhaust, temperature reduce due to heat loss to the reformer.

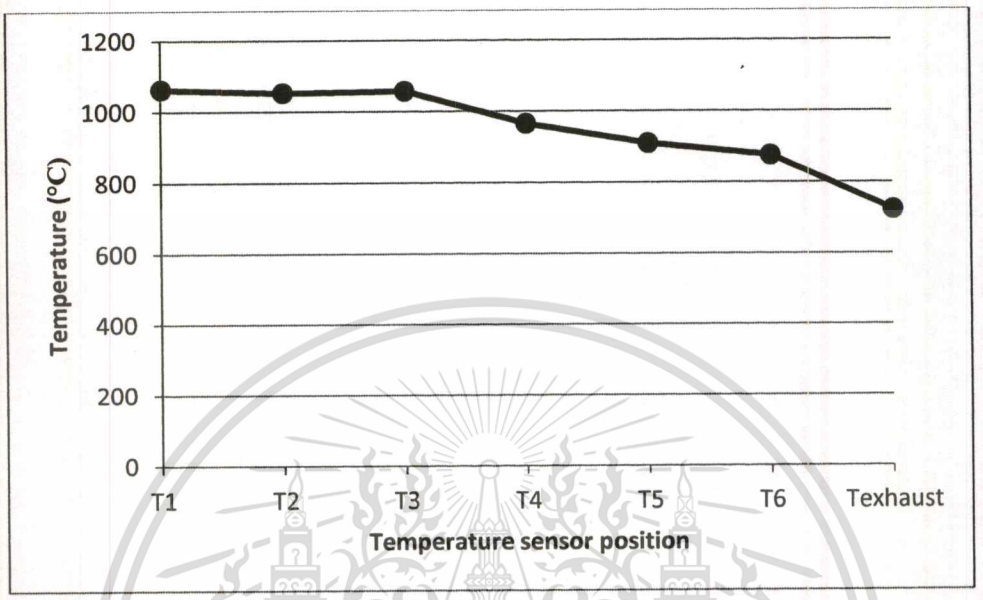

Figure 3.9 Temperature distribution inside the furnace at 85% excess air

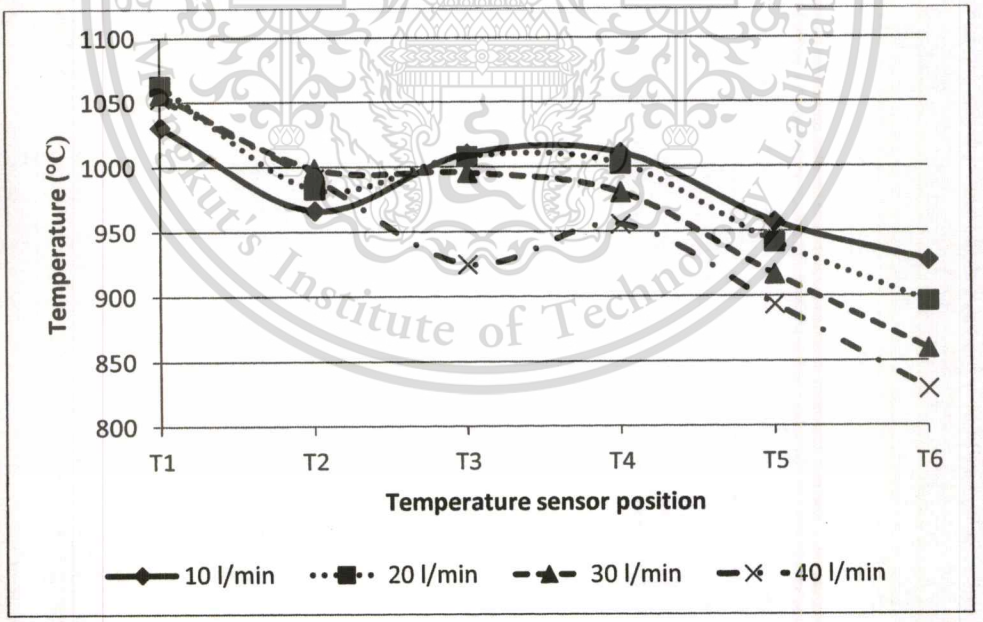

Figure 3.10 Temperature distribution along vertical location for different reactant gas flow rate

Figure 3.10 shows temperatures inside the reactor of reformer which receives heat from the furnace. These results vary with volume flow rate of reactant.

3.2.1.3 Mathematical Model of the Furnace

In this study, the heat energy of LPG combustion and heat loss from the exhaust gas were focused on. The assumption of the furnace for the mathematical model is;

- the reactor is assumed as the heat exchange unit

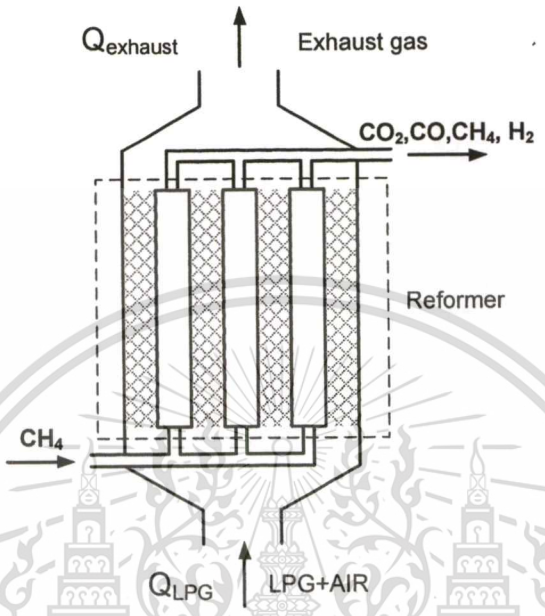

Figure 3.11 Furnace Diagram

Heat energy of LPG combustion can be calculated from lower heating value of LPG (LHV_{LPG}) as the following equation

$$\dot{Q}_{LPG} = \dot{m}_{LPG} \times (LHV_{LPG} \times 1000) \times \%\eta_{combustion} \quad (3.9)$$

From Figure 3.11, $\dot{Q}_{exhaust}$ is the heat energy of exhaust gas which can be defined as heat loss of the furnace. Heat loss can be calculated from Equation (3.10) by using exhaust gas emission results from Table 3.3. This result is used to calculate the mass flow rate of the exhaust gas see Equation (4.2) in chapter 4.

$$\dot{Q}_{exhaust} = \dot{m}_{exhaust} \times \Sigma C_{p\,exhaust}(T_{out} - T_{in}) \quad (3.10)$$

Heat from the combustion is transferred to the reformer which is inside the furnace. Heat energy is used in the steam methane reforming and water gas shift process to produce

hydrogen. Equation (3.11) is the energy balance between furnace and reformer including heat loss at wall.

$$\dot{Q}_{LPG} = \dot{Q}_{reformer} + \dot{Q}_{exhaust} + \dot{Q}_{wall} \quad (3.11)$$

3.2.2 Reformer

Reformer is an appliance used in the hydrogen production process. In this process, methane is converted to hydrogen by steam methane reforming process (SMR). In the SMR process, Ni/Al_2O_3 catalyst is used in the reaction as shown in Reaction (3.12).

SMR $CH_4 + H_2O \rightarrow CO + 3H_2$ $\Delta H = +206.1\ kJ/mol\ CH_4$ (3.12)

Water-gas shift $CO + H_2O \rightarrow CO_2 + H_2$ $\Delta H = -41.15\ kJ/mol\ CO$ (3.13)

Overall $CH_4 + 2H_2O \rightarrow CO_2 + 4H_2$ $\Delta H = +165.0\ kJ/mol\ CH_4$ (3.14)

For the SMR products, CO reacts with H_2O in the water gas shift reaction as shown in Reaction (3.13). Therefore, the overall reaction in the reformer unit is shown in Reaction (3.14) which is based on the endothermic reaction.

3.2.2.1 Experimental setup (Khemthong, B. 2009)

A drawing of the SMR experiment is presented in Figure 3.12. The reformer was located inside an electrical furnace. To produce a simulated biogas, CH_4 and CO_2 were mixed together by using a mass flow controller. Water was vaporized at the preheating zone inside the furnace and then mixed with simulated biogas prior to entering a reforming reactor. The steam was mixed with methane at a certain molar ratio or called S/C ratio. It was varied from two moles of steam per 1 mole of methane to six moles of steam per mole of methane. The reactor configuration used in this experiment, as shown in Figure 3.13, was a stainless-steel tube (inner diameter = 15 mm, length of packed bed = 150 mm). Alumina beads were packed in the reformer to generate a uniform flow inside the reactor. Ni/Al_2O_3 catalyst from Alfa Aesar was used in this experiment.

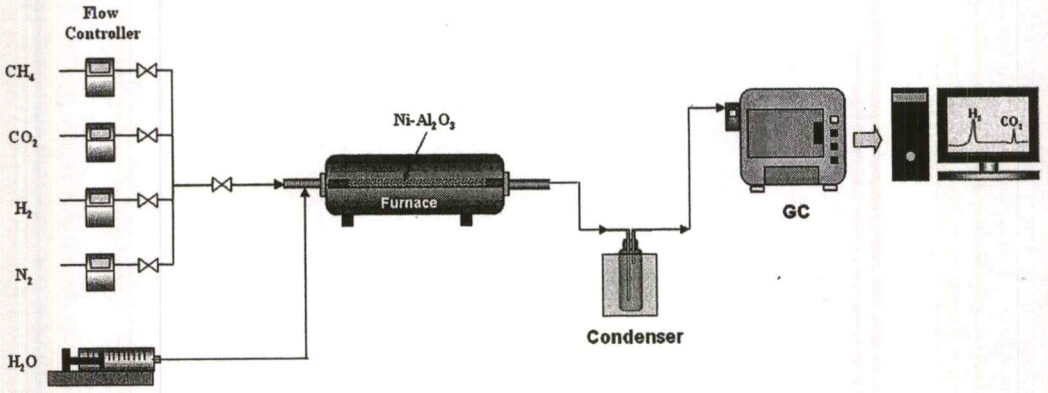

Figure 3.12 Diagram of the experimental apparatus

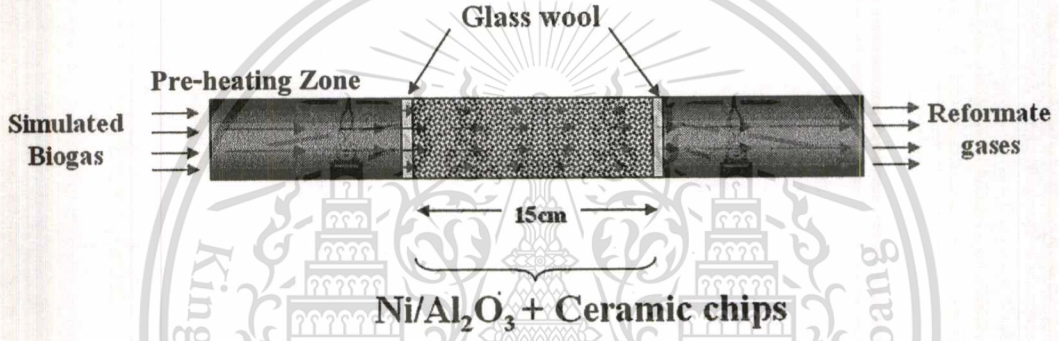

Figure 3.13 Schematic diagram of the reformer tube

The temperatures inside the reactor were measured and monitored continuously at the center and at the wall of the reformer tube using K-type thermocouples. To observe the temperature profile, three K-type thermocouple wires were inserted in the reformer bed at the inlet of the bed, 3.75 mm and 11.25 mm along the bed length. Beside those thermocouples, another K-type thermocouple was placed at the outer wall of the reformer to measure the actual operating temperature of the reformer.

Flow rates of CH_4, CO_2, N_2, and H_2 were controlled by using mass-flow controllers (MFCs), while a flow rate of water was controlled using a syringe pump. Moisture in the product gas was removed by means of a condenser. The compositions of dried reformate gas were analyzed using a gas chromatography technique (Shimadzu model GC-14B using a Porapak Q column). H_2, CO, CH_4, CO_2, and N_2 were detected using the TCD using argon as a carrier gas.

3.2.2.2 Experimental Results

Figure 3.14 shows the equilibrium condition for the overall reaction of steam methane reforming and water gas shift reaction from Reaction (3.14). At high temperature which is greater than 800°C. %Mole fraction of H_2 reach 80% and CO_2 reach 20%. Thus, %mole fraction total of product is equal to 100%. Reactants are not found.

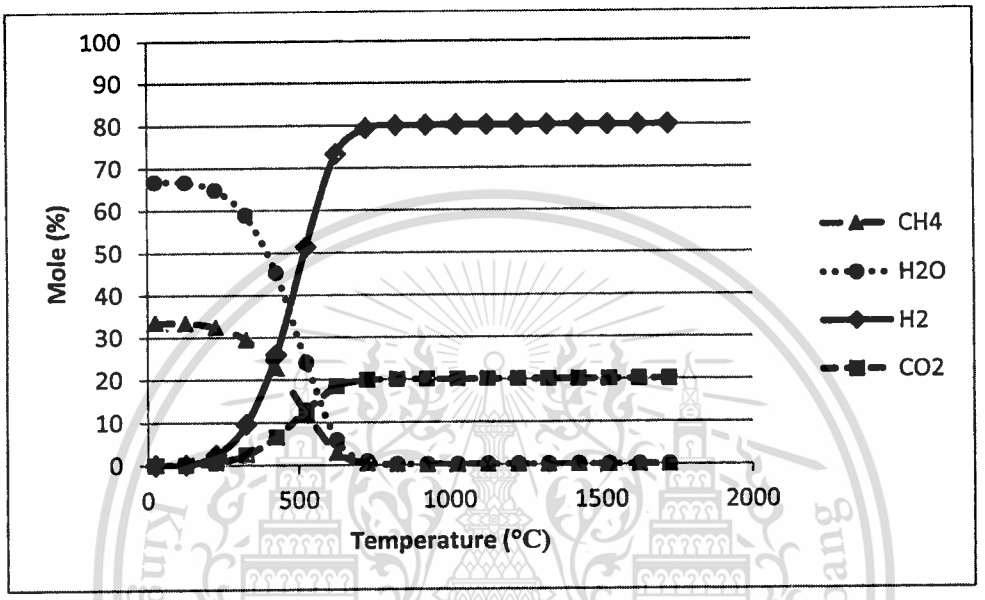

Figure 3.14 Equilibrium %mole fractions for the overall reaction of steam methane reforming and water gas shift reaction

Figure 3.15 shows the equilibrium condition of steam methane reforming reaction from Reaction (3.12). There is %mole fraction of H_2 = 75% and CO = 25%. Therefore, %mole fraction total of product is equal to 100%. CH_4 and H_2O are equal to 0%.

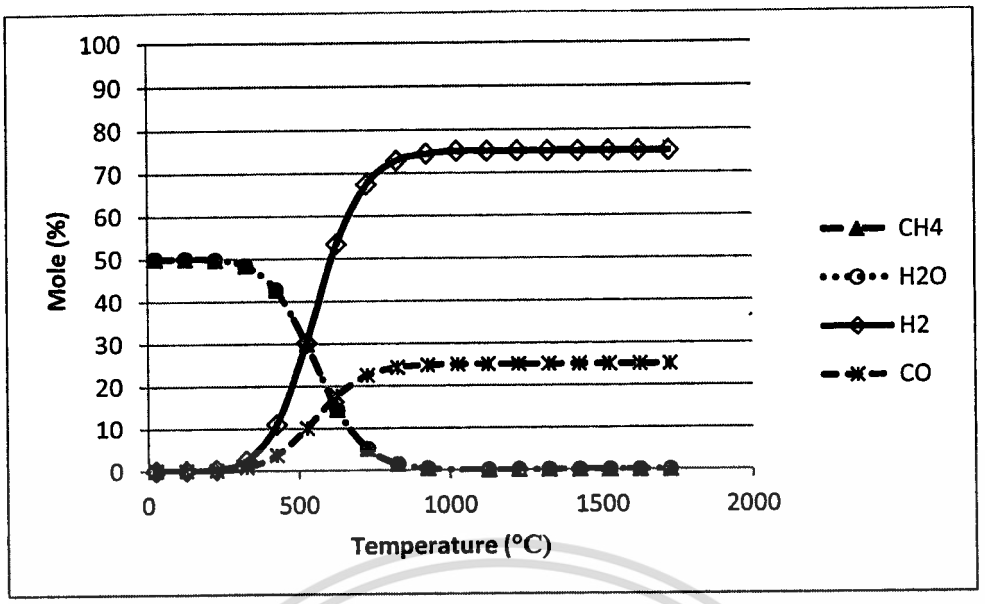

Figure 3.15 Equilibrium %mole fractions for the steam methane reforming reaction

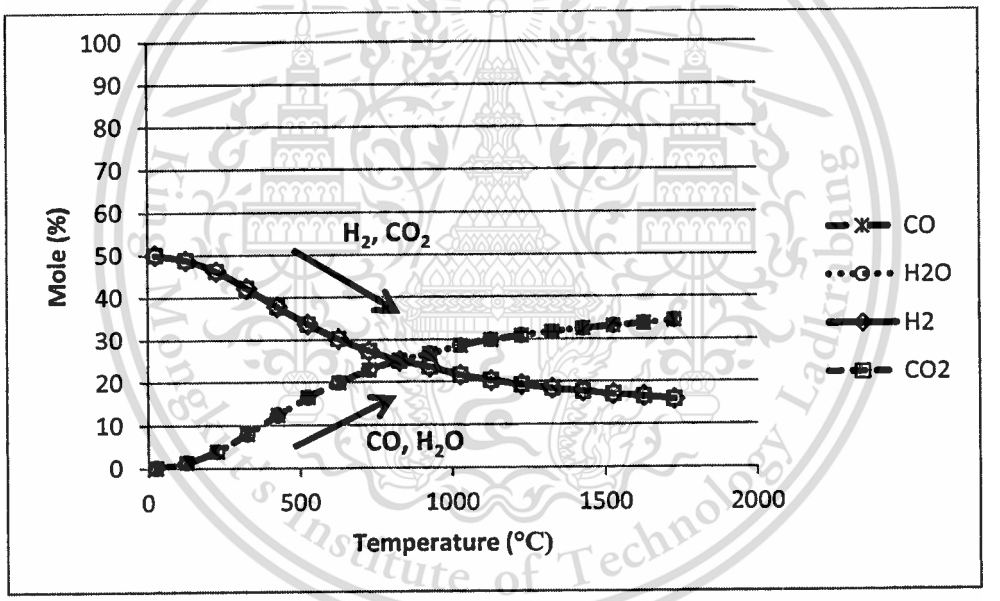

Figure 3.16 Equilibrium %mole fractions for the water gas shift reaction

Figure 3.16 shows %mole fractions in the equilibrium condition of the water gas shift reaction from Reaction (3.13). At stoichiometric ratio, it is founded that CO has more %mole fraction when temperature increase. On the other hand, %mole fractions of CO_2 go down with increasing temperature.

From the experimental results, the relationship between reformate gas and operation temperature in several S/C ratios are shown in Figures 3.17-3.20. The operation

temperature of the reformer were between 650°C -850°C at the S/C ratios of 2, 3, 4.5 and 6, respectively.

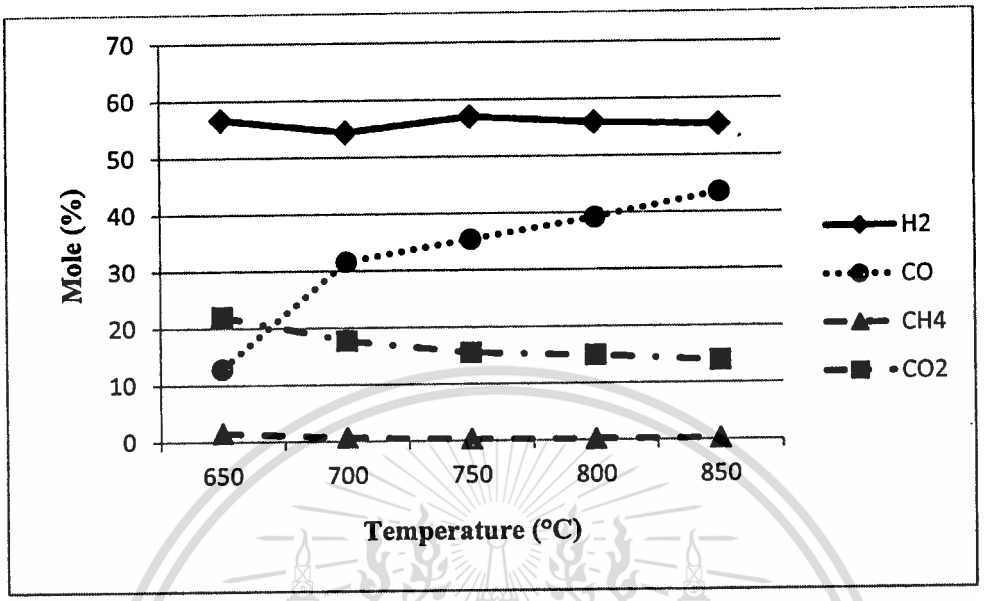

Figure 3.17 Composition of reformate gas as a function of temperature at constant S/C ratio = 2

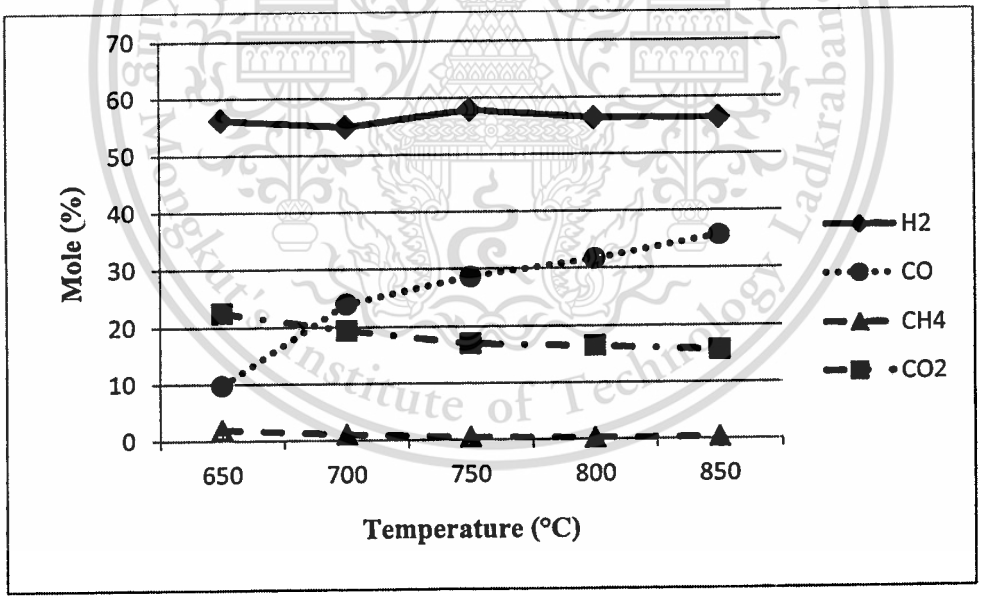

Figure 3.18 Composition of reformate gas as a function of temperature at constant S/C ratio = 3

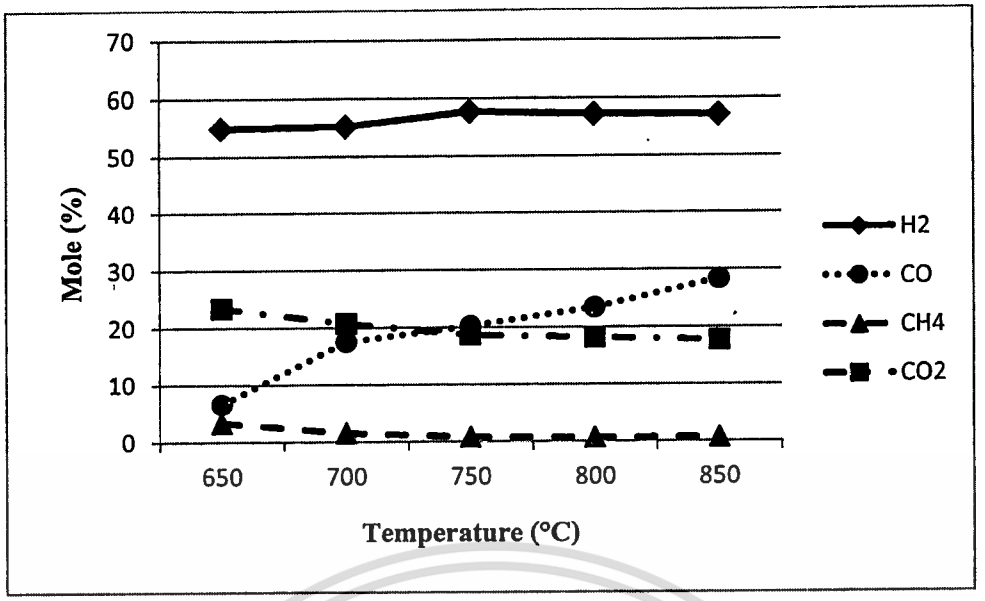

Figure 3.19 Composition of reformate gas as a function of temperature at constant S/C ratio = 4.5

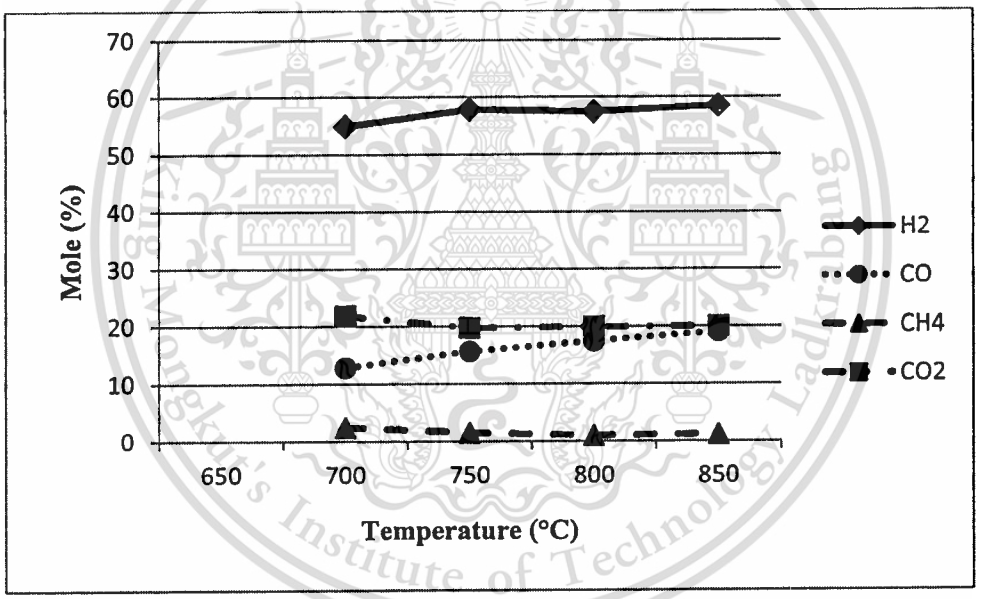

Figure 3.20 Composition of reformate gas as a function of temperature at constant S/C ratio = 6

Results from Figures 3.17-3.20, H_2 is a product gas which is similar to the equilibrium condition in Figures 3.14-3.15. CH_4 results is also relate to the equilibrium condition. It is close to zero because CH_4 is converted to H_2 product. Therefore, H_2 and CH_4 results agree well with those determined from the equilibrium condition.

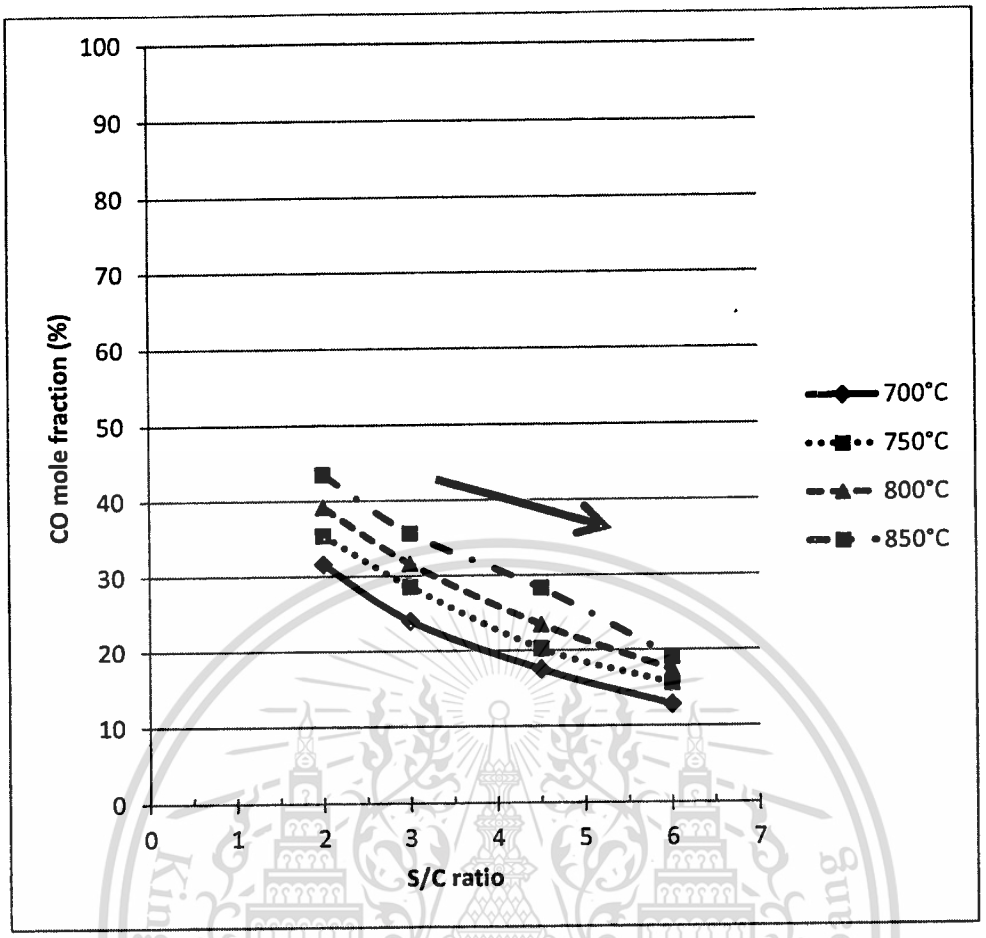

Figure 3.21 Tendency of %CO mole fraction results on S/C ratio

From SMR reaction Reaction (3.12), if S/C ratio is higher, it means mole fraction of CH_4 is lower or lean. Thus, mole fraction of CO decreases as observed in Figure 3.21.

Relationship between CO and CO_2 from Figure 3.17-3.20 can be explained from Figure 3.16 as mentioned before. Mole fraction of CO decreases when S/C ratio increases as shown in Figure 3.21. CO/CO_2 mole fraction ratio also decreases with decreasing S/C ratio. Thus, space between CO line and CO_2 line after cross section reduce following S/C ratio.

The relationship between reformate gas composition and S/C ratio from the experimental results is applied to empirical model for computer program of the reformer unit as mentioned in the next topic.

3.2.2.3 Mathematical model of reformer

To compare the results, a set of equations were calculated from the reformate gas compositions of the simulated biogas (BG) and the synthesis gas (SG) (Kolbitsch et al. 2007).

These are the conversion of CH_4

$$X_{CH_4} = 1 - \frac{y_{CH_4,SG}}{y_{CH_4,BG} \cdot y_C} \tag{3.15}$$

The conversion of CO_2

$$X_{CO_2} = 1 - \frac{y_{CO_2,SG}}{y_{CO_2,BG} \cdot y_C} \tag{3.16}$$

And the H_2 yield

$$Y_{CH_4} = 0.25 \frac{y_{H_2,SG}}{y_{CH_4,BG} \cdot y_C} \tag{3.17}$$

Where

$$y_C = y_{CH_4,SG} + y_{CO_2,SG} + y_{CO,SG} \tag{3.18}$$

The conversion from Equations (3.15)-(3.16) is used to calculate heat energy used in steam methane reforming and water gas shift processes as shown in Equation (3.19). ΔH_{SMR} and ΔH_{WGS} are the heat of reaction from Equations (3.12) and (3.13), respectively.

$$\dot{Q}_{reforming} = [(X_{CH_4} \times \Delta H_{SMR}) + (X_{CO_2} \times \Delta H_{WGS})] \times \frac{m_{CH_4}}{M_{CH_4}} \tag{3.19}$$

Equation (3.20) is used to calculate the heat energy of water-steam in the reformer. The first line of the equation is the heat energy which was used for an increase of temperature form normal temperature (NT) to boiling point (BP). The second line is the heat energy of latent heat which converts water to steam. The third line is the heat energy which is used from boiling point to reformer operation temperature.

$$\dot{Q}_{boiler} = [M_{H_2O} \times Q_{sensible\ water} \times \dot{n}_{CH_4} \times S/C \times (T_{BP} - T_{NT})]$$

$$+[M_{H_2O} \times Q_{latent} \times \dot{n}_{CH_4} \times S/C]$$

$$+[M_{H_2O} \times Q_{sensible\ steam} \times \dot{n}_{CH_4} \times S/C \times (T_{reform} - T_{BP})] \tag{3.20}$$

The heat energy of the reforming process and water-to-steam production is the net energy used in reformer unit as shown in Equation (3.21).

$$\dot{Q}_{reformer} = \dot{Q}_{reforming} + \dot{Q}_{boiler} \tag{3.21}$$

The temperature of the reformate gas is reduced to the normal temperature at the outlet of the reformer unit, before feeding into the SOFC stack. Thus, the heat loss occurs in this step. Then, we can calculate the heat loss as in the following Equation (3.22).

$$\dot{m}_{reformate\ gas} = \dot{m}_{H_2} + \dot{m}_{CO_2} + \dot{m}_{CO} + \dot{m}_{CH_4} \tag{3.22}$$

$$\dot{Q}_{loss,reformate\ gas} = \dot{m}_{reformate\ gas} \times (h_{reform} - h_{NT}) \tag{3.23}$$

Figure 3.22 showed the heat energy diagram which occur in the reformer unit. As mentioned before, the furnace and the hydrogen production unit or reformer, are called the reformer unit. The furnace is the energy input appliance for the reformer to produce hydrogen. There are heat transfer occurred between both of them as shown in Figure 3.22. Besides, there are heat loss occurred which are heat loss due to wall, heat of the exhaust gas, and heat loss of reformate gas.

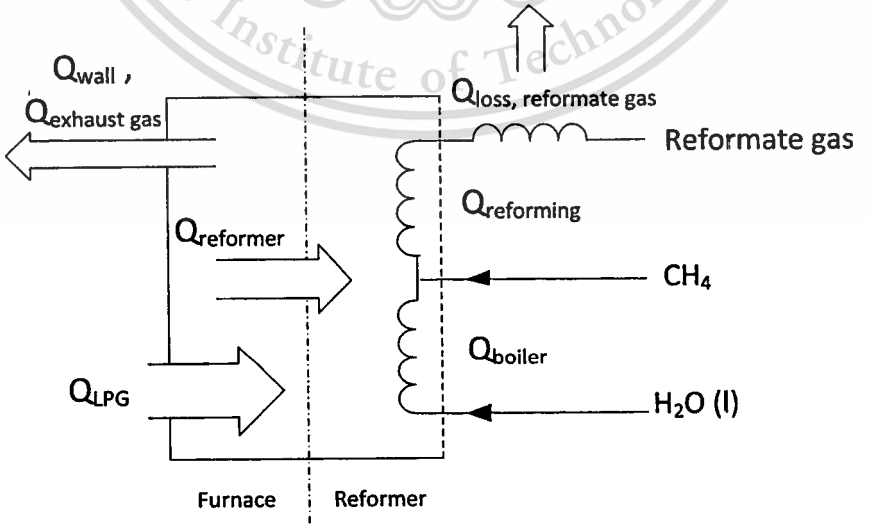

Figure 3.22 Furnace and reformer heat energy diagram

3.3 SOFC

SOFC is an energy conversion device which is based on an electrochemical reaction. This study was investigated the production of 1 kW electrical output of SOFC. The SOFC in this study is a tubular solid oxide fuel cell as shown in Figure 3.23. And the specification of SOFC bundle is shown in Table 3.4.

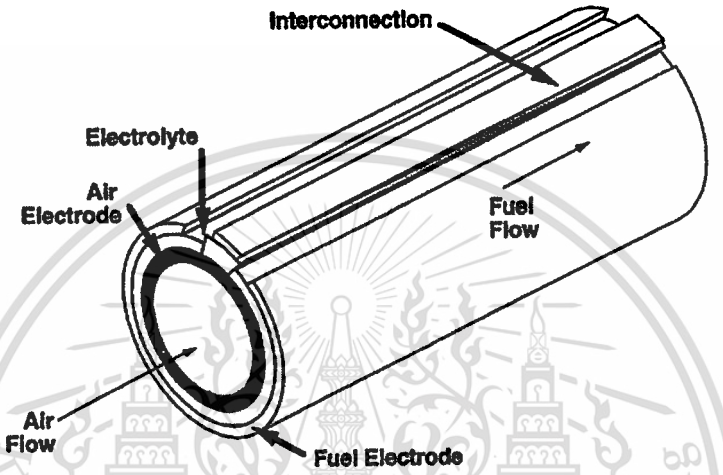

Figure 3.23 Tubular solid oxide fuel cell (S.C. Singhal. 2000)

Table 3.4 Specification of the 1 kW electrical output of SOFC

Specification	Amount
Total amount of SOFC	500 cells/bundle
Electrical power output	2 W/cell (1 kW/bundle)
Series connection	25 Cells/row
Parallel connection	20 row/bundle
Diameter of cell	5 mm
Length of cell	16.5 mm
Utilization of hydrogen	60%

3.3.1 Experimental Procedure

First, the start-up process, the SOFC bundle is needed to be heated up by electrical heater until reaching the operation temperature at 920°C. There were three electric heaters which were controlled by a proportional–integral–derivative (PID) controller box. This SOFC bundle is

fed with O_2 which is reactant of the reaction from air atmosphere. Air is conducted using an electrical fan under the SOFC tubes. While the SOFC is heated up, N_2 is also fed into the SOFC. After the temperature of the SOFC tubes reaching the temperature operation required, the temperature is controlled at steady state at 920°C. Next, hydrogen is fed into the SOFC to react with O_2 to produce electricity. An electronic load is used to pull electrical power by an addition of current. Then, the voltage drop of the SOFC was measured using a multi-meter. In the study, hydrogen is fed at 25, 30, 35, 40 and 45 l/min, respectively.

3.3.2 Experimental Results

The experimental results are shown in Figures 3.24-3.28. They are the relationship between current-voltage and power output from the SOFC at 25, 30, 35, 40 and 45 l/min of hydrogen flow rate, respectively.

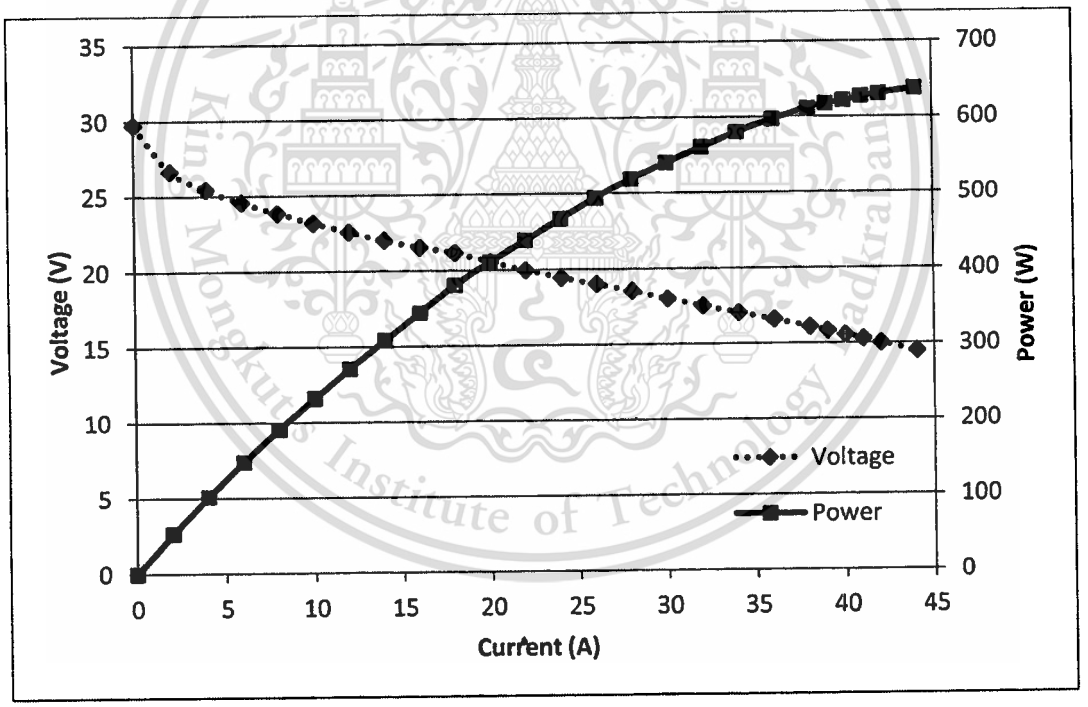

Figure 3.24 SOFC performance at 25 l/min of hydrogen

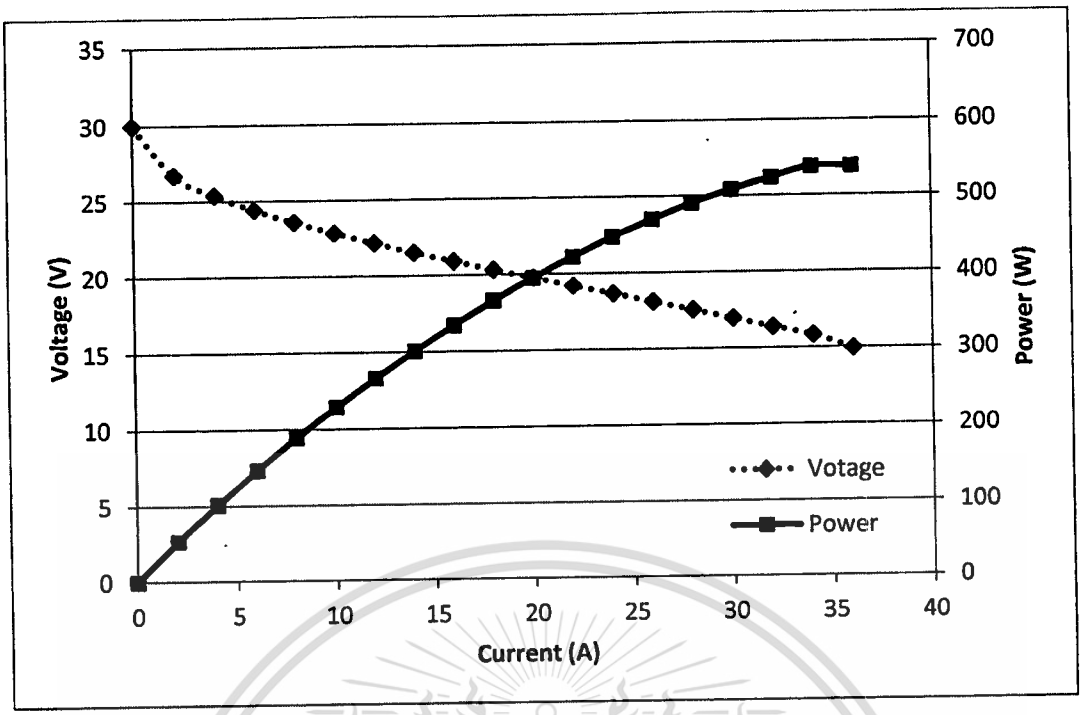

Figure 3.25 SOFC performance at 30 l/min of hydrogen

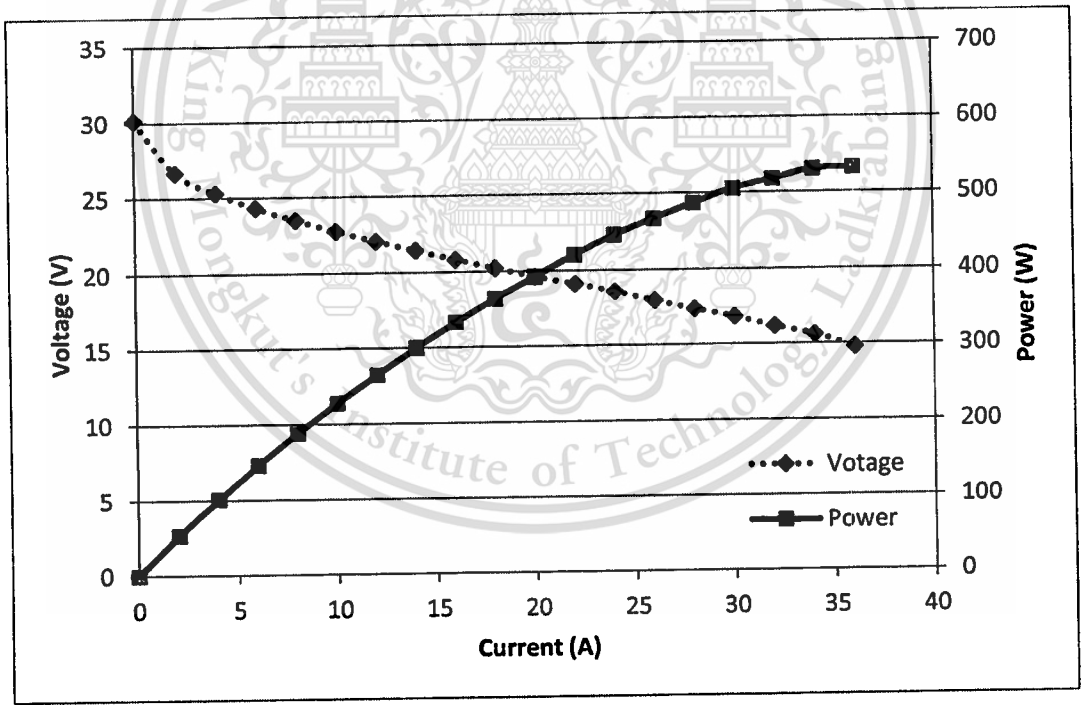

Figure 3.26 SOFC performance at 35 l/min of hydrogen

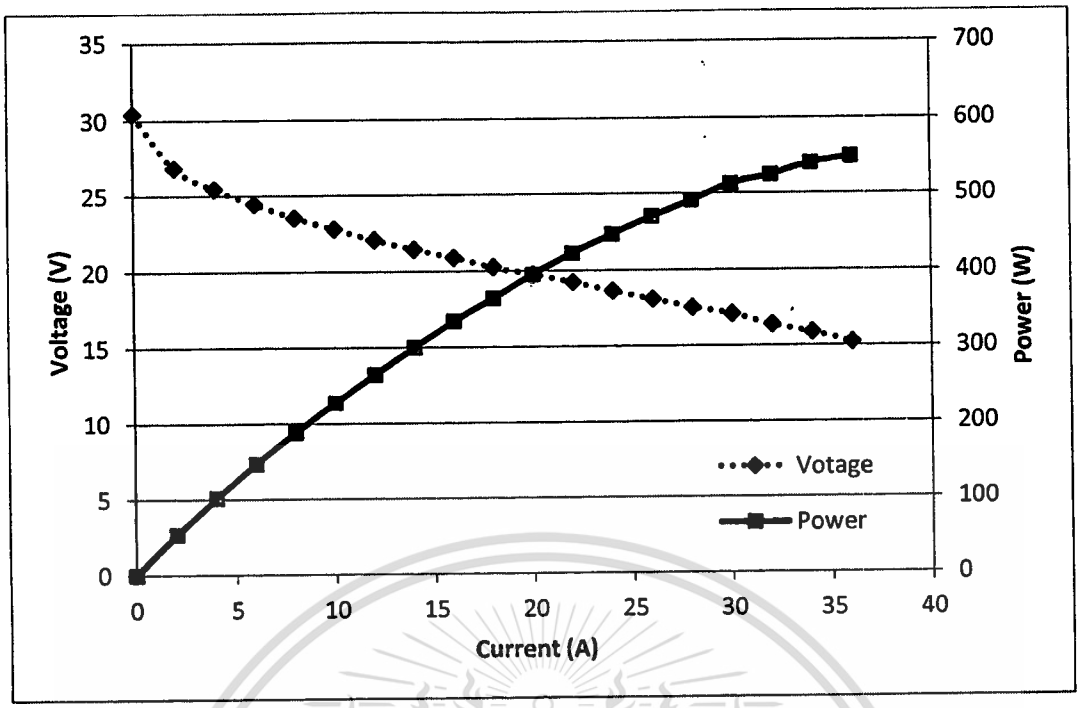

Figure 3.27 SOFC performance at 40 l/min of hydrogen

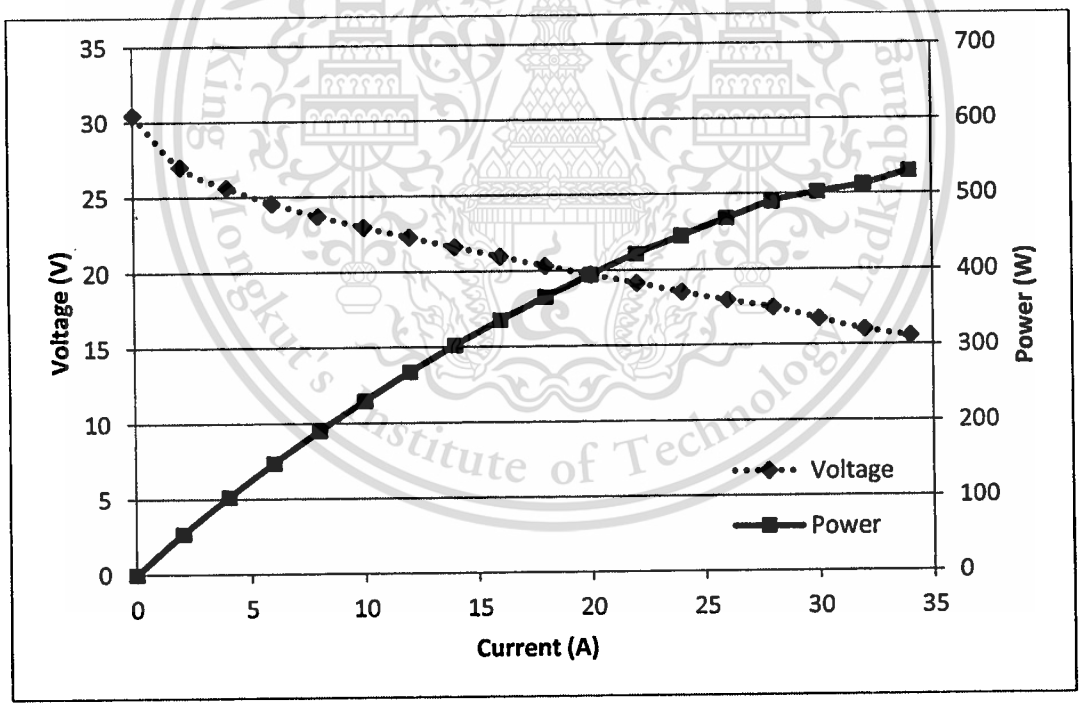

Figure 3.28 SOFC performance at 45 l/min of hydrogen

Hydrogen flow rate and electrical energy output is applied for use as an empirical model in a computer simulation.

3.3.3 Mathematical model of SOFC

Reformer products are fed into the SOFC at room temperature up to the operation temperature. Thus, heat energy occurred by transferring the heat energy of the SOFC to reformate gas as shown in Equation (3.24).

$$\dot{Q}_{SOFC} = \dot{m}_{reformate\ gas} \times (h_{sensible,\ reformate\ gas} - h_{reform}) \quad (3.24)$$

Electrical output of the SOFC can be calculated from the empirical model which depends on hydrogen volume flow rate at the inlet and addition of current to the SOFC. Then, the electrical voltage can be defined to calculate electrical output as shown in Equation (3.25).

$$Power_{SOFC} = VI \quad (3.25)$$

The efficiency of the SOFC can be determined by the following Equation in which the electrical output or power output of the SOFC is derived from the mass flow rate and lower heating value (LHV) of hydrogen.

$$\eta_{SOFC} = \frac{Power_{SOFC}}{\dot{m}_{H_2} \times LHV_{H_2}} \quad (3.26)$$

CHAPTER 4

MODELLING RESULTS AND DISCUSSION

4.1 Mathematical Modelling Program

This study has used MATLAB Simulink Program to simulate the empirical model of the SOFC system which comprises of CO_2 removal, furnace, reformer, and SOFC models as shown in Figure 4.1. In each sub-unit, there are three functions which are (1) input data as shown in Figure 4.2, (2) the empirical model and (3) output result. The first unit is the CO_2 removal unit which absorbs CO_2 from biogas. The CO_2 removal model has the mass flow rate of methane as the output. The mass flow rate of CH_4 is transferred to the next unit which is a reformer. The reformer unit used the empirical data to determine the reformate gas by following the condition of steam-methane (S/C) ratio and operation temperature. Heat energy is used in the steam methane reforming and water gas shift of the reformer. This heat is received from the furnace which uses LPG as fuel for the combustion. Hydrogen product of reformate gas is required for the SOFC model to investigate electrical energy output of the SOFC. The empirical model of electrical energy output of the SOFC can be separated by hydrogen flow rate. Thus, hydrogen mass flow rate of reformate gas is significant for the SOFC model.

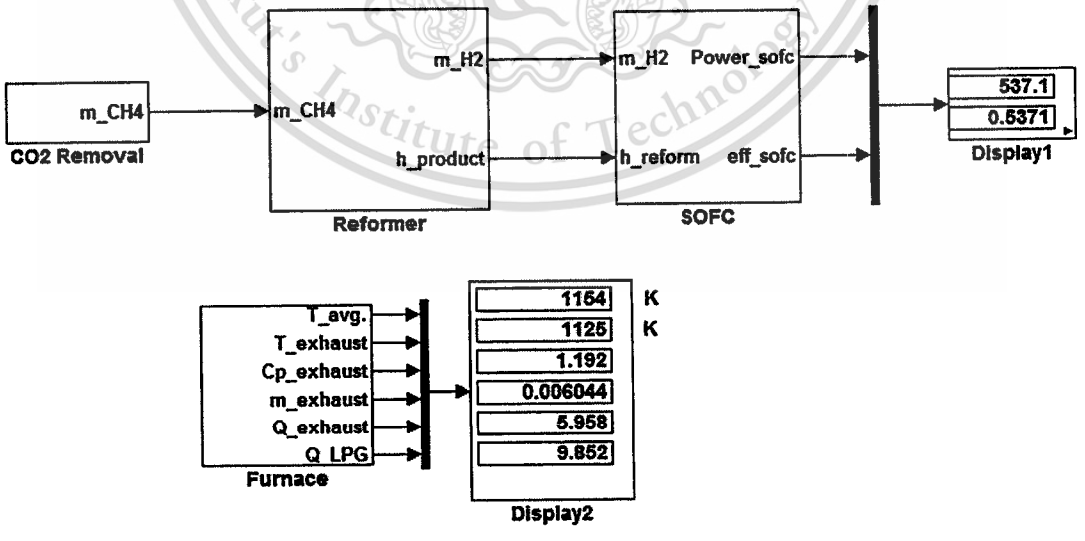

Figure 4.1 Mathematical modelling of the SOFC system

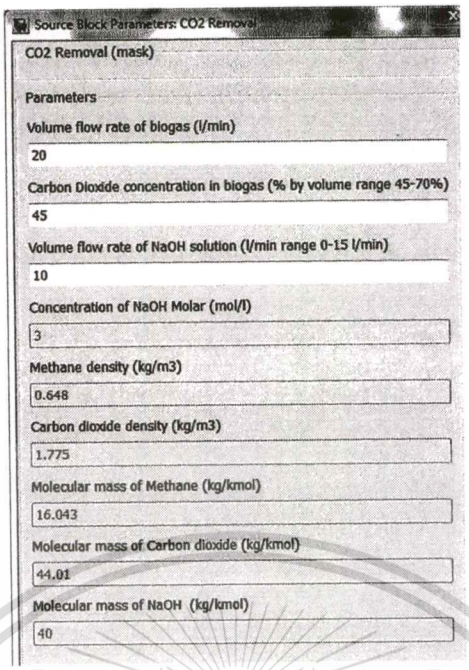

Figure 4.2 Block parameter

The empirical model used a function of look up table in the MATLAB Simulink program. The experimental results were fed into this function. Then, it can be determined the results from the input parameter in the empirical model. Details and results of the SOFC system are described in the following topic. The components in each model are explained. The energy usage for each unit is investigated.

4.2 CO_2 Removal Modelling

The mathematical of CO_2 removal is explained in the early chapter. It composed of CO_2 absorption period, the heat of reaction of CO_2 absorption, the consumption of NaOH solution and pumping power.

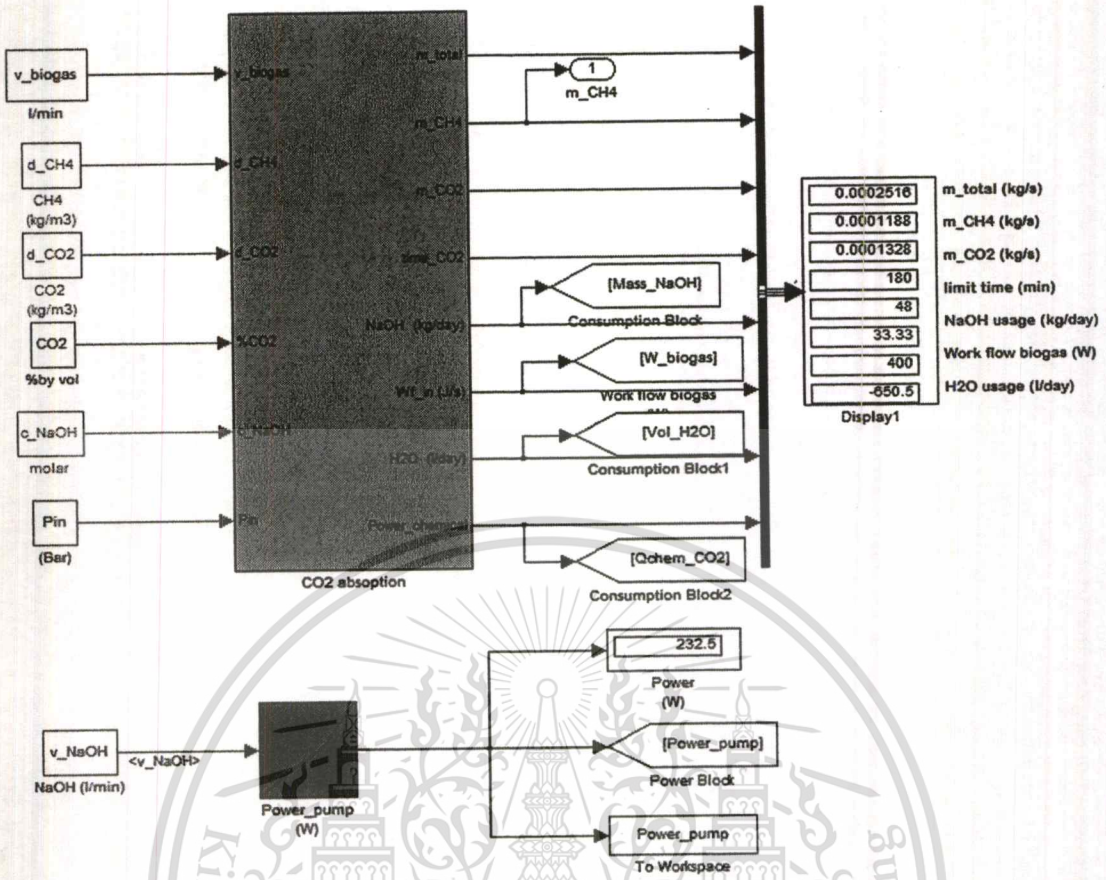

Figure 4.3 Mathematical modelling of CO_2 removal

Figure 4.3 shows the mathematical model of CO_2 removal. The absorption time of CO_2 removal was determined from the empirical model which depends on the %CO_2 by vol. at the inlet. Heat energy for the chemical reaction of CO_2 and NaOH solution can be defined by the heat of reaction as shown in Reaction (4.1).

$$CO_{2(g)} + 2NaOH_{(aq)} \rightarrow Na_2CO_{3(aq)} + H_2O_{(l)} \quad \Delta H = -107.52\ kJ/mol\ CO_2 \quad (4.1)$$

NaOH solution is prepared from solid NaOH. The condition of the empirical model is set that NaOH at 3 molar was used. The consumption of NaOH from the absoption time can be determined.

NaOH solution pump fed the solution into the absoption column. The power input for pump was determined from the empirical model of solution pump.

4.2.1 CO_2 Removal Modelling Results

First, the result of the empirical model was compared with the calculation of the absorption limit time as shown in Figure 4.4. The absorption limit time is defined as the absorption duration of CO_2 which is counted from the beginning until the last point of 0%by vol. of CO_2 concentration at the outlet. The operating condition is set at 1 bar, biogas inlet at 20 l/min and 3 molar of NaOH volume flow rate at 10 l/min.

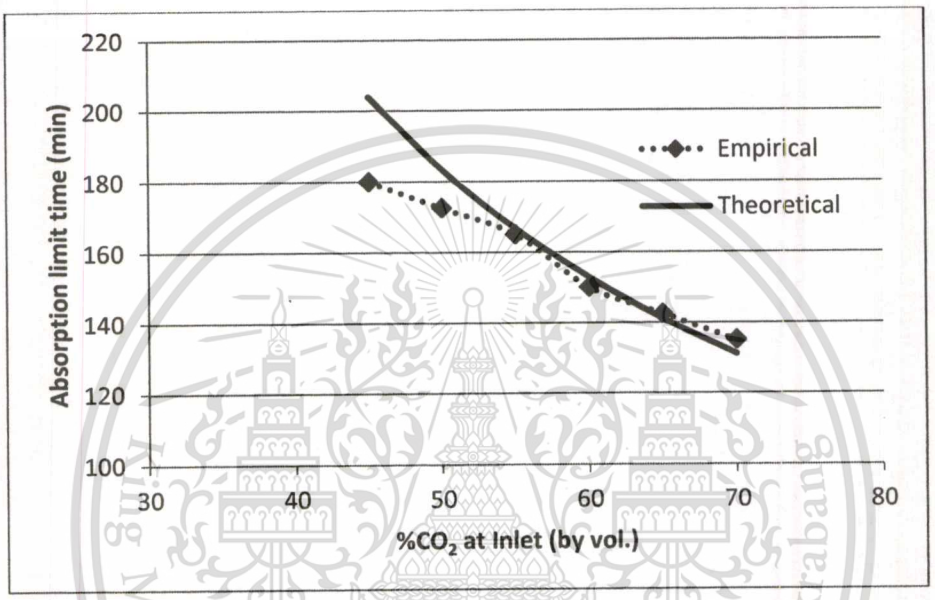

Figure 4.4 Relationship between absorption limit time and $\%CO_2$ at the inlet

From Figure 4.4, the absorption limit time decreases when increasing $\%CO_2$ at the inlet. The empirical and theoretical results have the same path. The $\%CO_2$ at 45 and 50% are different from the theoretical calculation, which may be caused by the CO_2 collection for measurement from the experimental which collected the output gas every 15 minute. If the CO_2 composition in biogas is high, 3 molar of NaOH solution is running out quickly.

In Figure 4.5, the same cause occurred at 45 and 50%CO_2 at the inlet. This figure shows the results of NaOH consumption. If biogas has high composition of CO_2, the consumption of NaOH is high too.

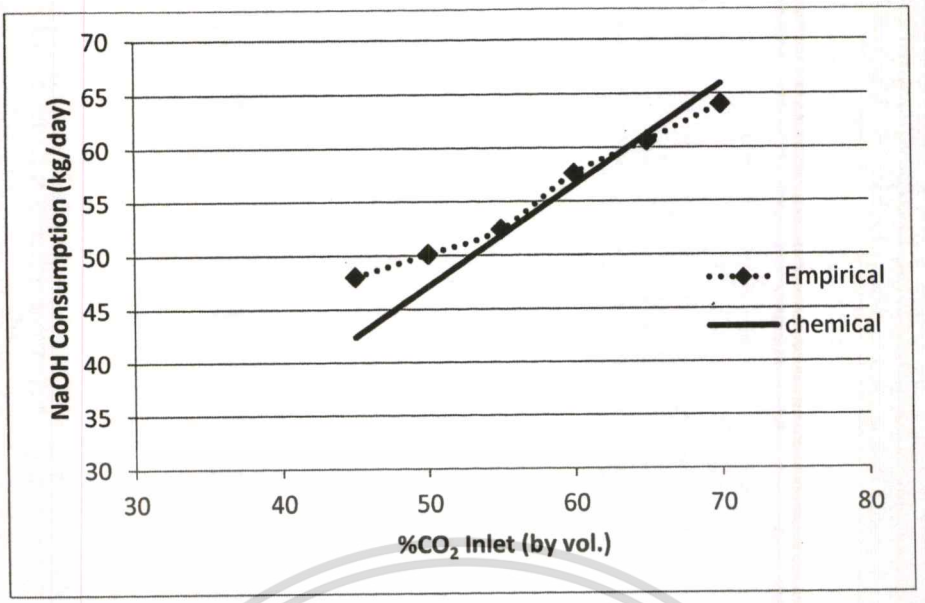

Figure 4.5 Relationship between NaOH consumption and $\%CO_2$ at the inlet

Figure 4.6 shows the chemical energy input which was used in the chemical absorption. At 45%-70% of CO_2 composition of biogas at the inlet, they use heat energy for the reaction between 600-1000 W referred to standard condition.

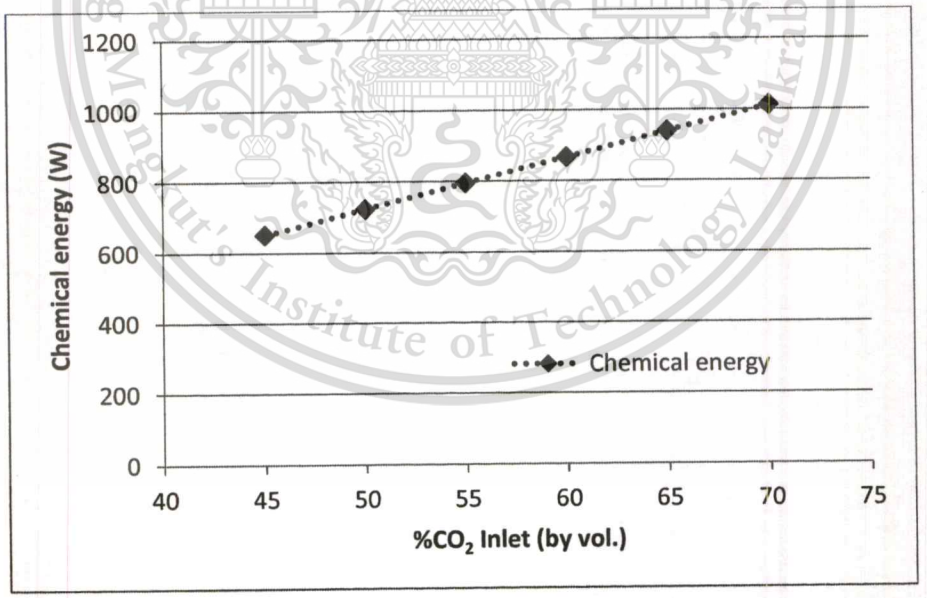

Figure 4.6 Chemical energy input for removing CO_2 from biogas at 10 l/min of NaOH solution

The empirical result of electrical power input of NaOH solution pump is shown in Figure 4.7.

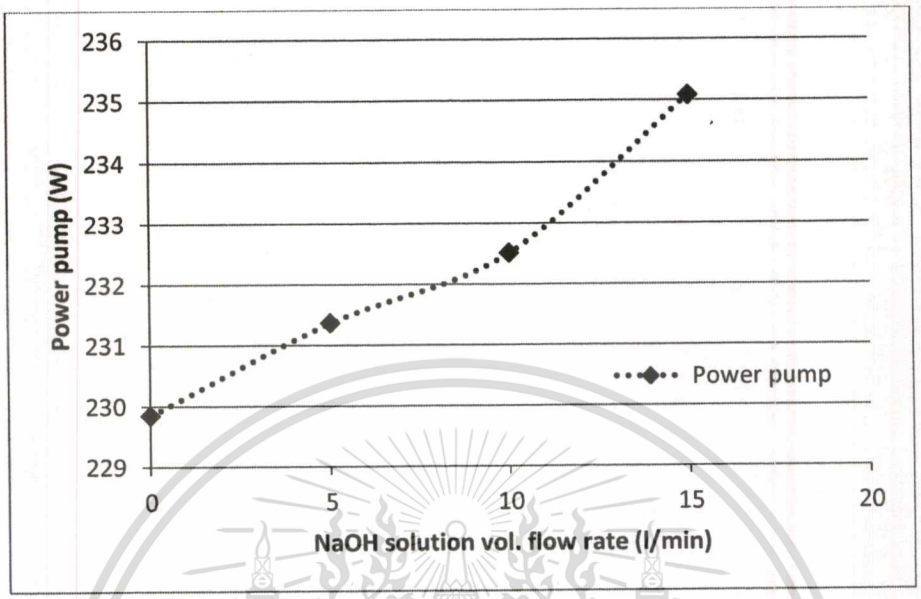

Figure 4.7 Relationship between electrical power of pump and NaOH solution vol. flow rate

Figure 4.8 shows the total energy input for the CO_2 removal unit which operated at 20 l/min of biogas at the inlet and NaOH solution flow rate at 10 l/min. Therefore, the CO_2 removal unit in this condition uses energy input at 850-1100 W following $\%CO_2$ at the inlet.

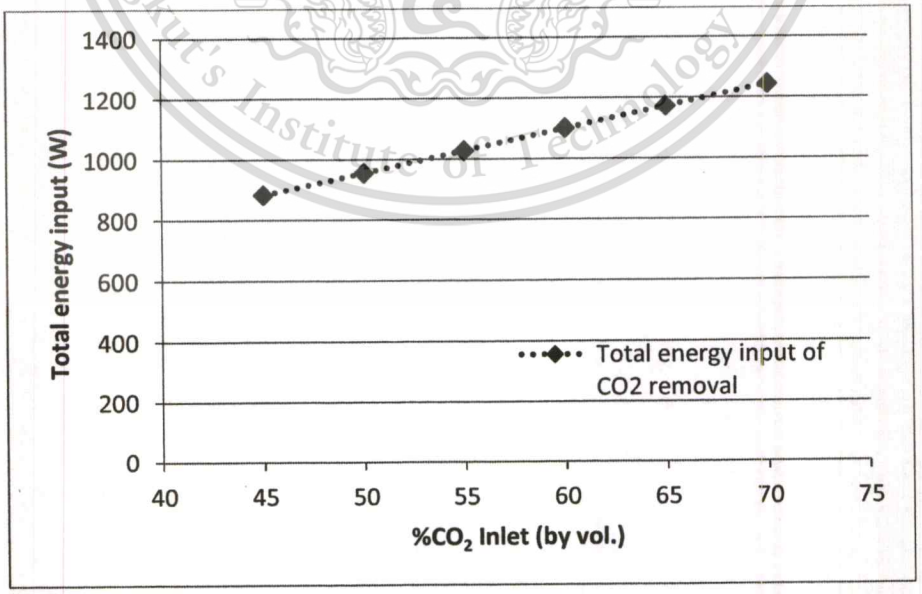

Figure 4.8 Relationship between total energy input of the CO_2 removal and $\%CO_2$ at the inlet

4.3 Furnace Modelling

The furnace transfers the heat energy to supply to the reformer unit. The furnace model composed of the mathematical model of heat energy of LPG combustion and heat loss of the exhaust gas as shown in Figure 4.9. The exhaust gas product is determined to investigate heat energy of the exhaust gas at the outlet of the furnace.

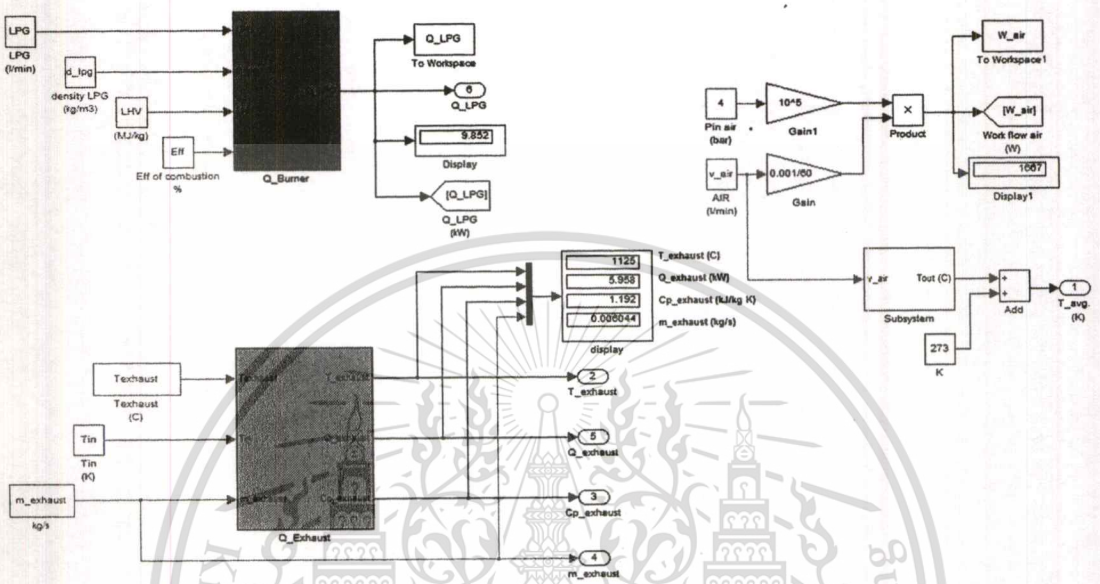

Figure 4.9 Mathematical modelling of furnace

Air used in the LPG combustion is calculated the pump power at 4 bar pressure inlet. The mass flow rate of the exhaust gas is determined from the empirical model of the exhaust gas. This empirical model is obtained from the experimental results which measure in %vol. of the exhaust gas. The mass flow rate of exhaust gas comprised of CO, CO_2 and O_2 as shown in Equation (4.2). This equation is used for calculating the heat energy of the exhaust gas model. Hydrocarbon is neglected because it is very small amount at the output.

$$\dot{m}_{exhaust} = \dot{m}_{CO} + \dot{m}_{CO_2} + \dot{m}_{O_2} \tag{4.2}$$

The efficiency of the furnace is calculated from heat usage in the reformer and heat of LPG combustion as shown in Equation (4.3).

$$\eta_{furnace} = \frac{\dot{Q}_{reformer}}{\dot{Q}_{LPG}} \times 100 \tag{4.3}$$

4.3.1 Furnace Modelling Results

In Figure 4.10, it shows the energy results at 85% excess air from the empirical models which are heat energy of LPG combustion, heat energy of the exhaust gas, and pumping power of air. The pumping power of air is the work done by pressurizing air at the inlet.

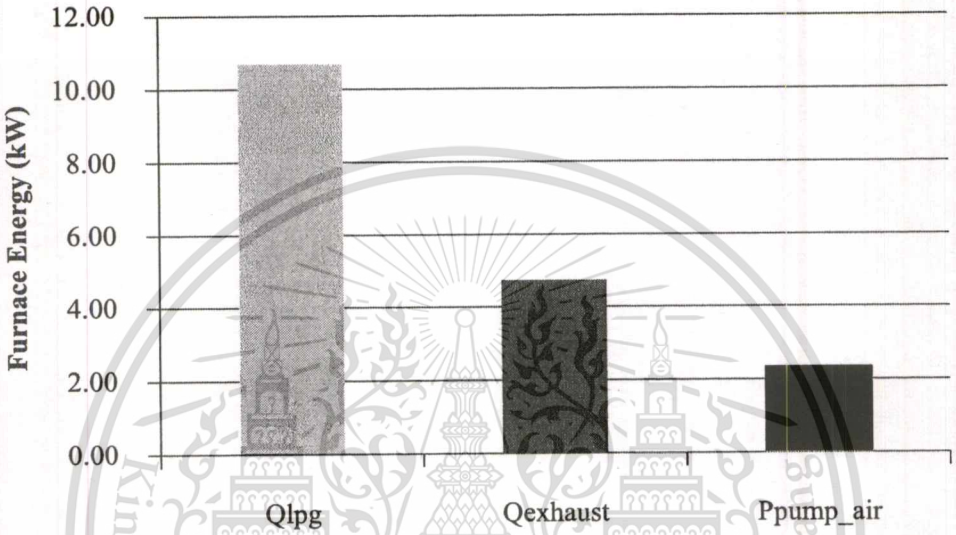

Figure 4.10 Energy on the furnace unit at 85%excess air of the LPG combustion

Heat energy of LPG combustion is the heat energy transferring to the reformer unit. It is about 10 kW energy input of the furnace. Heat energy of exhaust gas is a kind of heat loss of the furnace. From the experiment heat loss is about 5 kW.

Figure 4.11 shows the heat energy balance of the LPG combustion as mentioned in chapter 3 (Equation (3.11)). Heat energy of LPG is equal to 100% which can be separated into heat energy of exhaust gas, heat loss due to wall and heat energy of reformer.

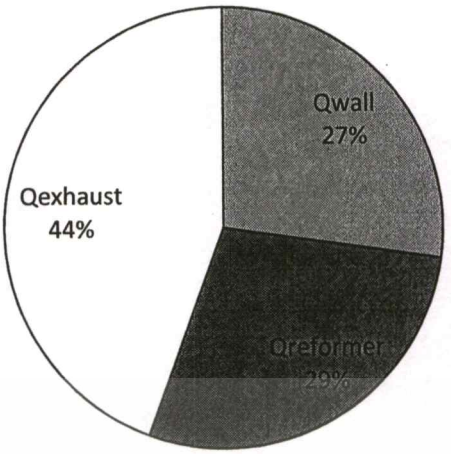

Figure 4.11 Heat energy balance of the LPG combustion

Heat loss from the exhaust gas and wall are estimate about 44% and 27%, respectively. Heat usage in the reformer is equal to 29% the heat of LPG combustion. Thus, the efficiency can be calculated which equals to 29%.

4.4 Reformer Modelling

The mathematical model of reformer comprised of; the reformate gas empirical model, the heat energy of reformer, the heat energy of boiler and heat loss at the outlet of reformer as shown in Figure 4.12. The heat energy of reformer calculated from the heat of reaction of stream methane reforming and water gas shift reaction. Steam is used as the reactant in both reactions. It needs heat energy to convert from water to steam at operation temperature. Thus, this energy is investigated as the heat energy of a boiler. After the reforming process is completed, the reformate gas has to be cooled down to the normal temperature before feeding into the SOFC. Therefore, the heat loss from the cooling down process can be calculated.

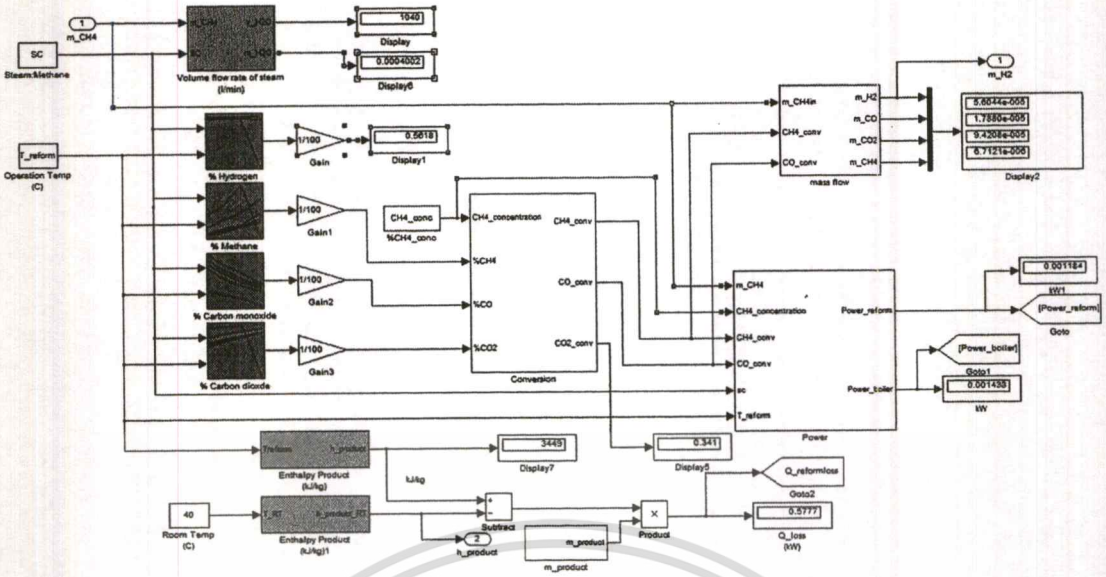

Figure 4.12 Mathematical modelling of reformer unit

4.4.1 Reformer Modelling Results

The energy conservation of reformer results following the S/C ratio is shown in Figures 4.13-4.16. They are heat energy of reformer ($\dot{Q}_{reforming}$), heat energy of water ($\dot{Q}_{boiler}$), heat loss at the outlet ($\dot{Q}_{loss}$). $\dot{Q}_{reforming}$ and $\dot{Q}_{boiler}$ are energy consumption unit and $\dot{Q}_{loss}$ is a waste energy in the reformer. The energy is calculated from the composition of reformate gas given in chapter 3. In Figures 4.13-4.16, there are slight increases in 3 lines of energy following an increase in temperature.

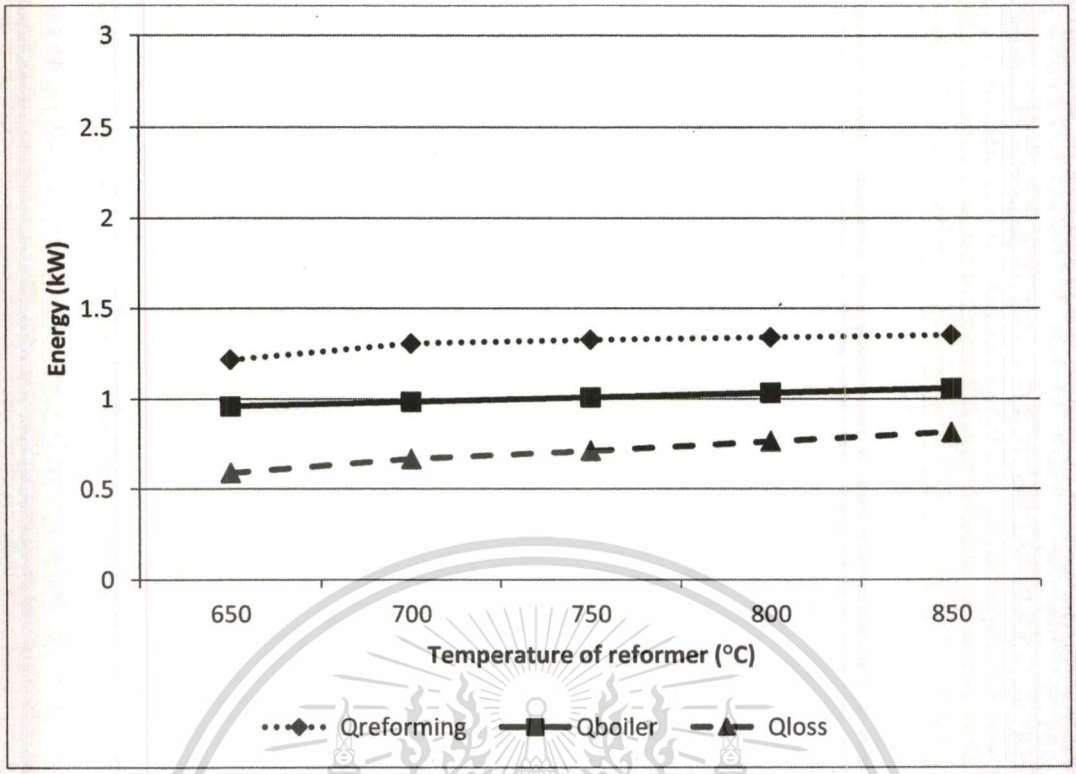

Figure 4.13 Relationship between energy conservation of reformer and temperature at S/C=2

In Figure 4.13, the dotted line has the highest the energy consumption. The heat energy of water is the solid line which is lower than the dotted line. It is at about 1 kW. The broken line has the lowest energy consumption. The heat energy of reforming process has a high energy consumption at S/C ratio = 2.

However, from Figures 4.14-4.16, they are different in order of energy. The heat energy consumption for water is the highest consumption. Next below is the heat energy of reformer and the heat loss, respectively.

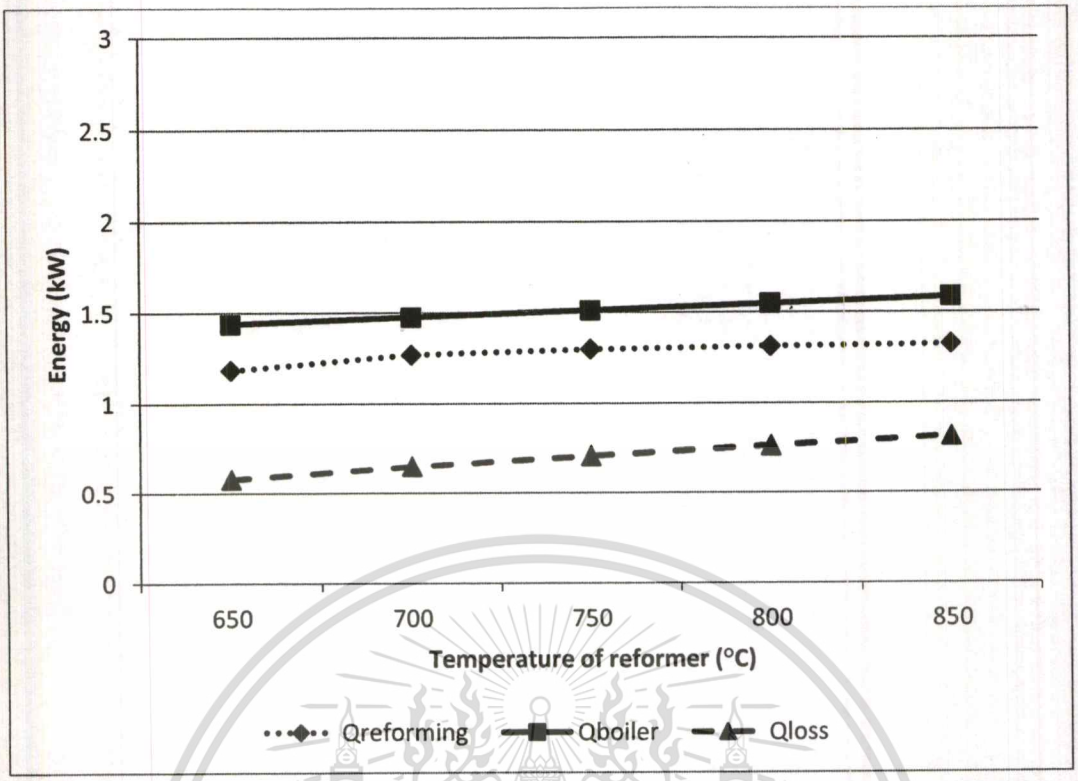

Figure 4.14 Relationship between energy conservation of reformer and temperature at S/C=3

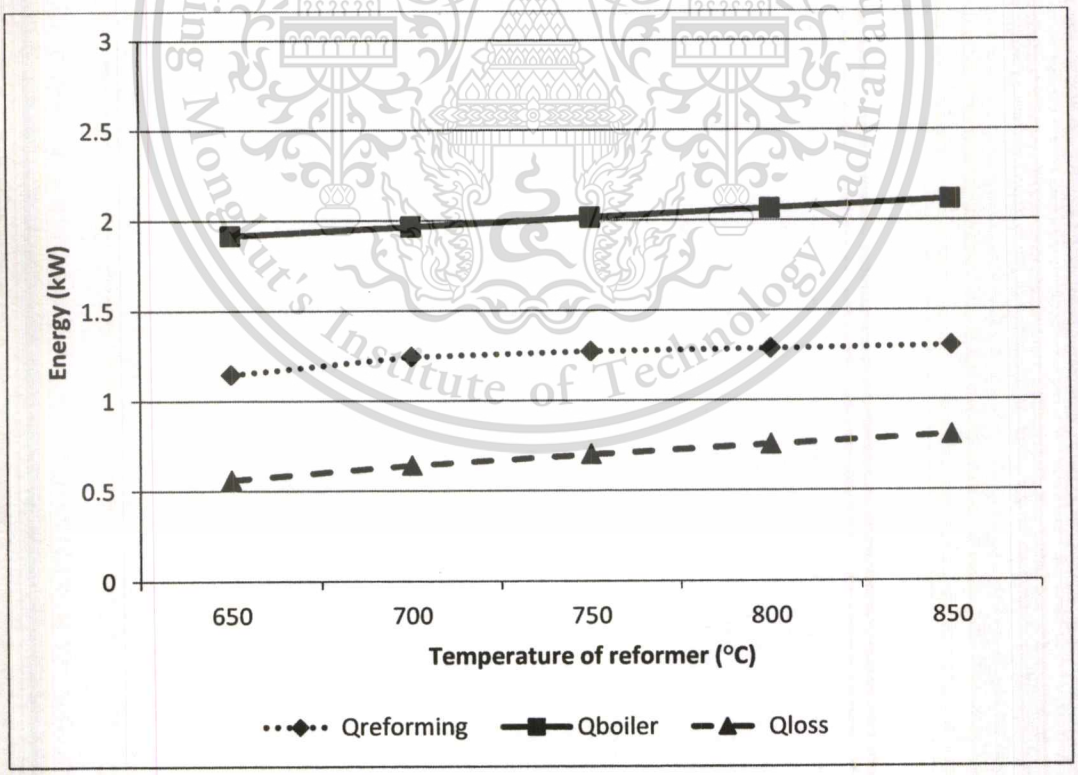

Figure 4.15 Relationship between energy conservation of reformer and temperature at S/C=4

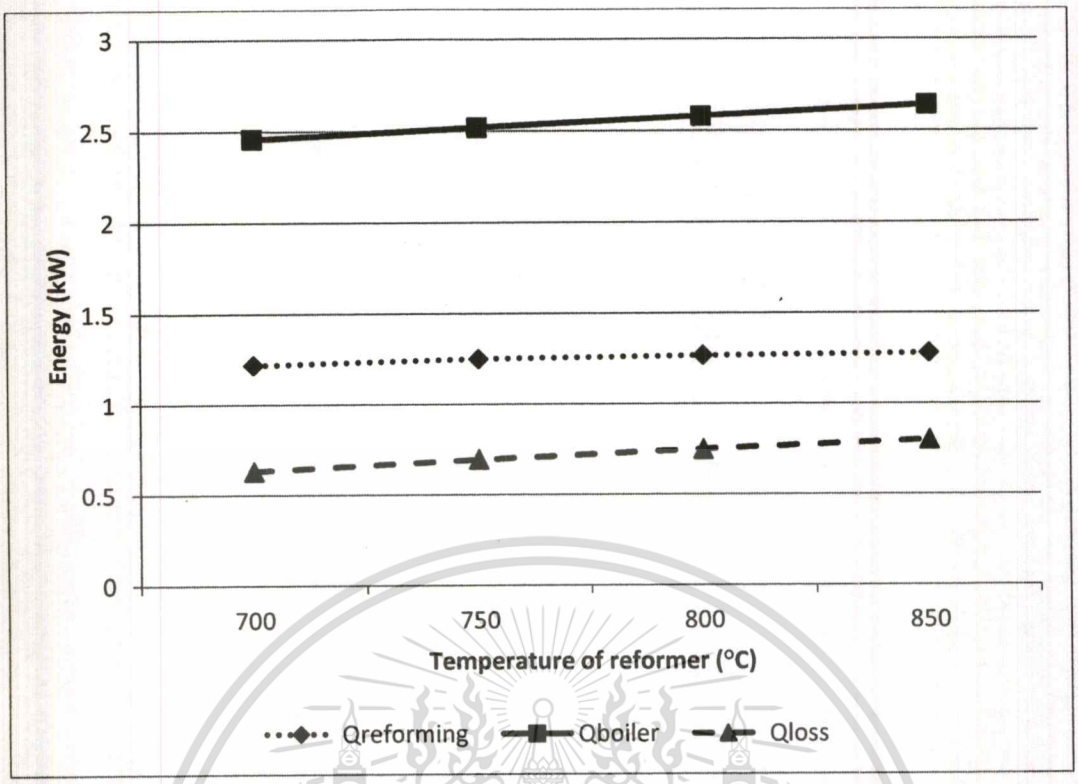

Figure 4.16 Relationship between energy conservation of reformer and temperature at S/C=5

When the results are compared with the S/C ratio, the high S/C ratio number has taken greater amount of energy. Especially, the heat energy of water consumed more energy to convert water to steam. If S/C ratio is a high the amount of water in the reformer system is high too. Other energies are slightly increased following the increase of S/C ratio.

In Figure 4.17, it is the relationship of reformate gas at the output of the reformer and the reformer operation temperature at 650, 700, 750, 800 and 850°C, respectively. The hydrogen production was investigated at S/C ratio = 3, because this ratio is the excess of water value which use less energy consumption for the reformer. The reformer must have has enough steam for the steam methane reforming and water gas shift process.

Considering the hydrogen production from Figure 4.17, the low operation temperature is given for the high hydrogen product. For example, at 650°C 62.19% of hydrogen can be produced. If the operation temperature is increased, the hydrogen product is decreased. These conditions of the reformer can produce hydrogen not less than 50% at the temperature between 650-850°C.

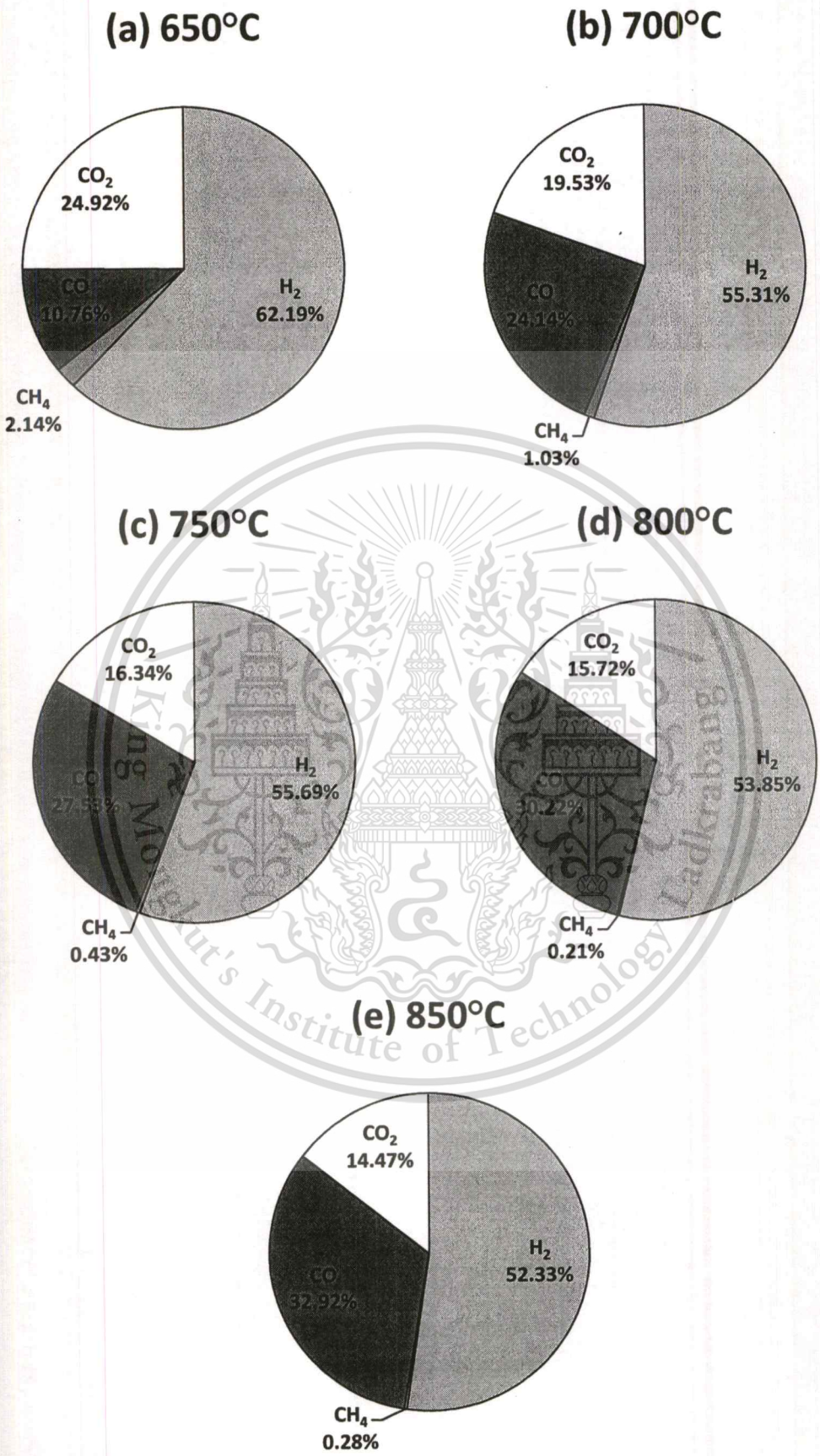

Figure 4.17 Chemical compositions of reformate gas results at S/C ratio = 3

4.5 SOFC Modelling

This model is an empirical model of the 1 kW electrical output of the SOFC as shown in Figure 4.18. The input of this model is mass flow rate of hydrogen obtained from the previous unit and current input to find the voltage drop in the SOFC and investigate the electrical power output of the SOFC. There is the heat energy in which the reformate gas receive from the heat input of the SOFC. The utilization of hydrogen on this unit is 60%.

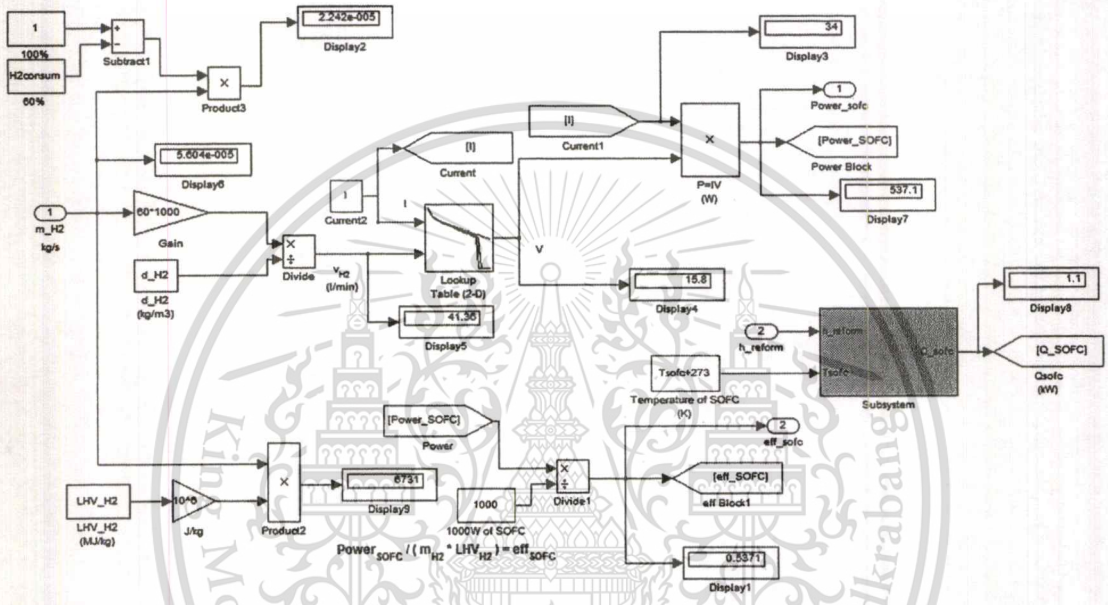

Figure 4.18 Mathematical modelling of the SOFC unit

4.5.1 SOFC Modelling Results

These results are set for the operation of 45% CO_2 by vol. composition of biogas. The reformer was operate at 85% excess air of furnace with S/C ratio = 3. The SOFC operated at 920°C. The result of the electrical power output is not reach 1 kW electrical output of the SOFC as shown in Figure 4.19. The SOFC unit is supposed to produce of 1 kW electrical output but the real electrical output was about 0.5 kW only. The similar electrical power output may occur at equilibrium of the reaction between hydrogen and oxygen.

The actual cause of underperformed result is due to cracking of the cells inside the SOFC bundle. When the SOFC was disassembled, the crack was found. This reason makes the electrical power output less than the 1 kW electrical output specifications.

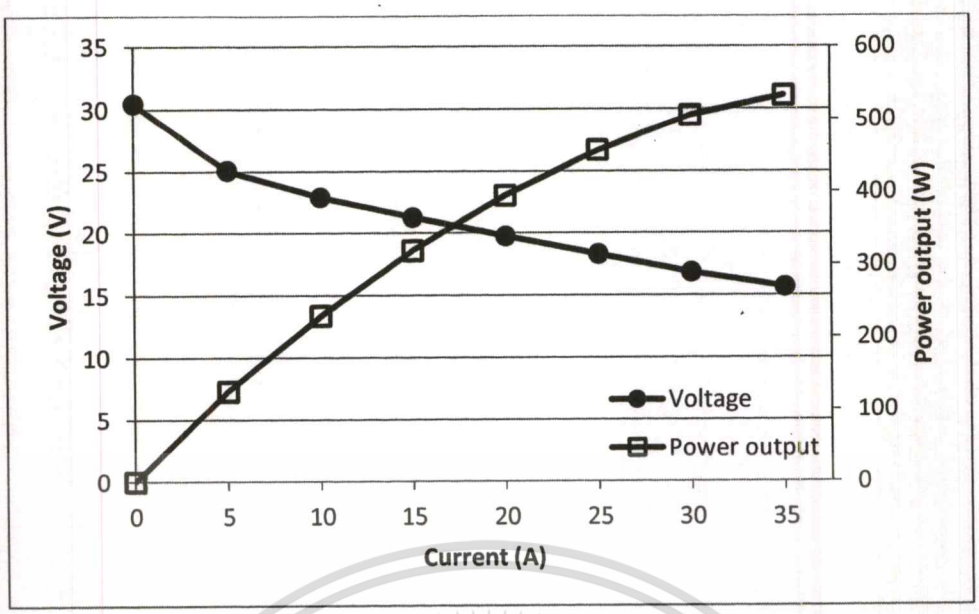

Figure 4.19 Electrical power output of the SOFC system

4.6 The SOFC System Results and Discussion

This is the overall energy consumption of the SOFC unit as shown in Figure 4.20. It uses the same condition with the pilot scale of the SOFC system detailed as follows; 45%CO_2 composition of biogas at the inlet, 10 kW furnace at 85% excess air, 650°C of reformer operation at S/C ratio = 3 and 920°C SOFC operation.

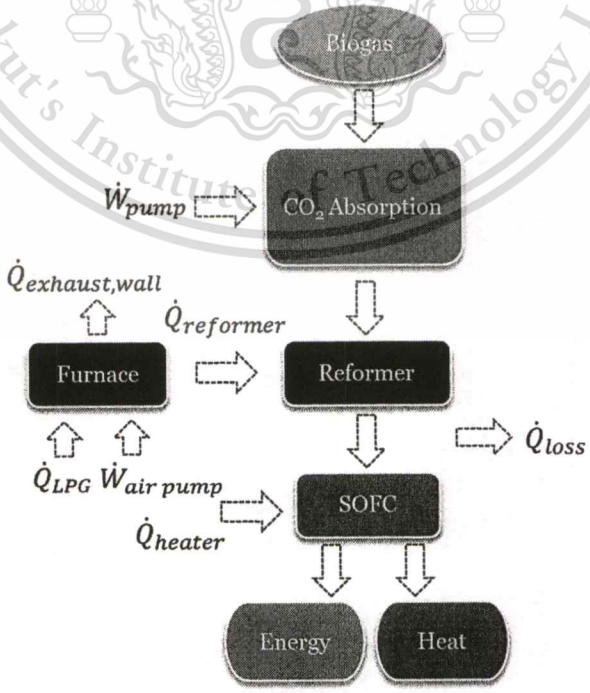

Figure 4.20 SOFC system flowchart

In Figure 4.21, the energy consumption is separated into sub-units of (a) CO_2 removal, (b) furnace, (c) reformer, and (d) SOFC, respectively. First, (a) the CO_2 removal has 2 parts of energy consumption which are 26% of electrical power of pump and 74% of chemical energy. Second, (b) the furnace produces 10 kW of LPG combustion, it can be estimated as 82% of energy on the unit. There are 29% heat energy of the reformer, 27% heat loss due to wall, and 44% heat loss from the exhaust gas as shown in Figure 4.11. Only 18% of energy from the furnace is the pumping power of air. Next, (c) the reformer has the heat energy for the hydrogen production and the steam production. These are followed by 34% hydrogen production and 42% steam production. The heat energy loss from the reformer is equal to 24%. Finally, (d) the SOFC unit has 3 sections which are the heat energy for hydrogen, the electrical power input for heater and the electrical power output. The energy input of the SOFC is equal to 8%Q_{SOFC} and 92%P_{heater}.

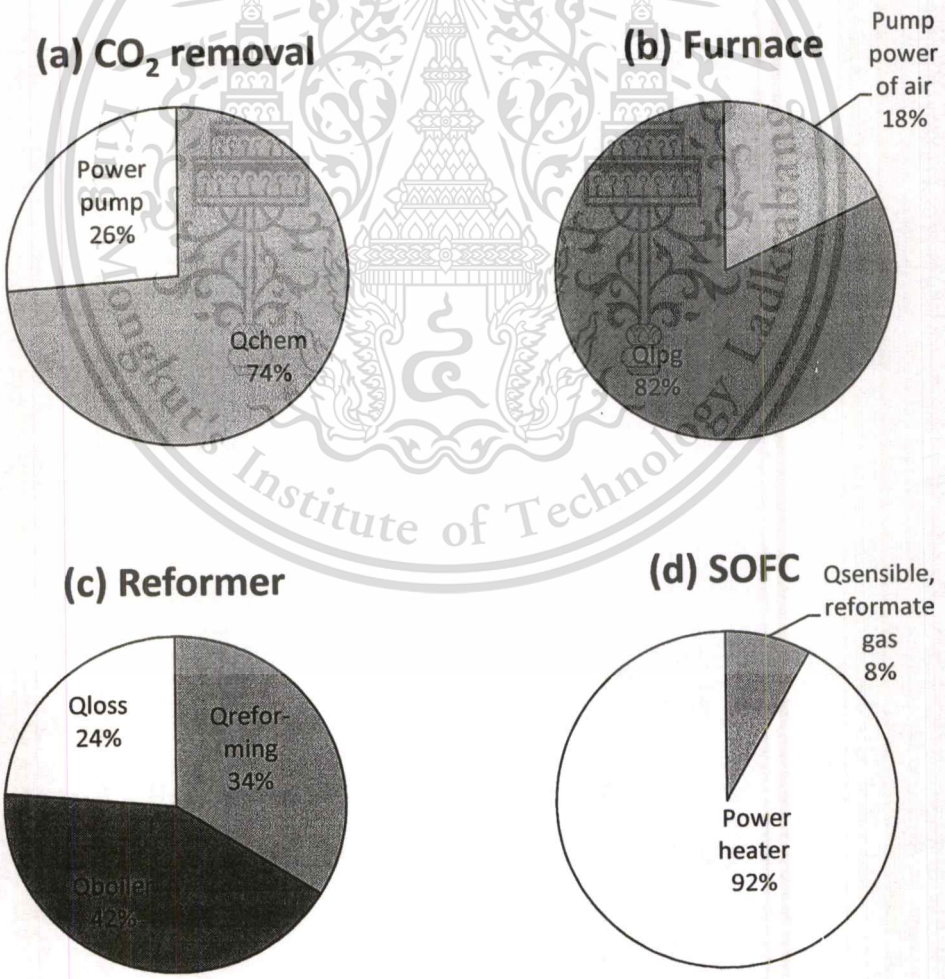

Figure 4.21 Energy consumption of the sub-unit in the SOFC system

The electrical output is 4% from the total energy input in the SOFC as shown in Figure 4.22. Other 96% is energy loss due to heat loss. The efficiency of the SOFC unit is equal to 7.53%.

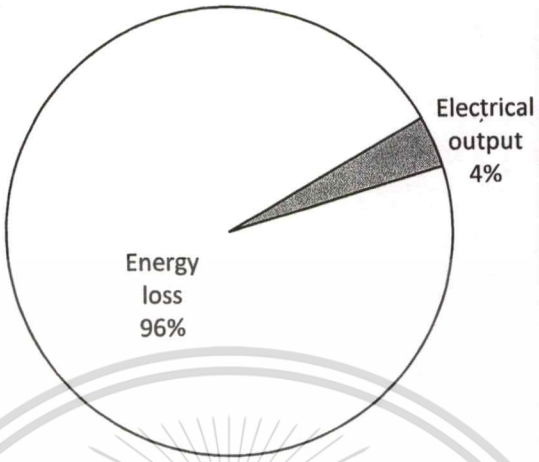

Figure 4.22 Energy output of the SOFC unit

Figure 4.23 shows energy consumption of hydrogen production system. The hydrogen production is comprised of CO_2 removal, furnace and reformer unit. It can be separated into 18% of mechanical input and 82% of heat of reaction.

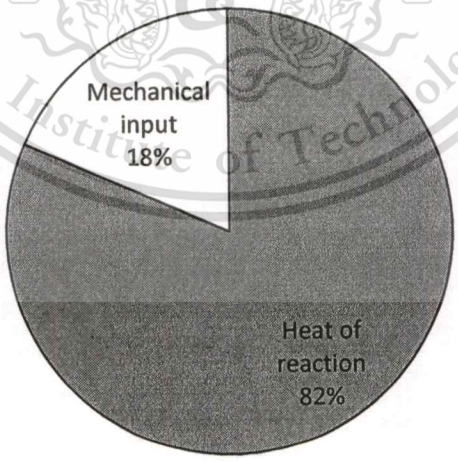

Figure 4.23 Energy consumption of hydrogen production system

The output of this system is hydrogen. It is calculated as heat energy of hydrogen as shown in Equation (4.4).

$$\dot{Q}_{H_2} = \dot{m}_{H_2} \times LHV_{H_2} \tag{4.4}$$

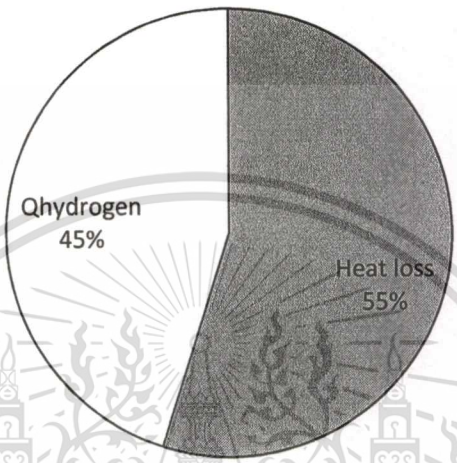

Figure 4.24 Energy output of hydrogen production system

Figure 4.24 shows energy output of hydrogen production system which is 45% heat energy of hydrogen and 55% of heat loss. Heat loss is heat from the exhaust gas, cooling of reformate gas at the outlet and heat transfer due to wall.

The overall energy input occurs in the SOFC system including chemical reaction, mechanical input and heat input are represented in Figure 4.25. All the sub-units are based on a chemical reaction. Thus, the chemical reaction consumed energy for the consumption of the SOFC system as shown in this pie chart which is equal to 42% of all energy. The heat supplied for the SOFC bundle about 48%. Only 10% of the energy consumption in the SOFC system is for the mechanical input.

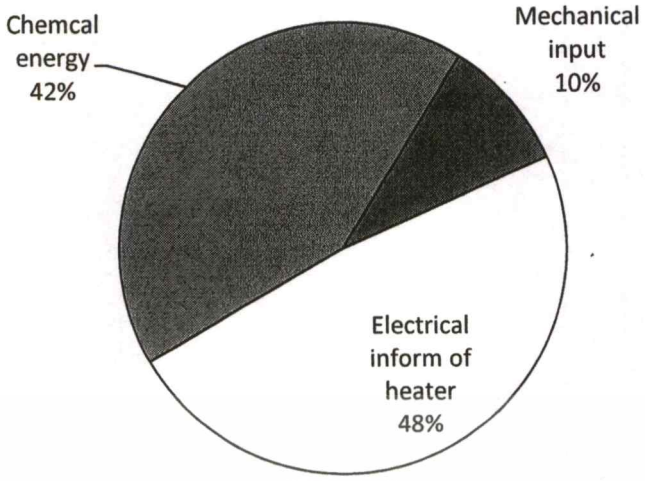

Figure 4.25 Overall energy consumption of the SOFC system

The SOFC system has the energy loss about 98% which are heat losses from the furnace, the reformer and the SOFC unit. The electrical power output from the SOFC system estimate only 2% from the overall system as shown in Figure 4.26. The heat loss from the furnace and reformer unit can be recovered by preheating the reactant before feeding into the reformer.

$$E_{total\ input} - E_{output} = E_{loss} \tag{4.5}$$

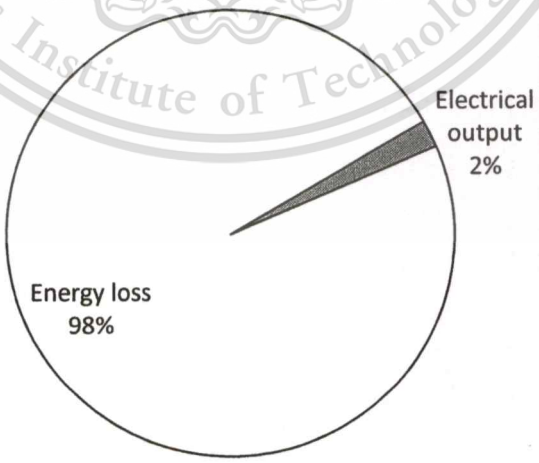

Figure 4.26 Overall energy output of the SOFC system

CHAPTER 5

CONCLUSIONS AND SUGGESTION

5.1 Conclusion and Suggestion

The energy conservation of the SOFC system has been investigated by using a computer program. The empirical model of the sub-units is set from the real experimental results. These results come from the pilot scale of the sub-units which are CO_2 removal, furnace, reformer and SOFC. Therefore, the empirical model simulated the operation of the real SOFC system using biogas fuel.

The CO_2 removal of the fuel processing for biogas consumes electrical power for pumping NaOH solution only while heat from the chemical reaction is not high enough to preheat gases. Thus, it can be neglected. On the other hand, the NaOH solution consumption is very high following the $\%CO_2$ in biogas because this unit cannot re-circulate NaOH solution. When NaOH solution cannot absorb CO_2 anymore, it is discarded. Therefore the chemical energy of this reaction has been taken into account.

A furnace is a heat supply for the reformer unit. It uses LPG as a fuel, but there is also a heat loss. If it can be used to preheat methane and water before feeding into the reformer, it will be advantageous for the SOFC system. It can then reduce the heat energy consumption in the reformer unit.

The hydrogen production unit, requires energy for the steam methane reforming and water gas shift reaction. Also with H_2O, it requires heat energy for convert water-to-steam. If S/C ratio increases, the heat energy is consumed higher. There is a heat loss at the outlet of the reformer. Therefore, it can be recovered for use in the system in a similar manner as energy loss from the furnace. From the start until this process of the SOFC system, 1 kW H_2 production consumes 3.8 kW energy input.

For the final unit, the SOFC can produce only 0.53 kW of 1 kW electrical performance. Because the problem of cell cracks inside the SOFC stack. The efficiency of the SOFC is equal to 7.53%. If the problem can be solved, the SOFC will achieve higher performance. This unit use high electrical power heater. If the SOFC can use another heat supply source for example heat from the furnace, it will reduce energy consumption of the SOFC unit.

The SOFC system is waste the energy mostly through the heat loss 98%. The energy output of the system is only 2% when compared with the energy input and the loss which occur in the system. There is more to do on energy management of this SOFC system by using biogas to get higher performance.

RERERENCES

Argonne National Laboratory. "Basic Research Needs for the Hydrogen Economy." U.S. Department of Energy, Office of Science Laboratory. 15 May 2003.

Aroonwilas, A. and Veawab, A. 2004. "Characterization and comparison of the CO_2 absorption performance into single and blended alkanolamines in a packed column." **Industrial and Engineering Chemical Research**. Vol. 43(9), April 2004, pp. 2228-2237.

Aroonwilas, A., Chakma, A., Tontiwachwuthikul, P. and Veawab, A. 2003. "Mathematical modeling of mass-transfer and hydrodynamics in CO_2 absorbers packed with structured packings." **Chemical Engineering Science**. Vol. 58(17), September 2003, pp. 4037-4053.

Aroonwilas, A., Tontiwachwuthikul, P. and Chakma, A. 2001. "Effects of operating and design parameters on CO_2 absorption in columns with structured packings." **Separation and Purification Technology**. Vol. 24(3), September 2001, pp. 403-411.

Astarita, G., Savage, D. W., and Longo, J. M., **Chem. Eng. Sci.** Vol. 36, 1981. pp. 581.

Austin, G.T. "Industrial gas: Hydrogen." **Shreve's Chemical Process Industrial.** 5th ed. Singapore : McGraw Hill. 1984. pp. 106-112.

Brettschneider, O., Thiele, R., Faber, R., Thielert, H. and Wozny, G. 2003. "Experimental investigation and simulation of the chemical absorption in a packed column for the system $NH_3 - CO_2 - H_2S - NaOH - H_2O$." **Separation and Purification Technology**. Vol. 39(3), November 2004, pp. 139-159.

Chan, S.H., Low, C.F. and Ding, O.L. 2002. "Energy and exergy analysis of simple solid-oxide fuel-cell power systems." **Journal of Power Sources.** Vol. 102, 2002, pp. 188-200.

Crabtree, G.W., Dresselhaus, M.S. and Buchanan, M.V. "The Hydrogen Economy." **Physics Today**. December 2004.

Dey, A. and Aroonwilas, A. 2009. "CO_2 absorption into MEA-AMP blend: mass transfer and absorber height index." **Energy Procedia**. Vol. 1(1), February 2009, pp. 211-215.

Esper, B., Badura, A. and Rögner, M. "Photosynthesis as a Power Supply for (bio-) Hydrogen Production." **Trends Plant Sci.** Vol. 11, 2006. pp. 543–549.

Fleischer, C., Becker, S. and Eigenberger, G. "Detailed Modeling of the Chemisorption of CO_2 into NaOH in a Bubble Column." **Chemical Engineering Science.** Vol. 51, no. 10, 1996. pp. 1715-1724.

Grove, W.R. **Phil. Mag.** Vol. 14, 1839. pp.127-130.

Halabi, M.H., de Croon, M.H.J.M., van der Schaaf, J., Cobden, P.D. and Schouten, J.C. "Modeling and Analysis of Autothermal Reforming of Methane to Hydrogen in a Fixed Bed Reformer." **Chemical Engineering Journal.** Vol. 137(3), 15 April 2008. pp. 568-578.

Hirschenhofer, J.H., Stauffer, D.B., Engelman, R.R. and Klett, M.G. **Fuel Cell Handbook.** 4th ed. US Department of Energy Federal Energy Technology Center, Morgantown, WV : Business Technology Books. 1998.

Hoang. D.L., Chan, S.H. and Ding, O.L. "Kinetic and Modelling Study of Methane Steam Reforming Over Sulfide Nickel Catalyst on a Gamma Alumina Support." **Chemical Engineering Journal.** Vol. 112, June 2005.

Hullu, J.D., Maassen, J.I.W., Meel, P.A., Shazad, S., Vaessen, J.M.P., Bini, L. and Reijenga J.C. 2008. "Comparing Different Biogas Upgrading Techniques" **Final Report Eindhoven University of Technology.** July 2008.

Jeffries-Nakamura, B., Narayanan, S.R., Valdez, T.I. and Chun, W. "Making Hydrogen by Electrolysis of Methanol." **JPL New Technology Report NPO – 19948, NASA Tech Briefs.** Vol. 26, no. 6, 2002.

Khemthong, B. **"Model Development and Validation of Steam Methane Reforming of Simulated Biogas for Solid Oxide Fuel Cell System."** M.Eng. Chemical Engineering Program Sirindhorn International Institute of Technology Thammasat University. 2009.

Kohl, A. and Nielsen, R. **Gas Purification.** 5th ed. Texas : Gulf Publish Company. 1997.

Kullavanijaya, P., Paepatung, N., Laopitinun, O., Noppharatana, A. and Chaiprasert, P. "An Overview of Status and Potential of Biomethanation Technology in Thailand." **King Mongkut's University of Technology Thonburi Research and Development Journal.** Vol. 30, no. 4, Oct.-Dec. 2007. pp. 293-700.

Lawal, A., Wang, M., Stephenson, P. and Yeung, H. "Dynamic Modelling of CO_2 Absorption for Post Combustion Capture in Coal-Fired Power Plants." **Fuel.** Vol. 88, no. 12, Dec. 2009. pp. 2455-2462.

Mangalapally, H.P., Notz, R., Hoch, S., Asprion, N., Sieder, G., Carcia, H. and Hasse, H. 2009. "Pilot plant experimental studies of post combustion CO_2 capture by reactive absorption with MEA and new solvents." **Energy Procedia**. Vol. 1(1), February 2009, pp. 963-970.

NASA Tech Briefs. "Improved Fabrication of Electrodes for Methanol Fuel Cells." (NPO-19941), Vol. 23, no. 4, April 1999. pp. 38.

Piroonlerkgul, P., Assabumrungrat, S., Laosiripojana, N. and Adesina, A.A. 2008. "Selection of appropriate fuel processor for biogas-fuelled SOFC system." **Chemical Engineering Journal.** Vol. 140(1-3), July 2008. pp. 341-351.

Piroonlerkgul, P., Laosiripojana, N., Adesina, A.A. and Assabumrungrat, S. 2008. "Performance of biogas -fed solid oxide fuel cell systems integrated with membrane module for CO_2 removal." **Chemical Engineering and Processing: Process Intensification.** Vol. 48(2) February 2009. pp. 672-682.

Pollution Control Department. 2001.

Seitarides, Th., Athanasiou, C. and Zabaniotou, A. 2008. "Modular biomass gasification-based solid oxide fuel cell (SOFC) for sustainable development." **Renewable and Sustainable Energy Reviews.** Vol. 12(5), June 2008, pp. 1251-1276.

SFC Smart Fuel Cell AG. 2009. www.sfc.com

Shiratori, Y., Oshima, T. and Sasaki, K. 2008. "Feasibility of direct-biogas SOFC." **International Journal of Hydrogen Energy.** Vol. 33(21), November 2008, pp. 6316-6321.

Sonntag and Van Wylen .Fundamentals Thermodynamics 6th ed., John Wiley & Sons, Inc. 2003.

Suwanwarangkul, R., Croiset, E., Entchev, E., Charojrochkul, S., Pritzker, M.D., Fowler, M.W., Douglas, P.L., Chewathanakup, S. and Mahaudom, H. "Experimental and Modeling Study of Solid Oxide Fuel Cell Operating with Syngas Fuel." **Journal of Power Sources.** Vol. 161, 2006. pp. 308-322.

T-Raissi, A. and Block, D. "Hydrogen: Automotive Fuel of the Future." **IEEE Power & Energy.** Vol. 2, no. 6, Nov.-Dec. 2004. pp. 43.

U.S. Department of Energy. **Hydrogen Program Annual Merit Review Proceedings.** 2008. www.hydrogen.energy.gov/annual_review08_proceedings.html

Van herle, J., Marechal, F. and Leuenberger, S. 2004. "Process flow model of solid oxide fuel cell system supplied with sewage biogas." **Journal of Power Sources.** Vol. 131(1-2), May 2004, pp. 127-141.

Van herle, J., Marechal, F., Leuenberger, S and Favrat, D. 2003. "Energy balance model of a SOFC cogenerator operated with biogas." **Journal of Power Sources.** Vol. 118, 2003, pp. 375-383.

Van herle, J., Membrez, Y. and Bucheli, O. 2003. "Biogas as fuel source for SOFC co-generators." **Journal of Power Sources.** Vol. 127(1-2), March 2004, pp. 300-312.

Wellinger A, Lindeberg A. "Biogas Upgrading and Utilization." **Task 24: Energy from Biological Conversion of Organic Wastes.** 1999. pp. 1–19.

Wiens, B. Consulting Inc. Metro Vancouver BC Canada. http://www.benwiens.com /energy4.html#energy4.10

Wittaya, W., Punbusayakul, N., Charoensuk, J. and Charojrochkul, S. "Effect of staged air on temperature distribution in a 10 kW porous burner." The 24th Conference of the Mechanical Engineering Network of Thailland, October 20-22, 2010 Ubonratchathani.

Won, J.C., Jong, B.S., Sang, Y.J., Jong, H.J. and Kwang, J.O. 2009. "Removal characteristics of CO_2 using aqueous MEA/AMP solutions in the absorption and regeneration process." **Journal of Environmental Sciences.** Vol. 21(7), 2009, pp. 907-913.

Xu, J. and Froment, G.F. "Methane Steam Reforming I: Intrinsic Kinetics." **AIChE journal.** Vol. 35, no. 1, January 1989. pp. 97-103.

Yeh, J.T. and Pennline, H.W. 2001. "Study of CO_2 absorption and desorption in a packed column" **Energy Fuels.** Vol. 15(2), February 2001, pp. 274-278.

APPENDIX A

CONFERENCE PROCEEDING

International Conference on Green and Sustainable Innovation 2009
December 2 – 4, 2009, Chiang Rai

Study Behaviour of CO_2 Absorption in Packed Bed Column form Synthesis Biogas to Produce Hydrogen for SOFC Operation

G. Pornsopin[1], N. Punbusayakul[3], T. Uttamote[4], K. Hanamura[5], S. Charojrochkul[6], and J. Charoensuk[2,*]

[1]Department of Automotive Engineering, International College and
[2]Department of Mechanical Engineering, Engineering Faculty, King Mongkut's
Institute of Technology Ladkrabang, Chalongkrung Road, Bangkok, 10520
[3]Department of Mechanical Engineering, Engineering Faculty, Mahanakorn University of Technology, Bangkok Thailand, 10530
[4]Department of Chemical Engineering, Sirindhorn International Institute of Technology, Thammasat University
[5]Department of Mechanical and Control Engineering, Tokyo Institute of Technology, Tokyo, Japan
[6]National Metal and Materials Technology Center, 114 Thailand Science Park,
Paholyothin Road, Klongluang, Pathumthani 12120
*Email: kcjarruw@kmitl.ac.th

Abstract

Biogas is used as a primary fuel and needed to be purified before entering to the hydrogen reforming unit of a Solid Oxide Fuel Cell (SOFC) system. Carbon dioxide (CO_2) is one of compositions needed to be removed. In this experimental study for a pilot plant scale, a CO_2 absorption unit is used to treat the gas mixture with sodium hydroxide (NaOH) solution. Normally, biogas contains about 50-60% methane (CH_4), 40-50% CO_2. The quality of biogas depends on the concentration of CO_2. Given that the CO_2 mixture with air (simulated biogas) is treated in an absorption column in which the concentration of NaOH solution is employed using the calculated values obtained from the chemical reaction theory with CO_2. The discussion of the results leads to an acceptable recommended CO_2 concentration and pH ranges for the given process. This is used as a criterion for allowable concentration of CO_2 at 5%. The CO_2 absorption unit is capable to operate within the designated operating condition. The experimental results show that the concentrations of CO_2 have effected the CO_2 absorption operation. If the CO_2 concentration at the inlet is high, the CO_2 absorption unit operation time will decrease. This study can predict the limit of absorbent used to absorb CO_2 concentration in the synthesis gas or biogas itself.

Keywords: NaOH, CO_2, Absorption, SOFC, Biogas

1. Introduction

Biogas is a source of renewable energy which is normally produced from waste in farm or domestic animal. Biogas can be applied for use in a solid oxide fuel cell to generate electricity [1-6] because solid oxide fuel cell can be operated using flexible hydrocarbon fuel. In our study, the solid oxide fuel cell system uses biogas as a fuel

and its needs to be reformed to hydrogen before feeding into the SOFC. The main compositions of biogas are methane, carbon dioxide and sulphur dioxide. Before reforming, carbon dioxide should be removed from the biogas composition to reduce excessive concentration of carbon dioxide which causes dilution of reaction and reduce hence the concentration of hydrogen in the reforming process.

The CO_2 removal is based on a chemical reaction absorption by using alkaline salt solution [7] in which the absorbent for carbon dioxide is located in a packed bed column. Spray of aqueous solution containing sodium hydroxide is used for our carbon dioxide absorption.

The CO_2 removal application is studied to optimize the carbon dioxide absorption process at 45, 55, 60 and 70 % of CO_2 concentration using a gas chromatography to measure CO_2 concentration at the outlet.

2. Experimental

2.1 CO_2 absorption unit

The CO_2 absorption unit diagram is shown in Fig. 1. The absorption column [8-15] is 4 inch in diameter packed with raschig ring packing of 1.5 m high to increase the surface area of gas-liquid contact. The absorption column is designed for a counter flow pattern. At the top of the column locates a spray nozzle to spray solution into the column. NaOH solution tank supplies and receives absorbed solution in the experiment [10]. Gas and liquid flow rates are calibrated using air and liquid rotameters. The CO_2 analysis is carried out using the gas chromatography (GC) which measures the CO_2 concentration from collected gas.

2.2. Experimental procedure

The experiment setup is shown in table 1. This experiment used synthesis gas between CO_2 and air as a simulated biogas. In various concentration of the mixed gas can be quantified using a GC. Then, each gas flow was adjusted at 10 l/min to mix in the line to be 20 l/min and to flow into the column as shown in Fig 1.

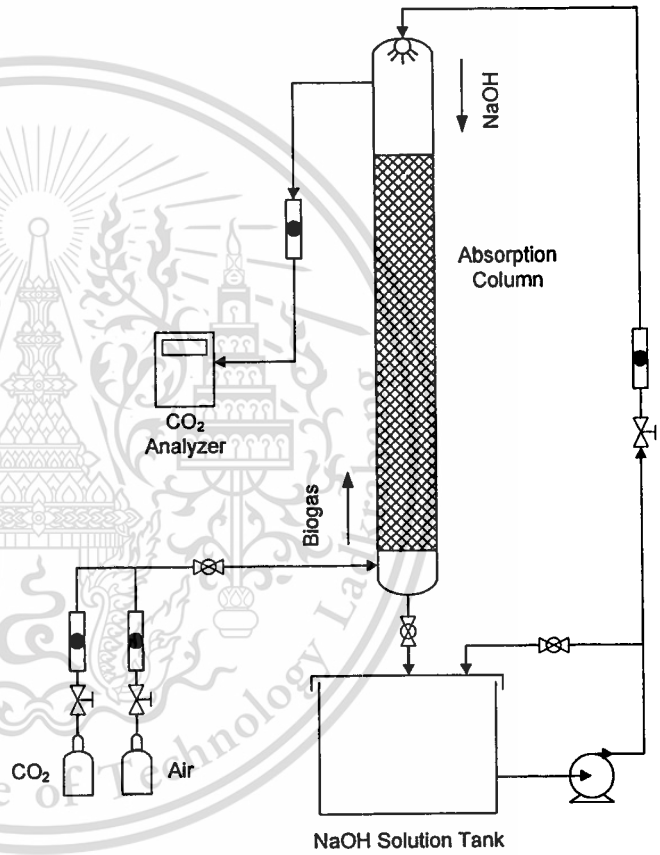

Fig. 1 CO_2 absorption unit

Leave the mixed gas blending for 15 minutes. For aqueous salt solution, 6200 gram of NaOH is prepared with 50 litres of water to obtain 3 molar concentrations. The solution is pumped up to the top of the column at 10 l/min and sprayed in to the column. Mixed gas and NaOH solution are flown in the opposite directions. A chemical

reaction between CO_2 and aqueous salt solution occurs in the packed bed column. And then after the solution is used in the reaction, it flows back to the NaOH solution tank and is circulated until the concentration of NaOH solution decrease which cannot absorb CO_2 anymore.

Basic chemical reaction of CO_2 and aqueous salt solution is represented by the following reaction [7].

$$CO_{2\,(g)} + 2NaOH_{\,(aq)} \Rightarrow Na_2CO_{3\,(s)} + H_2O_{\,(l)}$$

(Exothermic reaction) Eq. (1)

Products of the absorption reaction are disodium carbonate (Na_2CO_3) and water (H_2O). This is exothermic reaction which releases thermal energy. Heat absorption usually takes place about 55 °C.

The experimental product gases obtained from the reaction are collected every 15 minutes and analyzed using a GC to identify the concentration of gas compositions until CO_2 can be detected. The pH of the aqueous salt solution was checked using a pH paper [10]. Before starting the experiment, the pH is 14. If CO_2 occurs in the product gas, the pH of the solution is changed.

3. Results and Discussion

Effects of CO_2 concentration on CO_2 absorption are compared to identify the time limit in which the absorbent can absorb CO_2 at each rate. The results show both pH value and CO_2 concentration (%) at the outlet with time on Figs. 2 – 5. Results from Fig. 2 show that the absorption rate of CO_2 decreases when the resident time of absorbent is increased to 3.15 hours. After at the CO_2 outlet in 15 minutes later has increased at a slow gradient. In the end, CO_2 outlet has increased with a rapid gradient.

Table 1 Experimental setup data

	Case 1	Case 2	Case 3	Case 4
Gas				
CO_2 (% by volume)	45	55	60	70
Air (% by volume)	55	45	40	30
Flow rate (l/min)	20	20	20	20
Inlet pressure (Bar)	1	1	1	1
Liquid (NaOH)				
Concentration (M)	3	3	3	3
Volume (l)	50	50	50	50
Flow rate (l/min)	10	10	10	10

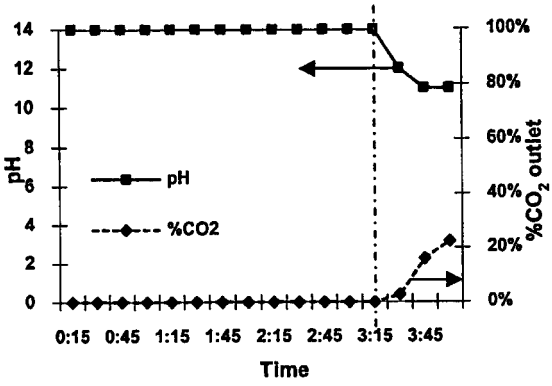

Fig. 2 Relationship between CO_2 at the outlet and pH with time at 45/55 CO_2/Air ratio

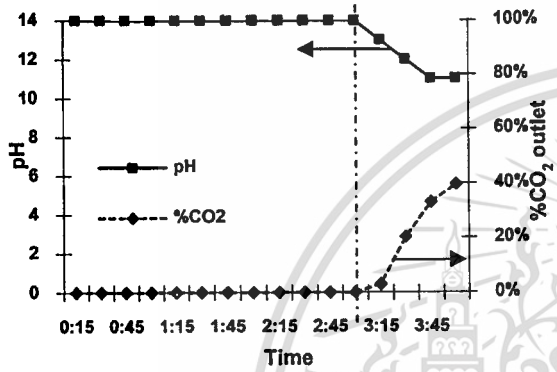

Fig. 3 Relationship between CO_2 at the outlet and pH with time at 55/45 CO_2/Air ratio

On the other hand, the CO_2 absorption unit may use a pH indicator to check the concentration of NaOH solution. The results show that pH value decrease from 14, after 3.00 hours, resident time at 55/45 CO_2/Air ratio by volume. pH line has rapidly decreased in a linear pattern caused by a precisions measured from the pH indicator as shown in Fig. 3.

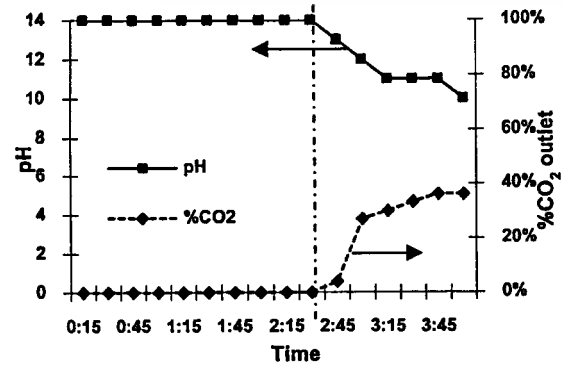

Fig. 4 Relationship between CO_2 at the outlet and pH with time at 60/40 CO_2/Air ratio

In the case of 60/40 CO_2/Air ratio has the same behaviour as 45/55 and 55/45 CO_2/Air ratios. The pH value starts to decrease from 14 rapidly at 2.30 hours. In the same time, CO_2 content at the outlet is found to increase.

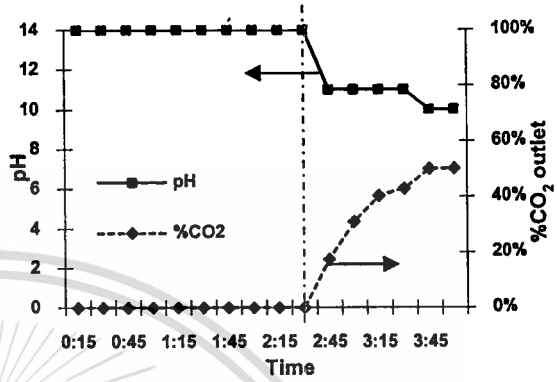

Fig. 5 Relationship between CO_2 at the outlet and pH with time at 70/30 CO_2/Air ratio

In the case of 70/30 CO_2/Air ratio, the concentration of CO_2 at the outlet was measured after 2.30 hours. Since, the gas collecting time was set at 15 minutes interval, the CO_2 leaves the absorption column during 2.15-2.30 hours. The concentration of CO_2 at 70 vol. % was obtained by interpolation at 2.23 hours.

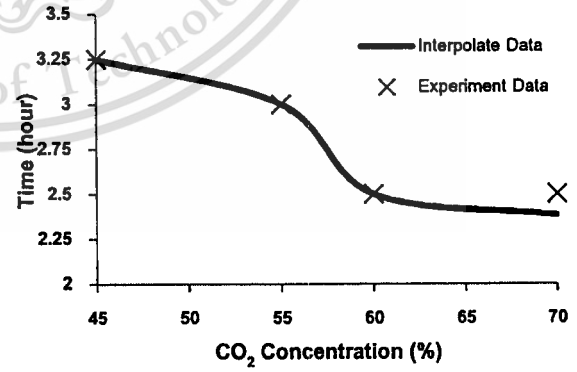

Fig. 6 Relationship between time and CO_2 concentration at the inlet

The Y axis as shown in Fig 6. is time in which the CO_2 content at the outlet is detected. This relationship shows a trend of NaOH solution

which reaches a limit to absorb CO_2 in various CO_2 concentrations at the inlet. The relationship between time and CO_2 concentration at the inlet is shown in Eq. (2).

$$T_{NaOH/C_{CO_2}} = 0.0004{C_{CO_2}}^3 - 0.0747{C_{CO_2}}^2 + 4.1663C_{CO_2} - 72. \quad \text{Eq. (2)}$$

Where,

$T_{NaOH/C_{CO_2}}$ · Limit time of NaOH solution on CO_2 concentration at the inlet

C_{CO_2} CO_2 concentration at the inlet

4. Conclusions

The CO_2 absorption in a packed bed column is based on a chemical reaction between CO_2 and NaOH. The results show a relationship between time and CO_2 concentration at the outlet. The results were compared with the CO_2 concentration at the inlet, the limit time of absorbent used to absorb CO_2 concentration in the synthesis biogas or biogas itself can then be predicted. In addition, the operation time of CO_2 absorption unit is identified which use remove CO_2 before reforming gas in the SOFC system.

5. Acknowledgements

National Metal and Materials Technology Center (MTEC) is acknowledged for research support.

6. References

[1] Piroonlerkgul, P., Laosiripojana, N., Adesina, A.A. and Assabumrungrat, S. (2008). Performance of biogas -fed solid oxide fuel cell systems integrated with membrane module for CO_2 removal, *Chemical Engineering and Processing: Process Intensification*, vol. 48(2), February 2009, pp. 672 – 682.

[2] Piroonlerkgul, P., Assabumrungrat, S., Laosiripojana, N. and Adesina, A.A. (2008). Selection of appropriate fuel processor for biogas-fuelled SOFC system, *Chemical Engineering Journal*, vol. 140(1-3), July 2008, pp. 341 – 351.

[3] Van herle, J., Marechal, F. and Leuenberger, S. (2004). Process flow model of solid oxide fuel cell system supplied with sewage biogas, *Journal of Power Sources*, vol.131(1-2), May 2004, pp. 127 – 141.

[4] Van herle, J., Membrez, Y. and Bucheli, O. (2003).Biogas as fuel source for SOFC co-generators, *Journal of Power Sources*, vol.127(1 – 2), March 2004, pp. 300 – 312.

[5] Shiratori, Y., Oshima, T. and Sasaki, K. (2008). Feasibility of direct-biogas SOFC, *International Journal of Hydrogen Energy*, vol.33(21), November 2008, pp. 6316 – 6321.

[6] Seitarides, Th., Athanasiou, C. and Zabaniotou, A. (2008). Modular biomass gasification-based solid oxide fuel cell (SOFC) for sustainable development, *Renewable and Sustainable Energy Reviews*, vol.12(5), June 2008, pp. 1251 – 1276.

[7] Kohl, A. and Nielsen, R. (1997). *Gas Purification*, 5th edition, Gulf Publish Company, Texas.

[8] Yeh, J.T. and Pennline, H.W. (2001). Study of CO_2 absorption and desorption in a packed column, *Energy Fuels*, vol.15(2), February 2001, pp. 274 – 278.

[9] Aroonwilas, A. and Veawab, A. (2004). Characterization and comparison of the CO_2 absorption performance into single and blended alkanolamines in a packed column, *Industrial and Engineering Chemical Research*, vol.43(9), April 2004, pp. 2228 – 2237.

[10] Brettschneider, O., Thiele, R., Faber, R., Thielert, H. and Wozny, G. (2003). Experimental investigation and simulation of the chemical

absorption in a packed column for the system $NH_3 - CO_2 - H_2S - NaOH - H_2O$, *Separation and Purification Technology*, vol.39(3), November 2004, pp. 139 – 159.

[11] Won, J.C., Jong, B.S., Sang, Y.J., Jong, H.J. and Kwang, J.O. (2009). Removal characteristics of CO_2 using aqueous MEA/AMP solutions in the absorption and regeneration process, *Journal of Environmental Sciences*, vol.21(7), 2009, pp. 907 – 913.

[12] Mangalapally, H.P., Notz, R., Hoch, S., Asprion, N., Sieder, G., Carcia, H. and Hasse, H. (2009). Pilot plant experimental studies of post combustion CO_2 capture by reactive absorption with MEA and new solvents, *Energy Procedia*, vol.1(1), February 2009, pp. 963 – 970.

[13] Dey, A. and Aroonwilas, A. (2009). CO_2 absorption into MEA-AMP blend: mass transfer and absorber height index, *Energy Procedia*, vol.1(1), February 2009, pp. 211 – 215.

[14] Aroonwilas, A., Tontiwachwuthikul, P. and Chakma, A. (2001). Effects of operating and design parameters on CO_2 absorption in columns with structured packings, *Separation and Purification Technology*, vol.24(3), September 2001, pp. 403 – 411.

[15] Aroonwilas, A., Chakma, A., Tontiwachwuthikul, P. and Veawab, A. (2003). Mathematical modeling of mass-transfer and hydrodynamics in CO_2 absorbers packed with structured packings, *Chemical Engineering Science*, vol.58(17), September 2003, pp. 4037 – 4053.

BIOGRAPHY

Name: Ms.Gunniga Pornsopin

Date of Birth: April 26, 1985

Place of Birth: Bangkok, Thailand

Education:

2003 – 2007 B.Eng. in Mechanical Engineering, Faculty of Engineering, Mahidol University

2008 – 2011 M.Eng. in Automotive Engineering (International program), International College, King Mongkut's Institute of Technology Ladkrabang (KMITL)

Scholarships:

2008 – 2010 Full scholarship for study in the master degree from National Science and Technology Development Agency (NSTDA)

Publications:

1. ***G. Pornsopin***, N. Punbusayakul, T. Uttamote, K. Hanamura, S. Charojrochkul, and J. Charoensuk "Study Behaviour of CO_2 Absorption in Packed Bed Column form Synthesis Biogas to Produce Hydrogen for SOFC Operation" orally presented in the International Conference on "Green and Sustainable Innovation 2009", December 2 – 4, 2009, Chiang Rai.
2. N. Punbusayakul, ***G. Pornsopin***, T. Uttamote, P. Onbhuddha, J. Charoensuk and S. Charojrochkul "Study the Concentrations of NaOH Solution which Effect to CO_2 Absorption from Biogas for Fuel Processing in SOFC System" orally presented in the National Conference on "The 24th Conference of the Mechanical Engineering Network of Thailland", October 20-22, 2010 Ubonratchathani.